A minerals research contract report
June 1, 1981

FINAL REPORT — EVALUATION OF COAL-MINE ELECTRICAL-SYSTEM SAFETY

Grant G0155003
The Pennsylvania State University

BUREAU OF MINES ★ UNITED STATES DEPARTMENT OF THE INTERIOR
Minerals Health and Safety Technology

DISCLAIMER NOTICE

50272-101

REPORT DOCUMENTATION PAGE	1. REPORT NO.	2.	3. Recipient's Accession No.
4. Title and Subtitle FINAL REPORT - EVALUATION OF COAL-MINE ELECTRICAL-SYSTEM SAFETY			5. Report Date June 1, 1981 6.
7. Author(s) Lloyd A. Morley, Frederick C. Trutt, Jeffrey A. Kohler			8. Performing Organization Rept. No.
9. Performing Organization Name and Address Department of Mineral Engineering The Pennsylvania State University University Park, PA 16802			10. Project/Task/Work Unit No. 11. Contract(C) or Grant(G) No. (C) (G) G0155003
12. Sponsoring Organization Name and Address Assistant Director - Mining U.S. Bureau of Mines 2401 E. Street, N.W. Washington, D.C. 20241			13. Type of Report & Period Covered Final 14.

15. Supplementary Notes

16. Abstract (Limit: 200 words)

This final report concludes the documentation under Grant G0155003 and details research not covered under foregoing report volumes. The first chapter lists all other reports. The following chapters are divided into three major research tasks: Continuous Safety Monitoring Systems, Battery and Battery-charging Safety, and Mine Power System Transients. The monitoring chapter discusses the prediction of power-system failures. The battery chapter details work on battery-box stresses, battery chargers, and the elimination of electrocutions. The final chapter covers transient instrumentation, distribution transients sources and suppression, and utilization transients on mine power systems.

17. Document Analysis a. Descriptors

b. Identifiers/Open-Ended Terms Mine Electrical Systems, Power-system Monitoring, Prediction of Failure, Mine Batteries, Mine-battery-box Stresses, Battery Chargers, Mine-power-system Transients, Transient Instrumentation.

c. COSATI Field/Group

18. Availability Statement	19. Security Class (This Report)	21. No. of Pages
Release Unlimited	Unclassified	200
	20. Security Class (This Page) Unclassified	22. Price Unknown

(See ANSI-Z39.18)

OPTIONAL FORM 272 (4-77)
(Formerly NTIS-35)
Department of Commerce

FOREWORD

This report was prepared by The Pennsylvania State University, College of Earth and Mineral Sciences, Department of Mineral Engineering, University Park, Pennsylvania, under USBM Grant No. G0155003. The grant was initiated under the Coal Mine Health and Safety Research Program. It was administered under the technical direction of the Pittsburgh Mining and Safety Research Center with Mr. G. J. Conroy acting as the technical project officer. Mr. J. A. Herickes was the grant administrator for the Bureau of Mines.

This report is a summary of the work recently completed as part of this grant during the period July 8, 1974 to May 30, 1981. This report was submitted by the authors on June 1, 1981.

This technical report has been reviewed and approved.

At the grant report date, no inventions have been developed from Grant G0155003. Consequently, no patents are pending.

The authors are grateful to the many individuals and companies who have cooperated with our efforts. Special thanks are given to battery-charger manufacturers and mine operators. Individuals that deserve specific mention are J. G. Bredeson, W. R. Chubb, R. C. Jamison, J. A. Keifer, R. H. King, R. A. Rivell, P. A. Sopko, S. A. Thomas, and D. J. Tylavsky. Each directly served on the project and were faculty, staff, or graduate students at The Pennsylvania State University.

TABLE OF CONTENTS

TABLE OF CONTENTS (Continued)

TABLE OF CONTENTS (Continued)

Page

TABLE OF CONTENTS (Continued)

LIST OF TABLES

LIST OF TABLES (Continued)

LIST OF FIGURES

LIST OF FIGURES (Continued)

CHAPTER I
EXECUTIVE SUMMARY

The overall objective of USBM Grant G0155003 was to gain extensive information about safety in underground coal-mine electrical systems. The performance period extended from July 8, 1974, through May 30, 1981. The original grant underwent nine modifications and, to obtain the project objective, the research contained therein covered numerous individual tasks.

Twelve major reports have been separately produced, all under the grant title, and are as follows:

1. Morley, L. A., "Evaluation of Coal Mine Electrical System Safety," Annual Report to the USBM, Grant G0155003, USBM OFR, August 1975, 172 p.

2. Morley, L. A., F. C. Trutt, R. A. Rivell, "Coal Mine Electrical System Evaluation - Computer Modeling," Annual Report to USBM, Grant G0155003, NTIS PB 283496/AS, December 1976, 168 p.

3. Morley, L. A., R. H. King, P. A. Sopko, "Coal Mine Electrical System Evaluation - Shielded Cables," Annual Report to USBM, Grant G0155003. NTIS PB 283492/AS. January 1977, 170 p.

4. Morley, L. A., J. L. Kohler, "Coal Mine Electrical System Evaluation - Continuous Monitoring." Annual Report to USBM, Grant G0155003, NTIS PB 283490/AS. January 1977, 270 p.

5. Morley, L. A., J. A. Kiefer, "Coal Mine Electrical System Evaluation - Battery and Battery-charging Safety." Annual Report to USBM, Grant G0155003, NTIS PB 283494/AS, February 1977, 65 p.

6. Morley, L. A., F. C. Trutt, R. A. Rivell, "APL Mine Electrical System Load-flow Program," Task Completion Report to USBM, Grant G0155003, NTIS PB 283496/AS, April 1977, 136 p.

7. Morley, L. A., J. L. Kohler, W. R. Chubb, "Coal Mine Electrical System Evaluation - Transient Analysis," Annual Report to USBM, Grant G0155003, NTIS PB 283491/AS, 68 p. May 1977, 68 p.

8. Morley, L. A., "Coal Mine Electrical System Evaluation - Executive Summary," Annual Report to USBM, Grant G0155003, NTIS PB 283495/AS, May 1977, 17 p.

9. Morley, L. A., F. C. Trutt, R. A. Rivell, "Extended APL Mine Electrical System Load-flow Program," Task Completion Report to USBM, Grant G0155003, NTIS PB 283497/AS, September 1977, 100 p.

10. Morley, L. A., F. C. Trutt, S. A. Thomas, "Dynamic Simulation of Coal Mine Electrical Power Systems," Task Completion Report to USBM, Grant G0155003, NTIS PB 292333/AS, January 1978, 169 p.

11. Morley, L. A., F. C. Trutt, R. C. Jamison, "Load Modeling of Continuous Miner Induction Motors," Task Completion Report to USBM, Grant G0155003, NTIS PB 292462/AS, January 1978, 138 p.

12. Morley, L. A., F. C. Trutt, J. L. Kohler. "Evaluation of Coal Mine Electrical System Safety." Annual Report to USBM, Grant G0155003. NTIS PB 80-119514, January 1978, 43 p.

Six graduate theses also have been produced as a result of the funding:

1. Kohler, J. L., "A Tentative Method for the Prediction of Mine Power System Component Failures by Pattern Recognition Techniques," An Unpublished M.S. Thesis, The Pennsylvania State University, March 1977, 227 p.

2. Sopko, P. A., "Shielded Low-voltage Trailing Cables for Underground Coal Mines," An Unpublished M.S. Thesis, The Pennsylvania State University, March 1977, 161 p.

3. Jamison, R. C., "Load-modeling Continuous Miner Induction Motors," An Unpublished M.S. Thesis, The Pennsylvania State University, November 1977, 130 p.

4. Thomas, S. A., "Dynamic Simulation of Coal Mine Electrical Power Systems," An Unpublished M.S. Thesis, The Pennsylvania State University, November 1977, 161 p.

5. Tylavsky, D. J., "A Microprocessor Based Implementation of the Sequential Events Detections, Analysis, and Prediction System," An Unpublished M.S. Thesis, The Pennsylvania State University, August 1978, 350 p.

6. Keifer, J. A., "An Assessment of Direct-current Mine-power-system Failure Parameters," An Unpublished M.S. Thesis, The Pennsylvania State University, March 1979, 86 p.

All required copies of these reports and theses have been forwarded to the Bureau of Mines in compliance with the terms of the grant agreement. Appendix I contains abstracts of each.

This final report concludes the documentation under Grant G0155003 and details research not covered under the foregoing report volumes. The following chapters are divided into three major research tasks:

1. Chapter II - Continuous Safety Monitoring Systems,
2. Chapter III - Battery and Battery-charging Safety, and
3. Chapter IV - Mine Power System Transients

Each chapter stands by itself and can be extracted with total comprehension. With this report, all objectives as specified by the grant scope of work have been obtained.

CHAPTER II
CONTINUOUS SAFETY MONITORING SYSTEM

2.0 BACKGROUND

2.0.1. General

The purpose of this research was to develop a continuous-monitoring system which could predict incipient electrical-safety hazards. It was originally funded under USBM Grant G0155003 as a two-year two-phase effort.

The first year was devoted to collecting extensive mine data concerning deterioration and the associated changes in the monitored electrical parameters. This information was used to characterize the incipient failures and related safety hazards. A system was subsequently designed and critically examined for its feasibility in the mine. The first-year results strongly indicated that a continuous-monitoring system could economically prevent electrical safety hazards.

The second-year effort focused on the hardware/software implementation of the safety-monitoring system. The package was primarily based on commercially available subsystems, such as a minicomputer, its peripherals, and A/D converters, but several portions were designed and built by this organization, including a sensor amplifier, interface, and communication subsytem. The system was given the name SEDAPS, an acronym for Sequential Events Detection, Analysis, and Prediction System. The following provides a brief description of the research facility.

2.0.2. SEDAPS

Information concerning the present state of the mine power system is collected by suitable transducers and presented to the computer. The information typically consists of the waveshapes and magnitudes of voltage and current being supplied to portable, mobile mining equipment. A computer-controlled analog-to-digital converter converts the analog transducer data into a digital form, which can be operated on by the computer. The computer performs a Fast Fourier Transform (FFT) on the digitized data, and the results are in the form of coefficients representing the spectral content of the analog signal sampled by the transducers. Manipulations are performed on these frequency-domain components by the processing system of the computer. The results can then be plotted and examined for changes in any electrical parameter which are unique for a specific failure.

Hardware. The central unit of the computing system is an Interdata Model 7/16 minicomputer. The processor is a 16-bit machine containing 64 kbytes of core resident memory. Peripheral equipment consists of a teletype for communicating with the processor, a 10-Mbyte disc-storage facility for storing software and data, and a line printer for data output.

Software. All computer processes, from raw-data input to information output, are done under the instruction of system software. There are two basic program sequences which are required before the computer can produce useful data. The first sequence involves defining the type of data to be analyzed (i.e., a-c or d-c, three phase or single phase, etc.). The second step is the specification of appropriate calculations. At this point, system software takes over and performs the required calculations.

2.0.3. Original Results

By simulating deterioration in Penn State's Mine Electrical Research Laboratory, the projected operating characteristics of the system were verified. SEDAPS was able to predict impending cable, transformer, and motor failures.

The general results of the two-year research effort were as follows.

1. A unique system was designed to predict incipient failures and potential electrical safety hazards.

2. New analytical techniques were developed to aid in the effort.

3. The system was found suitable for the entire mining industry, especially underground coal mines, regardless of size.

4. An unique and powerful tool was established for the investigation of many electrical safety problems that are too complex for standard instrumentation applications.

A complete description of these accomplishments was made available in reference 1. The last item listed above related the very general nature of the developed system, not only in terms of its versatility but also the immediate application to aid in resolving mine electrical safety problems.

2.0.4. Scope of Work

Based on the previous work, there were two specific areas where continuing research was strongly indicated. The first was to advance the hardware-software development of the monitoring system, with emphasis on user-oriented software that could be applied to many problem areas. The objective was to establish SEDAPS as both a continuous safety-monitoring system and a stand-alone research tool. The second effort was to use the monitoring system to study mine power deterioration. Using extensive in-mine and laboratory studies, the purpose was to gain further knowledge in electrical deterioration and its connection to mine safety.

As the continued research progressed, work was quickly divided into three distinct areas: system definition, a-c hazard prediction, and d-c hazard prediction. Approximately half way through the project, a fourth area was found necessary: an investigation into the feasibility of implementing the prediction system in a microprocessor-based system. Such a study became necessary after the system concept had been defined, and it was discovered that very fast execution times and large computational power were needed. This, of course, required a minicomputing system which is not feasible, both from cost and technical standpoints, in underground coal mines.

Near the end of the performance period, the Technical Project Officer requested that the continuous-monitoring-system hardware, along with a software package, be delivered to a suitable facility at the Bureau of Mines' Pittsburgh Research Center (Bruceton), reassembled, and made operational. Accordingly, the scope of work was modified. Because of personnel changes, this involved a subcontract to KETRON, Incorporated, Wayne, Pennsylvania, to perform the requested services. This subcontract was completed satisfactorily.

Beyond the material contained in this chapter, detailed descriptions of certain work portions can be found in references 2, 3, and 4. Additionally, research is still progressing, above the grant scope of work but without Bureau of Mines' support. The results of the present effort will be described in reference 5 and will be supplied to the Bureau of Mines.

2.0.5. Chapter Format

The next chapter section lists the major project conclusions as well as recommendations for future research. The third section contains a description of the prediction-system concept. Direct-current incipient-safety-hazard prediction is covered in Section 2.3, and the microprocessor feasibility study is briefly discussed in Section 2.4. Appendix II of the report is an in-depth description of the prediction-system software. Additional computer listings as well as test data and programs appropriate for general-purpose computer simulation of the prediction system can be obtained by writing to the authors.

2.1. CONCLUSIONS AND RECOMMENDATIONS FOR FUTURE RESEARCH

2.1.1. Conclusions

During the course of this research project, a number of significant results have been achieved. These conclusions can be divided into four general areas as follows.

1. The major conclusion is that incipient-electrical-safety hazards in either a-c or d-c power systems can be predicted. Electrical-safety hazards can be predicted in the following types of equipment:

a. squirrel-cage induction machines,

b. wound-rotor induction machines,

c. direct-current series-wound machines,

d. direct-current shunt-wound machines,

e. transformers,

f. power-factor-correction capacitor banks,

g. rectifiers, and

h. electrical cables.

Any deterioration, beyond normal tolerances, in the above listed components can lead to electrical-safety hazards. Usually the deterioration can be represented as a loss of, or decrease in, the integrity of an insulating material. It was also found that deterioration in one component, while it may not cause an immediate safety hazard, can initiate or accelerate deterioration in other components, which may present direct hazards to workers.

When excessive deterioration occurs, the mechanical frame may become electrically "live." If touched, electrical burns could follow. Nonfatal electric shock to the miner might result, which, in itself, may represent minimal danger, except that the rapid uncontrolled movement that follows the shock could cause physical injury to the miner. At worst, an electrocution can result or, if sparks are generated, a methane ignition might create a fire or explosion.

2. The research has established the feasibility of a microprocessor implementation of the safety-hazard prediction system for in-mine use. The study found that off-the-shelf hardware, consisting of a high-speed microprocessor unit with a front-end preprocessor, will meet the system requirements in terms of execution time, core size, and scratch-pad memory. The preprocessor is employed to handle the large number of arithmetic operations required by the FFT routine. The implementation was found practical from cost, reliability, and maintainability viewpoints. The most favorable network application for a mine appears to be a distributed microprocessor-based system, whereby many mining sections would be continuously monitored.

3. The developed algorithm for predicting incipient electrical safety hazards is general enough to include non-electrical parameters. For example, mechanical parameters, such as vibration and temperature, may also be input to the system and used to expand the number of safety-hazard modes which are detectable.

4. The pattern features that are extracted from the monitored parameters (three-phase voltages and currents) have value in a noncontinuous monitoring-system environment. Many of the features could be measured on an incremental basis and used to improve electrical safety conditions in underground coal mines. In fact, this may present an intermediate solution to the problem of electrical safety prior to acceptance of the continuous-monitoring system by the industry. The specific application of each pattern feature is apparent if the use of

the parameter in the algorithm is understood. An example of such use is in the monitoring of the phase shift on the sixth harmonic of 60 Hz, which is found on d-c power systems. Measurement of this shift, either on a one-time basis or several times over a long time period, can be used to detect high-impedance faults on the d-c system or detect incipient component failure on the system, respectively.

2.1.2. Recommendations for Future Research

It is the authors' opinion that several additional areas need to be investigated in more detail before the system's concept can be implemented in the mining industry. To prematurely introduce this technology without resolving these issues might condemn it to certain rejection, by the industry. The additional work which must be performed spans five diverse areas and includes basic research as well as additional in-mine investigations.

1. The performance of the hazard-prediction system must be evaluated by mathematically modeling electrical machines and cable-connected electrical machines under various deteriorating conditions to study the changes in pattern features. This type of research could be considered a sensitivity analysis to establish the relationship between specific deterioration modes and consequential changes in the pattern features. These relationships were established empirically during the course of the project and supplemented by some mathematical modeling. However, additional simulations are needed to explain several anomalies which have occurred during use of the present system.

2. A formal topological analysis of the decision space must be conducted to verify the uniqueness of the hyperplane boundaries. Homomorphic relationships must also be defined in the decision space so the probability of a false alarm and the probability of a missed signal can be accurately computed. Although brief analyses were conducted in this area, a much more formal approach should be taken.

3. A system error analysis should be performed as well as a sensitivity analysis of error. Project personnel conducted error analysis of the FFT routine but could not examine the interrelationships among the system components. Again, the work must be performed so the accuracy of various system components such as transducers, A/D converter, and the processing system can be precisely defined. This is also necessary to define the overall sensitivity of the system to a specific type of incipient deterioration.

4. After the first three items have been investigated and an improved classification algorithm has been formulated (if necessary), a microprocessor prototype with a few megabytes of bulk storage should be constructed and placed in the mine for several months. While the microprocessor is in the mine, the section should be time studied, and the collected data should be analyzed frequently. Any remaining weaknesses in the system design should become evident at this point and can be corrected. Subsequently, an operational prototype should be constructed.

5. Prior to construction of the prototype, an engineering study should be performed to define the most efficient method of processing the data. The structure of the algorithm is such that a large number of mathematical operations have to be performed on a continual basis. Approximately two to three million floating-point operations must be performed each second. If the system is to operate in real time or in the most likely acceptable worst case of 2.5 times real time, these parameters must be defined.

2.2. ELECTRICAL-SAFETY HAZARD-PREDICTION-SYSTEM CONCEPT

2.2.1. Fundamental Premise

The fundamental premise of the hazard algorithm is that an electrical component that is deteriorating is also an incipient safety hazard, since the component is no longer functioning to the original design specifications. This implies that a system which predicts incipient failure or deterioration satisfies the need to predict incipient safety hazards. For reasons discussed in reference 1, it is much easier to predict failure than safety hazards, and actually more meaningful (i.e., in terms of defining the source of the safety hazard). This premise was verified in the previous research.

2.2.2. Prediction Technique

After examining a number of methods of implementing a hazard-prediction system, project personnel settled upon pattern-recognition techniques. Such a system structure has the major advantage of being able to predict a large number of safety hazards without a proportional increase in the complexity or size of the algorithm. Additionally, the pattern-recognition algorithm can be extended, utilizing adaptive-information-processing techniques, so that it behaves as a learning system. Consequently, its performance can actually be improved with time. The technique can also be thought of as a "customizing process" where the system tailors itself to the monitoring environment. A functional diagram of the system is shown in Figure 2.1 and will serve as the basis for future discussion.

Referring to Figure 2.1, the first step is the raw-data input provided by the system's transducers, in this case current and voltage sensing devices. (The transducers could also be other types of devices, for instance those for vibration, strain, pressure, or flow.) The data, which is in analog form, must be converted to a form which is compatible with the processing equipment. This requires filtering and amplifying the analog signal to prevent aliasing in the FFT routine and to improve the signal-to-noise ratio, respectively. Next, the signal is converted to digital form, and appropriate control codes are added. Once this has been completed, the processing algorithm is called. The first step is that of attribute extraction, selecting key features which characterize the data. Selection of the attributes that are to represent the patterns (here, incipient electrical safety hazards) is traditionally considered the first part of the pattern-recognition system. This topic was the main emphasis of reference 1 and will be very briefly summarized later in

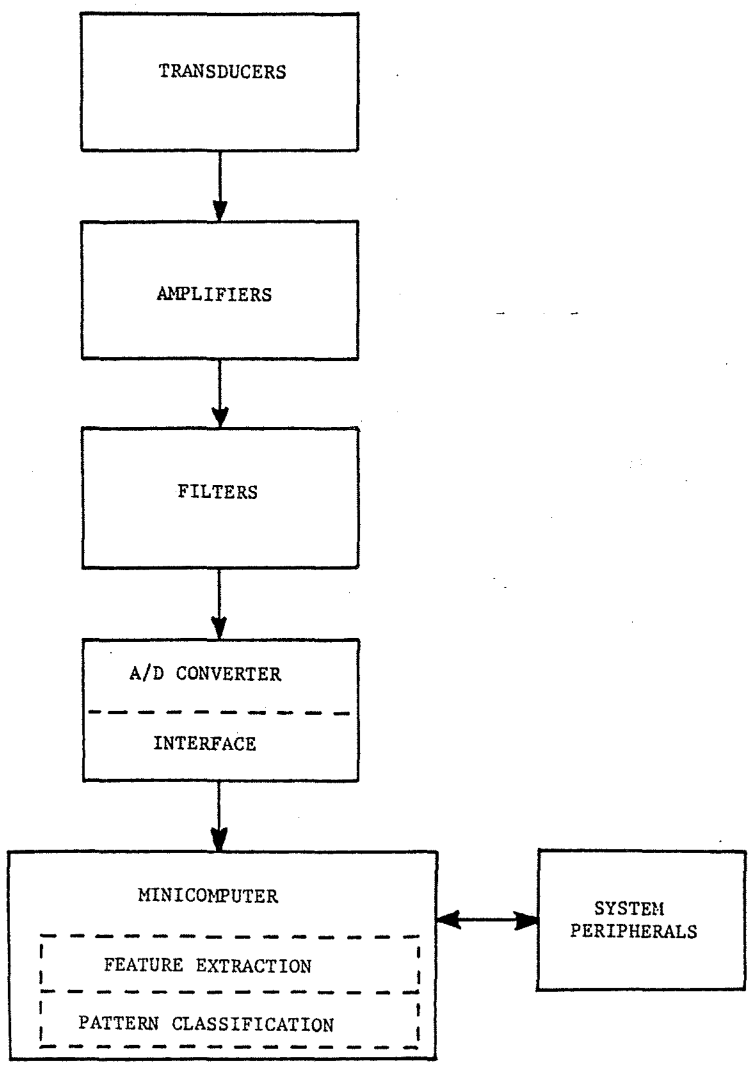

Figure 2.1. Functional Diagram of the Hazard Prediction System.

this section. The extracted features are then mapped into a decision space where the presence or absence of deterioration, as well as the type, is established. This aspect of the system will also be discussed later.

Classification Process. The features or attributes must adequately represent the pattern, be relatively easy to compute, and be invariant to translation at rotation of the pattern. Table 2.1 lists the features which were determined to meet the required criteria. Each of these attributes combines to form a unique "fingerprint" of an incipient electrical-component safety hazard. All of the attributes show varying degrees of sensitivity to different failure modes. These sensitivity relationships have been established largely on an empirical basis, but should be verified with formal mathematical models.

Figure 2.2 shows the data-flow process for attribute or feature extraction. After the features have been extracted, using standard signal-processing techniques, the resulting "pattern vector" is mapped into a decision space where any incipient electrical safety hazards are detected. The hazard classification or mapping process is really composed of two stages. The first is the determination of whether or not an incipient safety hazard exists. If the existence of such is established, then additional classification routines are called into the processing unit to define the nature of the hazard. Although this implementation has the disadvantage of requiring a more sophisticated software overlay structure, it significantly reduces the turn-around time for processing between successive samples in time and reduces the total core requirements. Therefore, the core must only be as large as the supervisor module and the largest subroutine to be overlaid.

In order for this multi-stage classification process to work successfully, it is necessary that the criteria for the first stage of classification be quickly executable and reliable. Based on the empirical investigations, it has been found that one of two features could be used as such an indicator. The transformed magnitude of the negative-sequence current for a machine will always change after some sort of deterioration has initiated. The transformed magnitude of the phase-A 60-Hz current for each machine being monitored will also change after the initiation of deterioration. Either one of these could be used in the first stage of classification. It has been decided to use the magnitude of the 60-Hz current.

With the aid of Figure 2.3, this first stage is easily explained. The figure shows a load cycle for a machine, where load cycle is defined as those events which occur between two successive excursions of the current through some arbitrarily selected reference value. This reference level is indicated in the diagram. It can be mathematically shown (see reference 1) that the value of the feature on its positive excursion through the reference value should be identical to the value of that same feature on a negative excursion through the reference level. In other words, the difference between the two should be equal to zero.

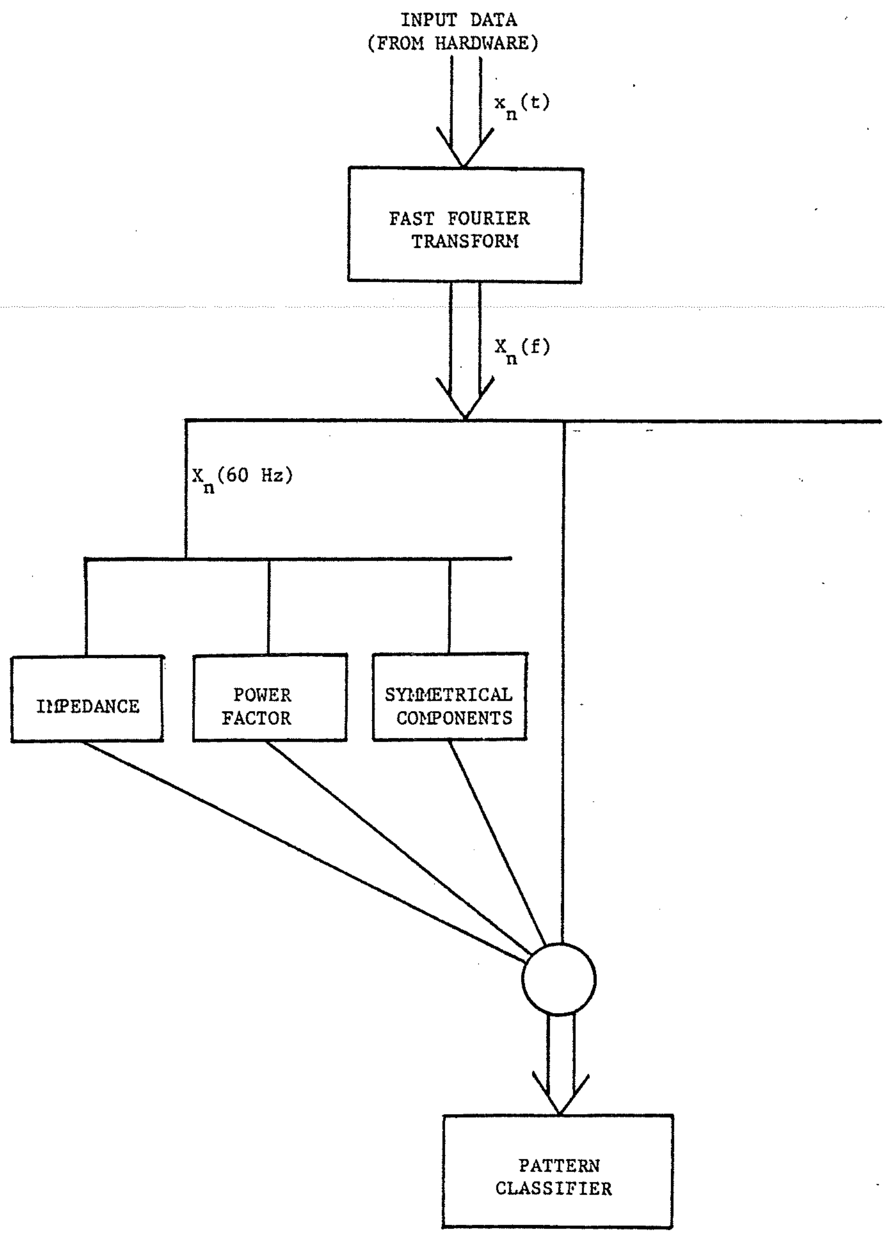

Figure 2.2. Information Flow Diagram for the Feature Extraction Process.

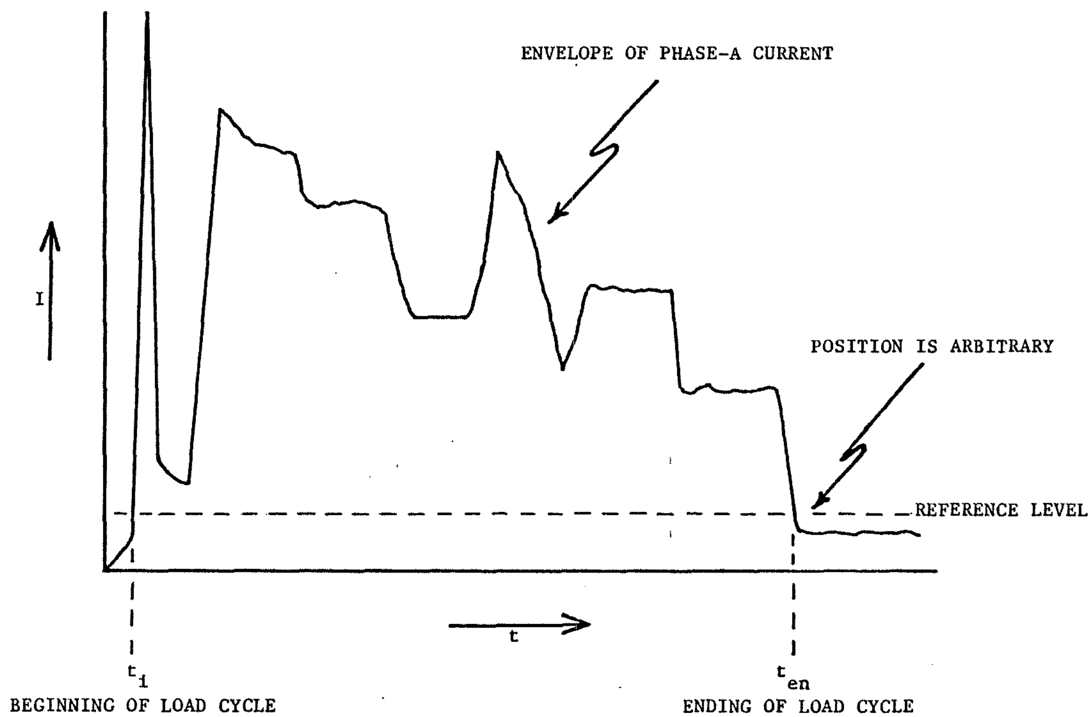

Figure 2.3. Graphic Definition of a Load Cycle.

Table 2.1. Pattern Features of the Hazard-prediction Algorithm.

	Magnitude	Phase Angle
60-Hz Voltage	x	
30-Hz Current	x	
60-Hz Current	x	
180-Hz Current	x	
360-Hz Current		x
Power Factor	x	
Impedance	x	
Complex Power	x	
Symmetrical Components of Current	x	
Symmetrical Component Impedance	x	

The algorithm has been constructed to sample the transducer input approximately six times each second with each discrete sample being taken at the Nyquist rate. When it has been determined that a datum point has gone through or made an excursion through the reference level, that point is saved. The difference between it and a stored value of that feature going through the reference level is computed. When the difference is zero, the algorithm goes back into a high-speed sampling mode. If the difference is non-zero, it is tested against a stored threshold value and, if this is exceeded, the initiation of deterioration has been detected. Now, additional routines are called in to compare the difference for each pattern feature. The algorithmic process from this point on constitutes the second stage of classification. The difference for the phase ϕ, jth feature of the ith load cycle is computed as:

$$d^{\phi}_{ij} = X^{\phi}_{ij} - X^{\phi}_{Rj} \tag{2.1}$$

where:

d^{ϕ}_{ij} = the difference for the phase ϕ, j^{th} feature of the i^{th} sample

X^{ϕ}_{ij} = the magnitude of the j^{th} feature for phase ϕ at the time when the phase a current passes through the reference level

X^{ϕ}_{Rj} = the stored reference value for the j^{th} feature of phase ϕ. This is also the value of X^{ϕ}_{ij} under normal operating condition

A column vector, D_{ϕ}, can be formed to represent these differences for all features of a given phase, d, at given point in time, i:

$$D^{i}_{\phi} = \begin{bmatrix} X_1 \\ X_2 \\ \vdots \\ X_n \end{bmatrix} \tag{2.2}$$

Empirically it has been found that the random variability of the sample can be reduced by introducing a second transformation:

$$P_n = D^{i}_{\phi} = D^{i}_{\phi+1} \tag{2.3}$$

where:

P_n = nth transform column vector, such that, (2.4)

$P_1 = D^{i}_{A} - D^{i}_{B}$; (2.5)

$P_2 = D^{i}_{B} - D^{i}_{C}$; (2.6)

$P_3 = D^{i}_{C} - D^{i}_{A}$, are the allowable states. (2.7)

It is the P transform which is used to predict incipient safety hazards.

If a column vector T is assumed where T contains a threshold value t_j for each feature, j, such that:

$$T = \begin{bmatrix} t_1 \\ t_2 \\ \vdots \\ t_n \end{bmatrix} \tag{2.8}$$

then the following test can be made:

if $|P_n| > |T + \varepsilon|$ (2.9)

then deterioration exists;

where ε is a column vector representing the error associated with the selected threshold.

When deterioration exists the following equations are evaluated:

$$\text{if } P_n < T + \varepsilon,\ L_n = -1 \text{ for each j;} \tag{2.10}$$

$$\text{if } P_n > T + \varepsilon,\ L_n = +1 \text{ for each j;} \tag{2.11}$$

$$\text{if } P_n = T + \varepsilon,\ L_n = 0 \text{ for each j.} \tag{2.12}$$

where L_n is nth column vector of state variables and ℓ_j is the value of the j^{th} test computed.

That is:

$$L_n = \begin{bmatrix} \ell_1 \\ \ell_2 \\ \vdots \\ \ell_j \end{bmatrix} \tag{2.13}$$

The vector L then becomes the pattern vector which is mapped into the decision space.

Mapping Functions. A number of mapping functions were developed and tested. The two most successful ones will be discussed here. The first is a polynomial function of jth order,

$$\sum_{j-1}^{J} \ell'_j k^j = H \tag{2.14}$$

where:

J = the number of features,

$\ell'_j = \ell_j + 1$

k = the number of allowable state of the variable ℓ, and is equal to 3 in this example.

H = pattern point from the nth P transform.

The character of this function is such that the phase in which deterioration occurs is easily defined. It also has the advantage of being simple and fast to compute. A disadvantage is that more than one pattern point, for a specific hazard, exists. This occurs because certain features (X_j) are relatively insensitive to a specific anamoly and may randomly vary within a small range. However, depending upon the value of the threshold

$(T + \varepsilon)$ with respect to this random variation of X_j, the state variable ℓ_j may also behave randomly. Consequently, the evaluation of equation 2.14, for many pattern vectors of a given hazard type, will result in a family of points.

The spread of these points is of course dependent on the order of the term of equation 2.14 in which the randomness is exhibited. Because more than one feature may exhibit this characteristic at any given time, the number of points within the family can become quite large. In practice, they have been found to vary from 12 to 65 points per family. Such presents a problem in tagging a given point with a specfic hazard. It is believed that this undesirable situation could be relieved by modifying equation 2.14 to include weighting factors, W_j, which can be computed or constants. The new equation would have the form,

$$\sum_{j-1}^{J} W_j \ell_j' k^j = H \qquad (2.15)$$

The other mapping function involves a tertiary masking process. There are various mathematical implementations of this process. The simplest (but not the most efficient) is a Boolean type of statement. Specifically,

if $\ell_j = b_{jm}$ for all j, then the mth hazard exists; (2.16)

b_{jm} = the apriori defined value which should be assumed be the jth state variable, ℓ, for hazard type m. These elements belong to a column vector B_m.

The method has the advantage that it is easy to use and modify. The obvious disadvantages are increased execution time and the inability to recognize hazards which were not defined apriori.

Tables 2.2 through 2.10 list the expected value of the state variables, ℓ_j of each L_n, for the fundamental modes of deterioration which can be predicted, and which relate to the safety hazards discussed previously. These tables represent the results of some 12,000 independent trials on cable-connected squirrel-cage (both wye and delta connected) and wound-rotor motors in the laboratory and in the mine.

This extensive data base permits the exploration of stochastic classification schemes; in fact, the error vector, ε, and the threshold vector, T, used in equation 2.9, can be defined in terms of the standard deviation and the mean of a distribution. Work is continuing in this direction (again to be presented in reference 5).

Table 2.6. Values of L vector for Line-line Deterioration in Phase B-C.

j		T transform		
		n 1	2	3
1	I	-1	-1	+1
2	Z	+1	+1	-1
3	R	0	+1	-1
4	X	+1	-1	-1
5	PWR	-1	-1	+1
6	PF	-1	+1	+1
7	IA1	+1	+1	-1
8	IA2	+1	+1	-1
9	IA0	+1	+1	-1

Table 2.7. Values of the L vector for Line-line Deterioration in Phase C-A.

j		T transform		
		n 1	2	3
1	I	+1	-1	+1
2	Z	0	+1	-1
3	R	-1	+1	-1
4	X	+1	+1	-1
5	PWR	+1	-1	0
6	PF	-1	+1	+1
7	IA1	+1	+1	+1
8	IA2	+1	+1	+1
9	IA0	+1	+1	+1

Table 2.8. Values of the L vector for Conductor Deterioration in Phase A.

j		T transform n=1	2	3
1	I	-1	+1	0
2	Z	+1	-1	0
3	R	+1	0	-1
4	X	-1	-1	+1
5	PWR	-1	+1	0
6	PF	0	0	-1
7	IA1	0	+1	0
8	IA2	0	+1	0
9	IA0	0	+1	0

Table 2.9. Values of the L vector for Conductor Deterioration in Phase B.

j		T transform n=1	2	3
1	I	0	0	+1
2	Z	0	0	-1
3	R	0	+1	0
4	X	+1	0	-1
5	PWR	0	0	+1
6	PF	-1	+1	0
7	IA1	0	+1	+1
8	IA2	0	+1	+1
9	IA0	0	+1	+1

Table 2.10. Value of the L vector for Conductor Deterioration in Phase C.

j		T transform		
		n 1	2	3
1	I	+1	0	-1
2	Z	-1	0	+1
3	R	0	-1	+1
4	X	-1	0	0
5	PWR	+1	0	-1
6	PF	0	-1	0
7	IA1	-1	-1	-1
8	IA2	-1	-1	-1
9	IA0	-1	-1	-1

The following probabilities have been empirically determined:

- probability of correct classification = 0.60
- probability of incorrect classification = 0.20
- probability of no classification = 0.20

These can be improved by requiring the classification of two or more load cycles of data to agree. In the case of three consecutive cycles, the probabilities are 0.8, 0.05, and 0.15, respectively.

2.3. PREDICTION OF INCIPIENT ELECTRICAL SAFETY HAZARDS ON DIRECT-CURRENT POWER SYSTEMS

2.3.1. Objective

The primary objective of the direct-current section of the research was to determine if the voltage and current waveforms supplying d-c contained any information which can be used to detect electrical hazards. This problem was approached in the same manner as the a-c safety-hazard-prediction problem where attributes were examined for their ability to characterize deterioration patterns. The work consisted of an extensive literature review, laboratory simulations, and in-mine data-collection and evaluation efforts. Complete discussion of the research in contained in reference 3.

2.3.2. System Hazards

Three types of d-c system hazards were considered. Two of these were very general in nature, being series failure and shunt leakages. The third type was very specific (and fairly common) and involved the loss of one diode in a six-diode full-wave bridge rectifier.

Shunt leakage currents can result from several types of activities including tracking across the motor commutator, shorting of armature windings, and short circuits in the field windings. A series failure is manifested as a gradual opening of a conductor or the degradation of any electrical connection. The detection of series failure is complicated particularly in series machines where it is impossible to distinguish between a series failure in the connecting cable and in the machine itself. The only way to resolve this dilemma is to monitor at both the machine and the d-c power source. Diode failures in rectifiers occur on a relatively frequent basis in mine power systems. In themselves, they present little danger except that the failure of the diode modifies the current waveform, causing inefficient operation of the d-c machines including additional dual losses. The unwanted heat accelerates insulation deterioration and may ultimately result in a failure or safety hazard.

2.3.3. Pattern-feature Behavior

A summary of the pattern-feature behavior for these types of deterioration is presented in the balance of this section.

Shunt-motor Deterioration. In shunt-motor deterioration, if the failure is on the d-c side of the rectifier, an unbalance of the a-c rectifier supply does not occur. The result is that the classification of either a shunt fault or a series failure in a d-c motor must be based on the absent value of some pattern characteristic and not on the value of an unfaulted phase (since none exists).

After extensive data collection and analysis, it was determined that the a-c harmonic present on the rectifier output contains useful information concerning the nature of the load connected to the rectifier (similar to the approach suggested in reference 1). In more specific terms, the magnitude and phase of the load impedance to the rectifier harmonic output can be used to indicate the presence of resistive faults (i.e., high-impedance deterioration) in the d-c system. The harmonic selected for analytical purposes is the sixth harmonic of the 60-Hz line frequency (360 Hz) which has the largest signal-to-noise ratio at the output of a three-phase bridge rectifier.

Table 2.11 shows the phase angle of the sixth-harmonic impedance of the shunt motor as a function of the motor load. The impedance angle for each increment of load current is actually an average value of 60 samples taken at the load. This averaging process is required to eliminate the impact of processing-system anomalies.

Table 2.12 shows the phase angle of the sixth-harmonic impedance as a function of the magnitude of shunt-fault leakage current. Motor current was held steady at 10 A. This test was performed near no load because a shunt fault of given magnitude is more apparent when motor impedance is at a maximum. Table 2.13 is similar to Table 2.12 with the exception that series failure is being modeled. The motor was operated full load for the series test because a series failure of given magnitude is more apparent at high line currents. Note that in both tables the impedance angle decreases as the fault magnitude is increased.

Tables 2.11, 2.12, and 2.13 show how the presence of both shunt faults and series failures may be inferred by observing the phase angle of the sixth-harmonic motor impedance. Importantly, a change in motor load causes only a minor shift in the impedance angle.

Once it is determined that motor deterioration is occurring, it is necessary to classify the failure as being either shunt leakage or series resistance. One way of accomplishing this would be to disconnect the motor in question and take resistance measurements with an ohmmeter. However, in the context of the continuous-monitoring system, the real and imaginary parts of the sixth harmonic motor impedance can be utilized by comparing to predefined values. Tables 2.14 and 2.15 illustrate this for the shunt fault and series failure, respectively. The data in Table 2.14 were taken at no load, and that of Table 2.15 was taken at full load.

Tables 2.14 and 2.15 show how the real part of the sixth-harmonic impedance increases in direct proportion to the fault magnitude for both failure types. The imaginary part, however, decreases with increasing shunt-fault current magnitude and increases with increasing series-failure magnitude. It should be noted that the imaginary part of the sixth-harmonic impedance is more sensitive to a series failure than a shunt fault. This suggests that the presence of a shunt fault may be inferred if it is observed that the phase angle is decreasing and the imaginary part has not changed significantly.

The sensitivity of this prediction method is ultimately limited by the precision in which the current and voltage of the machine under consideration can be measured. During this project, various techniques were applied to try and increase the accuracy of the method, including the development of special amplifiers which modified the incoming d-c signal, filtered out all components except 360 Hz, amplified the result, and then created a data bank upon which the calculations were performed. However, it would be desirable to do a sensitivity analysis of this aspect of the system to determine the precision in which the deterioration can be detected.

In-mine investigations revealed that the sixth-harmonic component of field current was too large to permit precise series-failure readings. It was found, however, that the magnitude of the sixth-harmonic field current was a good indicator of shunt leakage in the field circuit.

Table 2.11. Phase Angle of Sixth-harmonic Impedance as a Function of Motor Load.

Motor Current (A)	10	14	20	25	30	35
Impedance Angle (Degrees)	85.4	86.3	86.0	86.6	86.4	86.9

Table 2.12. Phase Angle of Sixth-harmonic Impedance as a Function of Shunt-fault-current Magnitude.

Fault Magnitude (A)	0	0.7	0.9	1.6	1.7	2.5	2.6
Impedance Angle (Degrees)	87.6	82.6	81.9	80.3	79.2	77.6	77.0

Table 2.13. Phase Angle of Sixth-harmonic Impedance as a Function of Series-failure-impedance Magnitude.

Failure Magnitude (Ω)	0.0	0.2	0.4	0.6
Impedance Angle (Degrees)	87.4	84.4	84.4	82.5

Table 2.14. Real and Imaginary Parts of the Sixth-harmonic Impedance as a Function of Shunt-fault-current Magnitude.

Fault Magnitude (A)	0	7.0	0.9	1.6	1.7	2.5	2.1
Impedance real part (Ω)	0.4	0.7	0.8	1.0	1.1	1.2	1.2
Impedance imaginary part (Ω)	5.7	5.7	5.7	5.6	5.6	5.4	5.3

Table 2.15. Real and Imaginary Parts of the Sixth-harmonic Impedance as a Function of Series-failure-impedance Magnitude.

Failure Magnitude (Ω)	0	0.2	0.4	0.6
Impedance real part (Ω)	0.2	0.5	0.6	0.8
Impedance imaginary part (Ω)	5.4	5.5	5.7	5.8

In shunt-leakage simulation, it was found that an increase in shunt leakage from zero to one third of the normal field current (the minimal obtainable with the shunt-fault model used) caused an increase in the sixth-harmonic field current over 700%.

Since the field circuit is essentially constant impedance, the presence of the series-resistance fault may be inferred by monitoring the field current.

Series Motors. Series-motor failures were also investigated in much the same manner as that described for shunt motors. A summary of this data is presented in Tables 2.16, 2.17, and 2.18.

Rectifiers. Diode failures and rectifiers were investigated in both the laboratory and the field. Figure 2.4 shows the time-domain representation of the rectifier voltage and current for a three-phase full-wave rectifier that has incurred the loss of one diode. It is interesting to note that the voltage waveform does not show a significant drop corresponding to that of the current. The same type phenomena was also found in the field work. In fact, in one mine visited, the mine electrical engineer complained about losing an abnormally high number of d-c locomotive motors. On further investigation, it was discovered that this same type of deformation of the current waveform existed in the time domain. Further examination revealed that the rectifiers supplying the d-c haulage system had also incurred the loss of one diode.

Table 2.16. Phase Angle of the Sixth-harmonic Impedance as a Function of Motor Load.

Motor Current (A)	7	9	11	13
Phase Angle (Degrees)	114.0	113.9	117.3	118.5

Table 2.17. Phase Angle of the Sixth-harmonic Motor Impedance as a Function of Shunt-fault-current Magnitude.

Fault Current (A)	0	.7	.9	1.6	1.7	2.5	2.6
Phase Angle (Degrees)	114	106	104	99	97	95	91

Table 2.18. Phase Angle of the Sixth-harmonic Motor Impedance as a Function of Series-failure-impedance Magnitude.

Fault Resistance (Ω)	0	0.2	0.4	0.6
Phase Angle (Degrees)	116	116	115	115

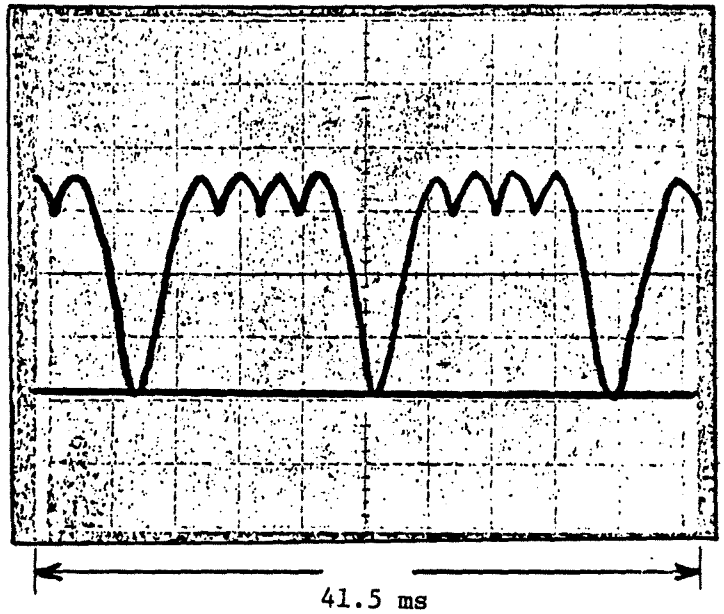

A. Time Domain

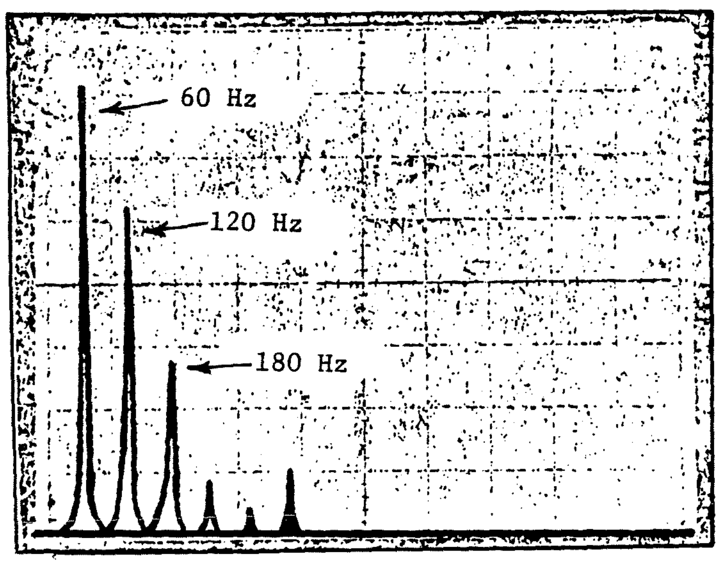

B. Frequency Domain

Figure 2.4. Time (A) and frequency (B) domain oscilloscope photographs of three-phase waveform with one-half of one phase opened.

2.3.4. Results

Results of this research section have indicated the following.

1. A method of improving d-c electrical system safety is available by monitoring the parameters described previously.

2. The d-c voltage and current waveforms in the mine have sufficient quality to use the methods described previously.

3. The problems detectable by these methods are presently being experienced by mine operators in the United States.

4. The sensitive features delineated in this research can be incorporated into the safety-hazard prediction system and can be classified in the same manner as a-c pattern features.

2.4. MICROPROCESSOR FEASIBILITY STUDY

2.4.1. Purpose

The purpose of the research summarized in the following paragraphs was to determine the technical and economic feasibility of implementing the hazard-prediction system with microprocessor-based technology. Although such a study would have been required ultimately, especially before this concept could be introduced to the industry, the main reasoning behind its inclusion in the project was to allow for the modification of and addition to the hazard-prediction algorithm in a manner which would be implementable on this technology. As a result of this study, various aspects of the hazard-prediction algorithm were modified to meet the constraints of existing state-of-the-art microprocessor technology. A complete description of the effort is contained in reference 4.

2.4.2. System Constraints

Process. Electrical-component failure is predicted by means of a complex failure-prediction algorithm. First, the 60-Hz three-phase voltage and current waveforms are sampled at a frequency of 960 Hz with 16 samples of the fundamental-frequency cycle. For the sixteen consecutive sample groups, each of sixteen samples are taken on each sampled channel. Then, a 16-point discrete fourier transform is performed on each 16-point sample group; this is accomplished by using a fast-Fourier-transform algorithm. The results of the FFT's are then processed by a series of complex signal-processing algorithms which extract the appropriate features as described previously (see reference 1). The results of these computations are then used to construct a pattern vector and ultimately a mapping function to predict a given incipient safety hazard.

Constraints. The microprocessor-based failure-prediction system has been designed around three system constraints.

1. The I/O capability of the microprocessor system must be able to sample minimum of 24 voltage, current, and/or other transducer-type channels at a frequency of 960 Hz.

2. All of the FFT calculations and failure-prediction calculations must be made within approximately 266 ms if the system is to run in near real time.

3. The results of the failure-prediction algorithm must be of a sufficient accuracy so erroneous failure predictions are not made because of the accumulation of excessive overflow in round-off errors. (Quantitatively, this means that the failure-prediction vectors used in the pattern-classification algorithm, that are as small as two percent of the maximum prediction vectors, must not be masked by errors due to the finite number of bits used to represent each data word in the calculations.)

2.4.3. Microprocessor-based System

A microprocessor-based system which meets these requirements is shown in Figures 2.5a and 2.5b. This hardware may be viewed as serving three functions. The sensors, amplifier, analog-to-digital converter, and ADC interface are responsible for signal acquisition. The microprocessor and FFT hardware make up the signal-processing portion of the system. The light-emitting-diode display and microprocessor keyboard are used as a man/machine interface for indicating incipient failures and allowing manual interrogation of microprocessor and/or modifying constants used by the mapping functions.

The most critical elements in the design, in terms of speed and accuracy, were the microprocessor and the FFT hardware. In order to estimate the time demands of the hazard-prediction system in terms of computations, the number of calculations required to make one pass through the hazard-prediction algorithm was developed, as shown in Table 2.19. State-of-the-art microprocessor technology was searched for systems that might be capable of meeting the requirements of the hazard-prediction system. A number of the microprocessors found have been listed in Table 2.20 along with the time it takes each to perform a given arithmetic operation. Using the information available on Table 2.19 and Table 2.20, the total time requirements of the system were computed. It was found that no existing microprocessor could perform the calculations in the time required (i.e., less than 266 ms). Accordingly, a decision was made to incorporate a hardware arithmetic processor on the front end of the microprocessor to handle the high computational overload. Such an approach is not unusual for complex signal-processing algorithms.

A hardware design which can be used to perform the high-speed FFT is shown in Figure 2.6. Being based around a 12-by-12 bit multiplier-

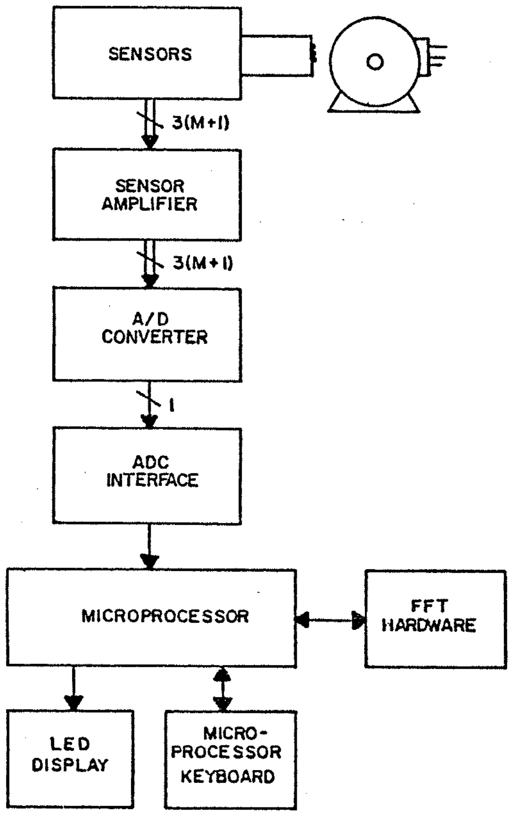

Figure 2.5a. Block Diagram of the Microprocessor-Based SEDAPS Hardware.

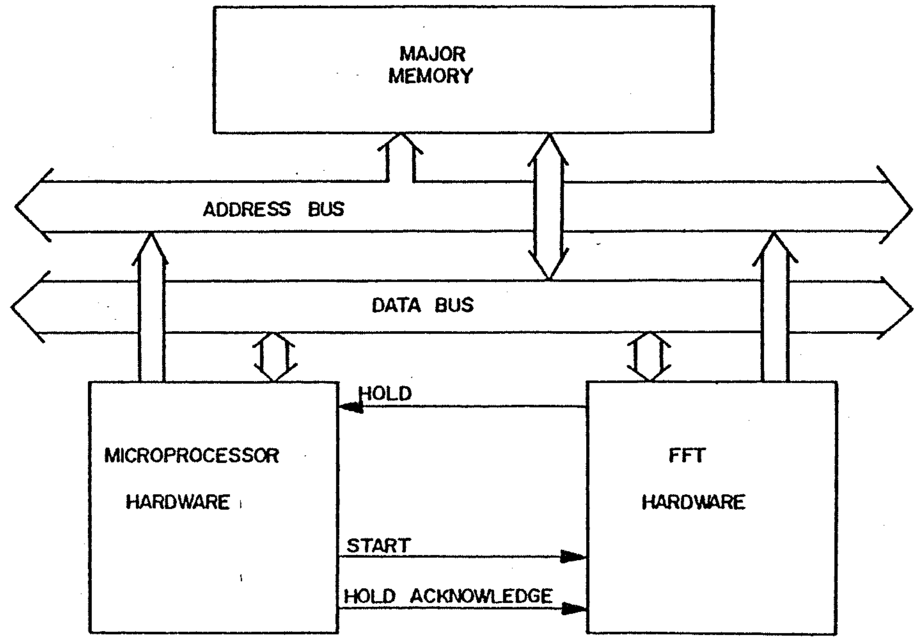

Figure 2.5b. Microprocessor-FFT Hardware Block Diagram.

accumulator chip which was available commercially, this chip functioned as the arithmetic element in FFT hardware. A functional block diagram of this chip is shown in Figure 2.7. The sequence of operations needed to perform a butterfly on a pair of complex data points as shown is listed in Table 2.21 (also see reference 4 for discussion).

Of course, the FFT hardware is used to perform only FFT calculations. The microprocessor is employed to sample data for use in these calculations and to process the results of them. Both the FFT hardware and the microprocessor must use the same memory. However, they cannot access this memory at the same time, hence an interfacing scheme as shown in Figure 2.5b is used. At the end of the input-data-sampling routine, the microprocessor sends a start level to the FFT hardware. The FFT hardware performs an initialization and sends a hold level to the microprocessor. The microprocessor then electronically detaches itself from the system buses and returns a hold acknowledge level to the FFT hardware. This then signals the FFT hardware to attach itself to the system buses and begin processing data. When all the FFT calculations are complete, the FFT hardware begins a termination routine which causes this hardware to attach itself from the system buses and remove the hold level to the microprocessor. Sensing the removal of the hold level, the microprocessor reattaches itself to the system buses and begins post-processing the results of the FFT calculations. One failure-prediction cycle ends with this incipient post-processing procedure and with incipient component-failure indications on the LED display in Figure 2.5a.

As mentioned in Section 2.2, there is a need to perform an error analysis of all computations used in the hazard-prediction algorithm. As stated previously, such an analysis has been made of the FFT, because any error in this stage of computation would seriously impact the accuracy of later computations.

Table 2.19. Microprocessor-Program Calculational Requirements.†

Calculation Description	+	x	÷	Cos	Arctan
FFT Calculations	36,864	24,576	0	0	0
Pre- and Post-FFT Calculations	7,968	1,266	36	21	24

† This table reflects the number of calculations required for running through the failure-prediction algorithm one time only.

Table 2.20. Preliminary Microprocessor Comparison.

Company and Microprocessor / Feature	Hardware Multiply	16 x 16 Multiply Time (μs)	16 x 16 Divide Time (μs)	Fix Instruction set	Software Support	Bit Slice Architecture	Assumed Clock Frequency (MHz)
Data General Corporation microNOVA	Yes	41.28	59.04	Yes	Same as NOVA	No	2.08
General Instrument Corporation CP 1600	No	250.0	375.0	Yes	Yes	No	2.5
Texas Instrument Incorporated TMS 9900	Yes	17.33	36.00	Yes	Yes	No	3.0
National Semicondictor Corporation Pace	No	1,270.0	Not Avail.	Yes	Yes	No	Not Avail.
National Semiconductor Corporation IMP-16	No	(Approx.) 544.0	(Approx.) 673.0	Yes	Yes	Yes	.714
Alpha Microsystems Incorporated (AM-100) WD 1600	No	73.2	80.8	Yes	Yes	Yes	3.0
Fairchild Semiconductor Macrologic	No	13.0	20.0	No	No	Yes	Not Avail.
Advanced Micro Devices AM 2900	No	3.2	Not Avail.	No	Yes	Yes	Not Avail.

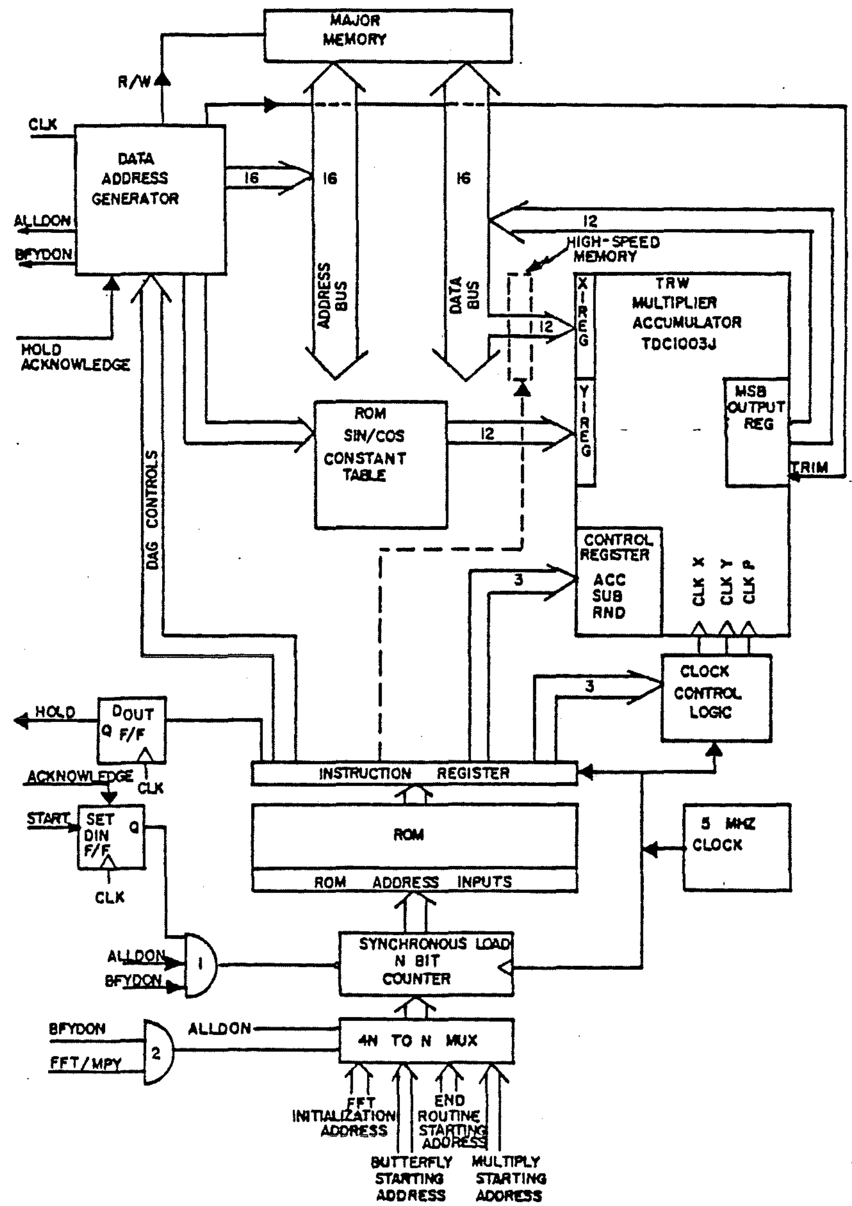

Figure 2.6. Preliminary FFT Hardware Design.

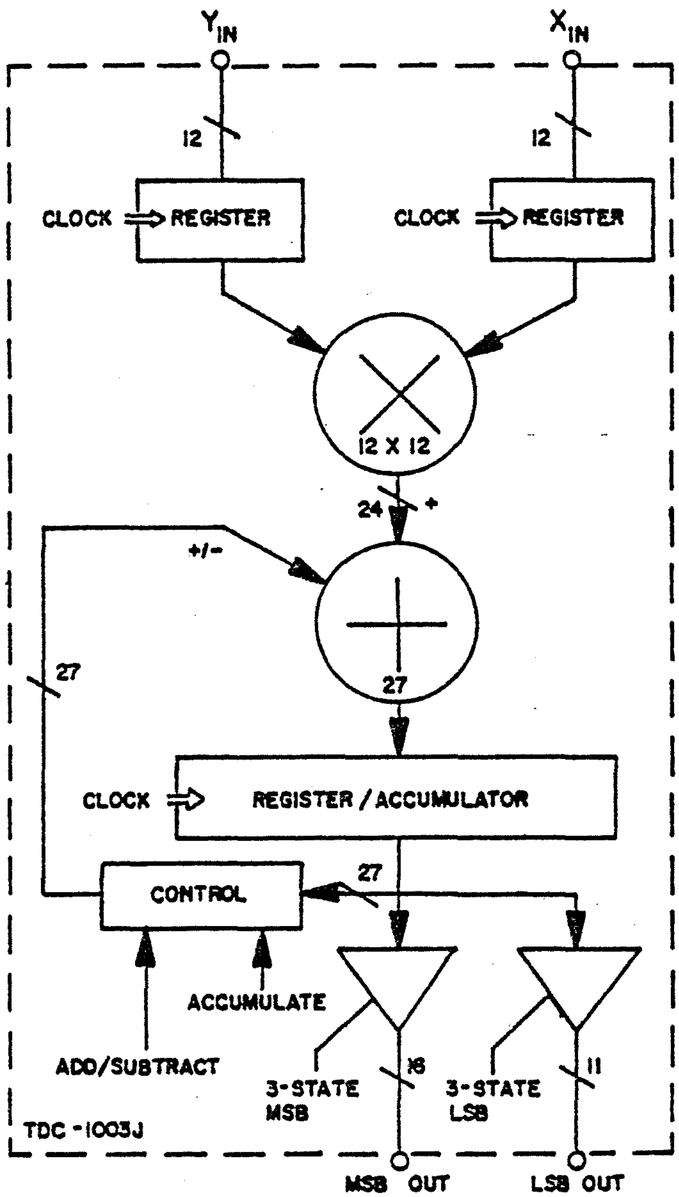

Figure 2.7. Multiplier-accumulator Functional Block Diagram.

Table 2.21. FFT Decimation-in-time Butterfly Sequence.

Operation Sequence					Contents of Output Registers at Completion of Operation	Cumulative Time at Completion of Operation
Step	Load/Hold (L/H)	ACC	SUB	RND		
1	L X_2, cos θ	0	0	0	$X_2 \cos \theta$	T
2	L Y_2, sin θ	1	0	0	$X_2 \cos \theta + Y_2 \sin \theta = Z_1$	2T
3	L X_1, 1	1	0	0	$X_1 + Z_1 = X_1'$ (transfer to destination)	3T
4	H X_1, 1	1	1	0	$-Z_1$	4T
5	H X_1, 1	1	0	0	$X_1 - Z_1 = X_2'$	5T
6	L X_2, sin θ	0	0	0	$X_1 - Z_1 = X_2'$ (transfer to destination)	6T
7	H X_2, sin θ	0	0	0	X_2 sin	7T
8	L Y_2, cos θ	1	1	0	$-X_2 \sin \theta + Y_2 \cos \theta = Z_2$	8T
9	L Y_1, 1	1	0	0	$Y_1 + Z_2 = Y_1'$ (transfer to destination)	9T
10	H Y_1, 1	1	1	0	$-Z_2$	10T
11	H Y_1, 1	1	0	0	$Y_1 - Z_2 = Y_2'$	11T
12	H Y_1, 1	0	0	0	$Y_1 - Z_2 = Y_2'$ (transfer to destination)	12T

Error Analysis. The FFT calculations can be made by using either floating-point or fixed-point arithmetic if some changes are made in FFT hardware. Floating-point arithmetic has the advantage of being more precise than fixed-point arithmetic but has the disadvantage of requiring more time. Fixed-point arithmetic is generally faster but is less precise than floating-point arithmetic. The selection of the type of arithmetic used depends on the amount of time available for computation, the amount of accuracy desired, and the degree of hardware complexity permitted. Since computational time and accuracy are both critical quantities, an error analysis should be performed for both procedures.

A floating-point error analysis of DIT FFT, shows that the output error variance (σ_E^2) in terms of the input signal variance (σ_x^2) is given by

$$\sigma_E^2 = (2/3)\nu \, 2^{-2t} 2^{\nu} \sigma_x^2 \tag{2.17}$$

where

$\nu = \log_2 N$

t = number of bits, including sign bit, used to represent each mantissa.

This result does not take into account the error introduced by quantization of the input signal by an ADC. If a "b"-bit ADC is used to sample the motor voltage and current waveforms, then it can be shown that the output error variance is given by

$$\sigma_E^2 = [(2/3)\nu \, 2^{-2t} + (1/3) \, 2^{-2b}] 2^{\nu} \sigma_x^2 \tag{2.18}$$

For the case of 16-point FFT, $\nu = 4$ and

$$\sigma_E^2 = [(2^8/3) \, 2^{-2t} + (2^4/3) \, 2^{-2b}] \sigma_x^2 \tag{2.19}$$

An error analysis of a fixed-point FFT requires that some type of rescaling technique be used at every stage in the FFT calculations. The signal being processed through the FFT signal-flow graph grows at most by a factor of two at each stage in the calculations. The fastest and simplest method to prevent overflows due to this growth rate is to insure that $|X_0| < 1/2$ to shift the mathematical results one place to the right after each stage in the FFT calculations. This method is the least accurate since it does not use all of the bits available to represent each data word and shifts all results to the right one place regardless of necessity. Using this method, it can be shown that the output error variance of a 16-point FFT is given by:

$$\sigma_{E'}^2 = (1/3)2^{-2t}\ (3296 + 12\sigma_x^2) + 16\ (1/3)2^{-2b} \qquad (2.20)$$

where the definitions of t and b are the same as in the floating-point error analysis.

The analysis leading up to equations 2.19 and 2.20 assumes that the errors from stage-to-stage are mutually uncorrelated and that the input signal is white. The signal sampled by the ADC is basically a sine wave. It can be shown that, for fixed-point calculations, the output error variance for a sampled sine-wave input is lower than the output error variance of a white input signal when both signals have the same variance. If the ADC digitizes the input sinusoidal signal to values between 1 and -1, then the variance of the input signal can be conservatively used in equations 2.19 and 2.20 as $\sigma_x^2 = 0.5$. The FFT hardware is a 12-bit device; hence $t = 12$ in equations 2.19 and 2.20. The ADC used in the design digitizes the sampled data to 10 bits which sets $b = 10$. Evaluating these expressions gives:

$$\sigma_E^2 = 5.086 \times 10^{-6} \qquad (2.21)$$

$$\sigma_{E'}^2 = 7.069 \times 10^{-5} \qquad (2.22)$$

Note that the output error variance of the fixed-point FFT calculation is one order of magnitude larger than that of the floating-point calculation. This effect was anticipated. The fast fixed-point FFT technique can be used, however, since its error variance meets the system specifications. Experimental results show that the minimum output error is of the same order of magnitude as the error variance. Hence, the maximum output error of 16-point FFT is conservatively expected to have a magnitude of less than 10^{-3}. The output values must be accurately resolved to within 2% of the maximum signal value. The smallest possible value of the maximum output signal will occur when all of the FFT output values are identical. Under this condition, the maximum output signal value is equal to the RMS output signal value which is:

$$X_{rms} = 2^2\sigma_x. \qquad (2.23)$$

Use has been made of the fact that the signal variance grows by a factor of 2 at each stage. Now if all results are to be resolved to within 2% of the maximum output signal, then the error associated with this result must be small enough so as not to obscure a 2% result. A maximum allowable error of 0.4% (i.e., 1/5 of a 2% result) will meet this criteria and is given by:

$$E_{max} = (0.004)X_{rms} = (0.004)2^2(.5) = 8 \times 10^{-3} \qquad (2.24)$$

Note that the maximum allowable error is greater than the maximum error expected.

The error analysis presented only includes the error due to the hardware FFT calculations. Additional error will be introduced from the calculations required by the failure-prediction algorithm. The failure-prediction algorithm is implemented using a 16-bit microprocessor which is much more accurate than the 12-bit FFT hardware. Further, many fewer calculations are required by the failure-prediction algorithm than by the FFT hardware. These two facts can be used to show that the error accrued by the failure-prediction algorithm is insignificant when compared with the error accrued by the FFT calculations.

2.2.4 Summary

The work discussed here shows the feasibility of using a microprocessor constructed with state-of-the-art integrated technology as a compact in-mine tool which can meet the speed and accuracy required for prediction of electrical-component failure. The cost and size of such a system permits its use where a minicomputer system is too bulky, costly, and vulnerable to adverse environmental conditions. Although problems, such as dust in the industrial environment and power regulation, have yet to be fully investigated, it is felt that any problems in system packaging can be overcome with minimal engineering effort.

2.5. REFERENCES

1. Morley, L. A., and J. L. Kohler, "Coal Mine Electrical System Evaluation Volume I - Continuous Monitoring," Annual Report on USBM Grant G0155003, NTIS PB 283 490/AS, Jan. 1977.

2. Morley, L. A., F. C. Trutt, and J. L. Kohler, "Evaluation of Coal Mine Electrical System Safety," Annual Report on USBM Grant G0155003, NTIS PB 80-119514, Jan. 1978.

3. Kiefer, J. A., "An Assessment of Direct-current Mine-power-system Failure Parameters," an unpublished M.S. Thesis, The Pennsylvania State University, University Park, PA, March 1979.

4. Tylavsky, D. J., "A Microprocessor Based Implementation of the Sequential Events Detection, Analysis, and Prediction System," an unpublished M.S. Thesis, The Pennsylvania State University, University Park, PA, Aug. 1978.

5. Kohler, J. L., "Algorithm to Predict Mine-power-system Failures," a Ph.D. Thesis in preparation, The Pennsylvania State University, University Park, PA, (expected completion Spring 1982).

CHAPTER III
BATTERY AND BATTERY-CHARGING SAFETY

3.0. BACKGROUND

The use of battery-powered vehicles has increased rapidly in recent years but, unfortunately, mining accidents involving batteries and chargers have also increased. Included have been several electrocutions, resulting from unsafe handling or faulty design of battery and battery-charging equipment. These problems provided the impetus behind this research into battery and battery-charging safety.

From accident reports, literature research, and communications with regulatory, research, operating, and manufacturing personnel, the following categories were delineated by this organization as the main hazards:

1. charging-station ventilation;
2. battery surface-leakage and ground-fault currents;
3. improper battery-handling practices;
4. defective batteries;
5. activated, unattended battery equipment;
6. battery-enclosure (box and cover) problems;
7. unsafe charger designs; and
8. grounding.

Most of these problems were researched in detail, and the results were reported earlier (see reference 1 and also Appendix I for abstract). Although several suggestions were made, an expanded effort was still needed in battery enclosures, battery chargers, and electrocutions. This chapter gives the final results for these three vital safety areas.

3.1. BATTERY ENCLOSURES

3.1.1. General

As proposed, the scope of work was to define the stresses involved or the withstand needs for underground coal-mine traction-battery enclosures. The principal concerns were possible specifications which might be included in a future Title 30, Code of Federal Regulations, Part 31.110, "Battery Boxes and Batteries." The specific enclosure areas were mechanical strength, insulation, ventilation, drainage, and electrical clearance. The objective was to provide a foundation from which other investigations can develop battery-enclosure requirements and testing procedures.

3.1.2. Current Manufacturing Practice

In order to gain a starting point, it was felt necessary to find the current manufacturing practices. Accordingly, several prominent manufacturers of batteries for underground battery-powered vehicles were consulted concerning the design criteria used in their battery-tray construction. The main reason was to catalog current practice, but the motivation was to discover if they were using any specific standards or tests to insure their design. It was known that such work would likely not define the required stress. However, the results were necessary to relate how present regulations were being met or exceeded and how any defined minimum requirements would affect current practice.

A summary of the consultation is presented in the next few paragraphs. In general, no testing program has been found to exist; either federal regulations or past practice has dictated design.

Tray-top Strength. All manufacturers use USBM Schedule 2G, (see reference 2), as published in Title 30, Code of Federal Regulations, Part 18, for a guide in determining the soundness of the steel used in fabricating the battery boxes (i.e., trays). Paragraph 18.44(a) contains a chart specifying wall thickness for three ranges of battery and tray weight. Because the tops are quite heavy for the larger sized batteries, some manufacturers use a split cover. In certain cases, the manufacturers said that they use a skirt around the cover for rigidity and, in the case of the split covers, some provide support for the split portion. In no cases was it found that testing was performed to determine the design of tray tops (i.e., covers) so they could withstand at least minor roof falls without the top being crushed down on the battery connections.

Tray-top Fasteners. Schedule 2G only requires that covers shall be provided with a means for securing them in a closed position. Each manufacturer has his own method for securing the tray-top, but none questioned had performed tests to determine fastener adequacy. One manufacturer referred to tests required of industrial trucks, Underwriter's Laboratories UL583 or ANSI B56-3-1972. Yet, the stress required by these standards (250 pounds per any one square-foot area) was generally considered inadequate.

Tray-top Insulation. Schedule 2G specifies only that the tray-top "shall be lined with a flame-resistant insulating material, preferably bonded to the inside of the cover unless equivalent protection is provided." There are various methods used for compliance. "Plastisol" is used by some manufacturers, but there is a production application problem. If the top is not properly heated during application, according to certain manufacturers, the "Plastisol" will not adhere well and can be abraded easily. At least one manufacturer uses a 30-mil polyurethane paint. Several others use an epoxy powder which is uniformily applied electrostatically. A discrepancy exists with this type; some considered it not field repairable while others do. Another manufacturer has a tray cover, which is molded thermoplastic resin. The result is a top not only having inherent dielectric, corrosion, and fire-resistant properties, but also being 77% lighter with higher impact resistance than steel. The plastic top has been accepted for use by representatives of MSHA's Division of Coal Mine Health and Safety. It has not, however, been approved by MSHA's Approval and Certification Center. Some manufacturers are advocating total encapsulation of the cell straps and terminals (the so-called "dead-top" battery), and they state that heat dissipation is not a problem.

Ventilation. "Adequate" ventilation is all that is specified in the federal regulations (together with terminal-access prevention). Each manufacturer has provided some means of natural air flow across the top of the battery, and cutouts or louvers are available from 40 to nearly 100% of the periphery of the tray-top. Yet, it has been found that no manufacturer performs tests to determine the percentage of hydrogen present or how such was dissipated. One company did relate their experience with charging batteries, saying that even under an unventilated hood, the hydrogen has a tendency to dissipate. Several stated that the real danger area is hydrogen trapped inside the cells.

Referring to the need to dissipate the hydrogen generated during the charging-cycle end, a manufacturer made a suggestion that a regulation should be written to require a minimum roof height of something like five feet, or whatever is needed, for easy removal of tray covers during charging. When asked about forced ventilation to allow closed covers during charging, the response was that it would be difficult to implement and that it appeared to be not needed. No criteria for this judgement was volunteered.

Drainage. Schedule 2G calls for tray-bottom drainage without specifying size, number, or location. One-inch diameter holes, placed at the cell intersections, are used by most manufacturers. No tests have been made to determine the adequacy of this arrangement.

Clearances. The electrical clearance between bare live parts is not mentioned in Schedule 2G. Manufacturers often refer to ANSI Specification B56.3 (UL583), which supposedly dictates limitations, and ANSI-C1, Article 374-7, "Clearance of Bare Live Parts," which states that a clearance of one-inch shall be maintained between uninsulated current-carrying metal parts and any metal surface (3). One manufacturer said that they use one-half inch as a minimum; it is possible that this might not be sufficient in the event of a badly bent top in combination with a compromised insulation lining.

3.1.3. Discussion of Present Practice

It is obvious in the foregoing that manufacturers closely follow Schedule 2G for their mining-application battery boxes. Some problems with these present regulations, however, have been created through the use of indefinite terms (for instance, "adequately ventilated") and also design specifications instead of performance standards. In this section, insulation, drainage, and clearance requirements for battery boxes will be discussed in light of these problems, present practice, and the possible involved stress or withstand needs. Afterwards, because of the necessary presentation lengths, mechanical strengths and ventilation are given separately.

Insulation. There does not seem to be an apparent difficulty in insulating the inside of the battery box and cover. Yet, after the enclosure goes into service, scratching or abrading the insulating material can defeat its electrical-isolation advantages. Thus, especially for metal covers, some method to verify the scratch and abrasion resistance of any applied insulation is necessary.

American Society of Testing Materials (ASTM) (4) has standards for abrading coatings and insulation but, from past experience, these are considered too general for each specific application. Therefore, the common stresses to which this insulation is exposed should be defined and, using these, a testing procedure developed.

Two likely sources of such scratches and abrasion would be:

1. a cover dropped from about waist high, say four feet, onto the mine floor and

2. the inside of the cover being scraped across the corner of the battery tray.

Application of the first could cause an impact "scratch," chipping the insulation. This could be simulated quite easily, for instance, by taking the maximum weight of a normally handled cover, or 150 lbs, and dropping it from a height of 4.0 ft onto the cover insulation so that a near point loading is obtained. The second stress simulation could also use this same weight magnitude of a force applied (say, through a piece of angle iron) to the cover insulation, having the abrading surface rub back and forth at a specific velocity, a preset number of times. An average removal of once a day, and a common battery life of two years, could be employed to set the maximum number of abrading strokes. Probably, situations could be found that would subject the insulation to more stress, but it is believed that the foregoing would be rather representative.

These thoughts directly apply to vehicles where the cover is completely removed for charging. It might be argued that vehicles which have hinged lids substantually reduce the problem. However, though misuse, even hinged-covers can be exposed to the same scratch and abrasion stresses. Thus, any test procedure should apply to all enclosures.

Drainage. Two items arise about battery-box drainage and the rate of fluid flow that the box must allow (or that the box might be subjected to): electrolyte and cleaning fluids. The accumulation of either within the box can both enhance surface-leakage-current problems and quite possibly lead to a ground fault. One example would be a cracked cell leaking electrolyte, the fault existing from the cell electrodes through the electrolyte to the battery tray or machine frame. Accordingly, a situation that could be input to drainage requirements is the occurrence of rupturing battery cells and allowing for "safe" electrolyte drainage in a specified time. A question arises from this concept however. As such could perhaps create a greater personnel hazard, is it wise to allow electrolyte to leave a battery tray freely? Regardless, cell rupture is not a common situation (although it can happen), but the periodic application of a cleaning fluid (soda wash) is. Drainage must be available for cleaning, and this might be the only requirement necessary.

The usual maintenance recommendation is periodic cleaning with one "bucketfull" of a sodium-bicarbonate solution (sometimes one-half a bucketfull is specified). A common bucket contains 10 quarts. Hence, a drainage requirement could be based on the box being able to drain this volume, which has been evenly distributed over the battery surface with the batteries in place. The drainage should occur within a reasonable period of time (for instance, 5 min.), without accummulation inside the enclosure. Any need for testing beyond this appears to be impractical.

An extensive literature search was made to see if any other country had a performance standard for drainage. None could be uncovered, yet it has been found that Australia employs a design specification similar to the one-inch practice used by most manufacturers just reported (one square inch of drainage area per cell) (5). The criteria behind this specification could not be found. However, design specifications are rather bothersome because of the restrictions they might place on manufacturers, sometimes without improving safety. Drainage-hole size also can be dependent of closed-box ventilation needs, as will be discussed shortly.

Clearance. The main problem for electrical clearance is in the application of uninsulated conductors. The National Electrical Code, Article 374-7, appears more than adequate for any system under 600 V and also seems to be followed closely by the manufacturers. The important portions of this article state that (3):

1. two bare current-carrying metal parts of opposite polarity mounted on the same surface shall be separated by not less than two inches, and

2. the clearance between the bare current-carrying conductor and any metal surface shall be no less than one inch.

Earlier in this chapter, the use of subjective statements has been discouraged. However, clearances are perhaps one area for exception, with the concern being component layout and workmanship. Thus, in addition to the above clearances, a subjective requirement also might be in order. An example statement would be: the layout of batteries, battery cables, and other electrical apparatus within the battery enclosure should be placed so as to minimize the risk of electrical faulting. (Frankly, such might be all that is required in terms of clearance.)

3.1.4. Battery-box Cover Strength

A prime worry when designing a battery box is the strength of the cover. The concern is the amount of deflection which would occur if the cover is deformed. Under external impact, the lid should be strong and rigid enough so it cannot be crushed down on the battery. Such could possibly short out the cell terminals, even though a lining of insulating materials is required.

Cover deformation could result from any of the following:

1. collision of a battery vehicle into a object,
2. collision of a battery vehicle into another vehicle,
3. impact of a battery vehicle into a rib,
4. rib fall on a battery cover, or
5. roof fall on a battery cover.

To obtain the "worst-case" situation would require analyzing all of the above for their quantitative effect on cover deformation. This could be accomplished by obtaining structural-component properties of the battery container (both cover and frame) and of the battery-powered equipment frames. The information, along with the maximum allowable deformations, could be input into the PLASTIC CANOPY program described in the Bureau of Mines IC 8795 (6) or into SAP and Elastic/Plastic SAP as described by Woodward Associates (7). However, the time constraints and available funding for this grant task do not allow for such a detailed study.

Fortunately, a few subjective "facts" about underground-coal-mine openings and vehicles might resolve the likely worst case. With vehicle collisions, the maximum stress would be received by the vehicle frame and only a portion would be transferred to the battery enclosure. Here, buckling of the cover could occur, but direct cover impact is not probable. Battery-box covers are exposed vertically; they are thus very susceptible to rib or roof falls. Because of the mechanics involved, a roof fall will likely contain more energy than a rib fall. Hence, direct dynamic cover loading from a roof fall would probably cause the worst-case stress on a battery-box cover.

The maximum probable roof fall is almost impossible to anticipate or predict. Because of the inevitable uncertainties associated with rock conditions, the best survey for an individual mine cannot accomplish more than just a very crude estimate. Even if methods were available for accurately computing such an event, they would be of little practical value (8). Furthermore, records of roof-fall heights, or of the volume and weight of material displaced, are not kept by mine operators. Only in the case of a fatality is such information available.

Formulae. An alternative is to rely on empirical approximations, specifically those employed to design support for underground openings. The applicable techniques are based on "rock load," the height of the mass of rock which tends to drop out of the roof. If support is inadequate, the rock load drops into the opening by increments whereby the roof assumes, in time, the character of an irregular vault.[1] Here, geological conditions have been found to have a definite input.

Terzaghi (8) has summarized the rock load for each general condition; those parts very applicable to underground coal mining are shown in Table 3.1. Simply, the rock load per condition is related to the opening width, B, and height H_t. As each condition does not have well-defined boundaries, rock load can have a range of values.

Yet, from Terzaghi's formulas, the following has been accepted as a general conservative estimate of rock load for underground openings in the United States (9):

$$H_p = 0.5(B + H_t) \qquad (3.1)$$

where,

H_p = the rock-load height (ft)

B = the width of the underground opening (ft)

H_t = the height of the opening (ft).

This height times the roof-rock density yields a good approximation of rock-load weight per unit area of roof, or

$$W_p = 0.5(B + H_t)\ \rho \qquad (3.2)$$

where,

W_p = the rock-load weight (lbs/ft^2)

ρ = the average roof-rock density (lbs/ft^3)

For stratified rock, ρ is the weighted average depending on bed thickness.

---

[1]It is realized that adequate roof support is mandatory under 30 CFR Part 75. However, the use of roof bolts is generally considered to meet this federal requirement. Unfortunately, even with approved roof-control plans, roof falls have occurred with the bolts in place.

Table 3.1. Rock Load on Roof of an Underground Opening.

Rock Condition	Rock Load, H_p, in feet[1]
1. Hard and Intact	zero
2. Hard Stratified or Schistose[2]	0 to 0.5B
3. Massive, moderately Jointed	0 to 0.25B
4. Moderately Blocky and Seamy	0.25B to $0.35(B + H_t)$
5. Very Blocky and Seamy	$(0.35 \text{ to } 1.10)(B + H_t)$
6. Completely Crushed but Chemically Intact	$1.10(B + H_t)$

[1]Roof of the underground opening is assumed located below the water table. If permanently above the water table, rock load for conditions 4 and 6 can be decreased by 50%. For all conditions, depth of opening must be more than $1.5(B + H_t)$, where B is the opening width and H_t is the height.

[2]Some rock formations contain shale and, in an unweathered state, shales perform like other stratified rocks. However, the term, "shale" is often applied to firmly compacted clay sediments which have not acquired full rock properties. When roof consists of such so-called shale in horizontal layers with sandstone or limestone, the roof pressure may be as high as in very blocky and seamy rock.

Estimated Stress. Applying this concept to underground coal mining, an example roof-rock density for designing mine support is 160 lbs/ft^3. Considering that the typical roof width is 20 ft, the rock load for a seven-foot high room would be

$$W_7 = 0.5(20 + 7)160 = 2160 \text{ lbs/ft}^2$$

and for an eight-foot room

$$W_8 = 0.5(20 + 8)160 = 2240 \text{ lbs/ft}^2.$$

These values can be considered as probable rock loads per square foot of roof area that are available for "worst-case" roof falls. Obviously, a greater room height (and also width) will give larger values, but cuts greater than eight feet are seldom taken. However, some Western U.S. operations take 12-foot or higher cuts on development.

To use these rock loads in terms of a required cover strength, the available potential energy must be considered. With conservation of energy, this would be converted into the kinetic energy that is transmitted to the battery cover. Perhaps the maximum energy for cover impact would be when an enclosure is resting on the mine floor (say the battery on charge, separated from the vehicle). If a battery-box height of 24 in. is taken, then two feet must be substracted from the room height. The energy involved in the roof fall is then for the seven-foot room

$$W_7 = 2160 \text{ lbs/ft}^2, \ Y_{drop} = 5 \text{ ft.}$$

$$PE_7 = 10{,}800 \text{ ft-lbs/ft}^2$$

where,

PE = the roof-fall potential energy per unit area of roof,

for the eight-foot room

$$W_8 = 2240 \text{ lbs/ft}^2, \ Y_{drop} = 6 \text{ ft}$$

$$PE_8 = 13{,}440 \text{ ft-lbs/ft}^2.$$

Interestingly, a common engineering response in industry to the question of roof-fall intensity is "a ton of rock dropping five feet."

An additional thought needs to be made about the volume of roof rock which could be critical in cover strength. Impact of the rock mass at a point should provide maximum cover deflection. The worst condition may be the deformation that occurs when one rock in the fall hits the center of the cover. Yet, turning of a block of rock during a fall, so a corner hits the cover, will probably result in lower cover stress. Further, rock often descends during a fall with little turning, coming down horizontally oriented with the roof. Thus, in "worst-case" terms, the shape of the falling mass would be that of a rectangular column, the height being defined by the rock load. So the cover sides do not restrict cover deflection, the other two rock-column dimensions would be defined by the maximum battery-box inside dimensions (or the unsupported portion of the cover, usually a rectangle). The rock-column weight should impact at a point, symmetrically centered with the cover. To find the largest single-cover dimensions, battery-manufacturer specifications must be consulted.

Comments. These rock loads, drop distances, and energies (or just the concepts involved) should provide the necessary background for determining battery-box strengths, especially that of the cover. However, a caution should again be made about the uncertainty of roof falls. The values given here cover unsupported roof conditions under typical mining conditions, thus they conservatively relate to roof falls when roof support fails. There could exist a situation where these could be exceeded, and an example might be a fall in a previously caved area. However, it is highly unlikely that battery equipment, let alone a charging station, would be placed under such unstable roof conditions for extended periods.

Because of the uncertainty involved in quantitatively predicting roof falls, additional research may be called for. An avenue might be through questionnaire or interview with mine operators and by examination of MSHA accident-investigation reports. Here, the forces imposed on structures from roof and rib falls (note, the force is not vertical in the rib-fall case) might be further clarified or even determined. If successful, such could verify the preceding calculations. Regardless, these computations are based on sound underground-opening design criteria.

Woodward Associates (7), under Bureau of Mines Contract J0357110, has performed a survey similar to that suggested above for rock falls in underground metal mines. Roof (back) and rib conditions in these mines are typically much different than that in underground coal, but the numbers they developed are informative:

1. number of falls analyzed, 138;

2. median fall distance, 10 ft.;

3. mean fall distance, 13.7 ft.;

4. median fall weight, 12,460 lbs;

5. mean fall weight, 20,760 lbs;

6. median protection level (energy), 46,560 ft-lbs; and

7. fatalities--only median protection level, 21,975 ft-lbs.

They found that 70% of rock falls produced kinetic-energy levels less than 50,000 ft-lbs and 40,000 ft-lbs will protect for 55 to 65% of rock falls. These values are very comparable with the energies previously computed (for a seven-foot high room, 50,000 ft-lbs would be available with a 4.63 ft^2 fall area, with 3.72 ft^2 of area for the eight-foot room).

Some other comments need stating. First, it is recommended that individuals developing standards and testing procedures for battery-enclosure strength (using this or any information) should read references 6, 7, 10, and 11. They not only contain siginficant information related to this area but also include some possibly applicable performance standards. Next, a dynamic test is obviously more realistic, but a static test may be acceptable. The latter is actually more desirable since dynamic procedures are often destructive and, therefore, expensive. It is very likely that, if a static test is selected, the dynamic situation can be simulated with a computer, perhaps using existing programs (e.g., reference 6). Finally, the resulting test procedure should be compared with the capabilities of present covers to assess its practicability.

3.1.5. Battery-box Ventilation

General. The ventilation of a traction-battery enclosure includes two areas, during charging and during discharge; the problem is the maintenance of hydrogen safety below its lower explosive limit. Federal-regulations (12) require that battery-box covers be removed while charging. With proper charging-room ventilation and the cover removed, hydrogen concentrations are definitely no hazard (1). However, following the charge cycle, the covers are closed, and the vehicle is placed in service. From chemical reactions and entrapped gas within the cells, lead-acid batteries continue to emit gas for several hours after receiving a charge, be they open circuited or on discharge (13). Considering the ignitability of hydrogen, there is a possibility of a dangerous air mixture accumulating. Hence, the safety worry here is adequate ventilation for the evolved hydrogen in a closed box while the battery is not on charge. Fortunately, the U.S. Department of Defense (Navy) and the United Kingdom have performed considerable work in this area; the results are likely adequate enough to employ as a basis for closed-box ventilation requirements.

United Kingdom Effort. Prior to 1945, there was little mention in the literature of possible gas emissions from lead-acid batteries during discharge. In fact, many early publications stated that there were no emissions under normal conditions (14). This thinking was also extended to early battery applications in U.S. underground mines (15).

As reported by Robinson (13), this gas-generation question, however, received much attention from authorities responsible for high-capacity battery installations in confined spaces, such as on submarines. He related a report stating that lead-acid batteries in these locations are always able to emit considerable quantities of hydrogen and oxygen for the first few hours after charge (16). Although actual quantities varied greatly from battery to battery, an 80-Ah cell, standing idle at 80°F (26.7°C) with 1.26 specific-gravity electrolyte, would probably emit 5 to 20 ml of hydrogen per hour for about 12 hours after charge. The approximate rate was found to be:

1. directly proportional to the battery capacity,

2. doubled for each 15°F (9.5°C) rise in temperature, and

3. doubled for each 0.050 unit increase in electrolyte density.

As a result of antimony contamination of the negative plates, the open-circuit emission also increased with cell age. Upon discharge, additional hydrogen was evolved from the negative plates (thought to be a release of entrapped gas during charging). Combining the open-circuit and discharge emissions on a worst-case basis, it was postulated that a lead-acid battery cell, at the end of its useful life, could release up to 500 ml (about 0.2 ft^3) of hydrogen per hour.

An advisory committee on coal mining was formed in the United Kingdom during the mid 1940's, and part of its effort was to investigate underground battery vehicles (17). Realizing the hydrogen-generation problem on discharge, the committee recommended that traction-battery enclosures be properly ventilated to prevent a hazardous accumulation. Accordingly, a regulation was promulgated in 1949 (18). (For the U.S., Bureau of Mines Schedule 2G instituted a similar requirement stating that "battery boxes shall be adequately ventilated" (2).)

Test Procedure. During 1946 and 1947, Robinson (13) performed research on hydrogen concentrations for battery discharge with the outcome being a test for hydrogen accumulation in battery boxes. The test procedure was made statutory for the United Kingdom in 1949 by the then Ministry of Fuel and Power (now the Department of Energy) (19).

The salient test conditions are as follows.

1. Hydrogen generation is calculated at 3.0 ft^3/hr per 25,000 cell-Ah.

2. Tests are made in still air.

3. Maximum hydrogen concentration within the box under these conditions must not exceed 2.0% with tolerance.

Robinson states that the emission calculations assume that all factors which contribute to the hydrogen-emission rate (i.e., cell temperature, acid specific gravity, and discharge rate) are simultaneously at worst case. Still air is selected to simulate the vehicle traveling at the same velocity as mine ventilation, thereby the container natural ventilation receives no assistance. The maximum concentration provides a safety factor of 2.0 from the lower flammable level of hydrogen (4.0%).

Other aspects of the U.K. test procedure include (19).

1. Dummy batteries (closed boxes) take the place of, and have the same volume as, the actual batteries.

2. Hydrogen is fed into the unoccupied space at the above calculated rate and is suitably distributed over the whole area.

3. Hydrogen-air-mixture samples are withdrawn from the air space at intervals of about one hour, and the hydrogen concentrations ascertained.

4. Usually, four series of tests are made, each of approximately six-hours duration, but the duration and number of samples are at the testing officer's discretion.

5. The enclosure ventilation is considered adequate if the mean value of the hydrogen concentration does not exceed 2.0% plus a tolerance. The tolerance is determined by the number of samples taken and by the standard deviation of the results.

6. The ventilation tests are performed in a chamber that is substantially free from drafts.

7. The venting is checked to insure it excludes falling water and so the vents are unlikely to become choked with dirt.

Robinson also researched simple arrangements of container vents that would provide sufficient natural ventilation to meet these ventilation requirements. He used the fact that hydrogen has the highest coefficient of diffusion into air of any gas and, from its extreme mobility, it is very difficult to retain within a leaky enclosure. The investigation used a simulated battery box, containing a dummy 56-cell, 288-Ah lead-acid traction battery. Hydrogen liberation for discharge was calculated at 2.0 ft^3/hr (by the foregoing relationship). While hydrogen was pumped in at this steady rate, hydrogen concentrations were measured in the space between the battery top and cover (volume of 6.1 ft^3). Eleven different venting arrangements in the enclosure top were used, ranging from 40 to 140 in^2, and sealed top vents were also investigated. End-plate venting was available in all tests and consisted of six 2-1/4-inch diameter holes (covered with a protective grid). The test period for all experiments spanned seven hours.

Robinson's findings were as follows.

1. Equilibrium between the battery rate of hydrogen emission and rate of hydrogen escape through the vents was established within one hour after each test commenced. Afterwards, the hydrogen concentration remained almost constant.

2. Maximum concentrations with natural top venting ranged from 1.3% to 2.8%, inversely with vent area, following a near logrithmic curve.

3. When the top vents were sealed and the side vents open, hydrogen concentration rose sharply to 5.3% obtaining 4.2% in 8.0 min. However, with 31 cfm of forced ventilation through the side vents, the 5.3% maximum dropped to 1.7% hydrogen. He hypothesized that normal haulage speeds and mine-ventilation flow rates would create a high factor of safety.

Robinson's overall conclusion was that a battery box could be readily vented to meet the British requirements. Forced ventilation was not needed.

Higher Hydrogen Emission Rates. Titman (21) studied lead-acid-battery gas emissions for the period of 45 minutes after charging (he earlier did a similar study for alkaline cells). The impetus behind the work was a knowledge that gas-emission rates from a battery immediately after charge might be greater than that (later emitted) after a standing period. Titman also investigated the parameters causing emission variations, mainly acid strength, discharge rate, and increased cell temperature. The experiments employed a new 6-V, 309-Ah traction battery. The research conclusions were.

1. Total gas emission for similar cells varied as much as 15%.

2. Hydrogen emission rate doubled for an increase of 0.050 in acid specific gravity (1.260 to 1.360). (Note: this increase could easily happen if a battery electrolyte is not topped up (20).)

3. The rate doubled for a 12.5°C increase in electrolyte temperature.

4. Overall rates were on the same order as for alkaline cells.

5. Immediately after charging, hydrogen rates up to 5.0 l/hr per cell were observed (corresponding to 14.30 ft^3/hr per 25,000 cell-Ah).

6. After 45 min, the cells were found to liberate as much as 1.3 l/hr per cell (3.72 ft^3/hr per 25,000 cell-Ah).

7. The minimum emission rate was always reached within 5.0 to 8.0 minutes standing after charging.

As can be seen, the findings for specific gravity were similar to that previously stated. However, hydrogen emission rates were considerably in excess of the 3.0 ft^3/hr testing standard: 376% higher immediately after charging, and 24% higher after a brief standing period.

Using these emission rates as a basis, Titman (22) further investigated the effect of high hydrogen rates in relation to typical battery-box ventilation. The enclosure was basically the same as used by Robinson (13). The findings included.

1. A 2.0% hydrogen concentration was not exceeded until the emission rate was ten times the 3.0 ft^3/hr standard rate.

2. After one-half hour, the hydrogen became uniformly distributed with no tendency to accumulate at a specific place.

3. For hydrogen concentrations of 2.0% or less, the enclosure concentration varied as the 2/3 power of the emission rate. (This was also verfied theoretically.)

4. With the high emission rates, acid-drain holes assisted enclosure ventilation.

Titman also provided a detailed description with illustrations of the hydrogen feed and collection apparatus.

Comments. It would seem that any test standard should consider the higher rates observed and used by Titman. After charging, it does take a reasonable amount of time for disconnecting the charger cable and replacing the cover. Noting that the minimum emission rates were obtained within 8.0 minutes after charging, the lower rate of about 3.75 ft^3/hr per 25,000 cell-Ah seems reasonable for testing. The balance of the U.K. procedure could be adopted almost directly. Interestly, however, it appears as the United Kingdom has not made any adjustments in their original battery-box ventilation testing schedule (19). Regardless, if this standard were to be employed in the United States, correlation would first need to be made with Title 30, CFR, Section 75.301-5, which restricts the maximum concentration of hydrogen to 0.8 volume percentum.

A direct comparison of hydrogen emission rates versus the top venting area of the enclosure would be advantageous. Yet, no direct relationship has been found (13). In practice, however, it has been discovered that about 25 in^2 of top vent area will allow 1.0 ft^3 of hydrogen to escape per hour, while meeting the United Kingdom testing requirements (20, 23).

Catalytic battery caps have been discussed in the earlier report (1), and one the their principal advantages should again be stated. By converting any emitted hydrogen and oxygen back into water, they prevent the escape of hydrogen from the cells (24). Accordingly, no tray ventilation is required, whether the battery is on charge or discharge. A problem with these caps, however, is that the palladium catalyst may be destroyed if the cap is turned over, say during maintenance.

Although not yet mentioned directly, there is an ever present hazard when using lead-acid batteries in any environment: an explosive hydrogen-air mixture can always be available inside the cell. (This is true even with catalytic caps.) If ignition energy is sufficient within the cells, or even close to the vent cap, the internal mixture can explode, possibly spraying acid and blowing bits of the cover towards personnel in the vicinity. Internal faults can produce this kind of explosion. Virr and Pearson (25) relate that a common source of such events also occurs when electrolyte leaks from a cracked cell producing a spark when the acid level falls below the bottom of the plates. There is no known method of preventing nor suppressing these internally initiated cell explosions. However, ground-fault protection which is discussed in the next chapter section, will detect electrolyte leakage.

3.2. BATTERY-CHARGER DEMONSTRATION

3.2.1. Personnel Hazards

One of the primary objectives of this research is to clearly define what is required in underground coal mining to prevent electrocutions on battery-powered systems. To arrive at such recommendations, the involved personnel hazards must be pinpointed.

As covered in a past report (1), the two most outstanding contributions to mine-charger accidents and electrocutions have been poor grounding and component failure (most seriously the power transformer), causing the a-c source power to be impressed on the d-c charging circuit. For instance, the charging circuit must be isolated from ground (the safety reasons will be discussed later). Thus, a primary-to-secondary power-transformer fault can elevate the charging circuit by the primary potential. If this is coupled with a fault which energizes a battery tray and grounding is unsatisfactory, the battery tray presents a shock hazard. The serious situation is grounding, because an intact ground system insures that frame potentials do not exceed reasonably safe levels, regardless of what other factors contributed to the hazardous condition. Obviously, a paramount hazard always exists when personnel are exposed to live conductors, irrespective of grounding.

From accident analyses (26) and input from operators, manufacturers, and state and federal regulatory agencies, the rash of other problems causing such accidents has included:

1. bad charging-cable insulation;

2. unconnected, exposed charging couplers (plugs) still energized;

3. charging couplers designed to allow cable damage and also having exposed ungrounded metal parts where the cables are attached;

4. charging couplers being damaged frequently or maintained inadequately, thereby causing poor contact;

5. battery surface leakage and internal faults;

6. no overcurrent protection for the a-c power input;

7. faults causing the control circuitry and components to have an elevated potential;

8. connecting a charger to a battery of wrong polarity;

9. repair work performed by unauthorized personnel; and

10. charging stations in abnormally wet locations.

An initial listing of safety features, which hopefully would eliminate charger electrocutions from these sources, was presented earlier (1). (Note: the statements, referring to battery-charger design contained there, were interim in nature.) Part of the present study involved the specification, purchase, and in-mine demonstration of a battery charger, containing as many of these recommendations as possible. The rest of the section will discuss the charger as well as the demonstration results.

Adhering to the scope of work, the suggestions and discussions contained in this and the subsequent sections apply directly to a-c to d-c chargers. However, many comments also relate to d-c to d-c charging systems.

3.2.2. Demonstration-charger Features

For clarity and to use as an argument basis, the following is the original list of recommended charger features:

1. The charger input cable should contain a monitored ground to insure that the charger frame remains at ground potential.

2. The charger should be equipped with panel interlocks which de-energize the charger at the outby source when access panels are removed.

3. The charger should have an emergency-off switch located in a conspicuous place on the charger frame. This switch should not be spring-loaded, thus requiring resetting after use.

4. The charger frame should be coated with an insulating material on the inside and outside. Such a requirement is not absolutely necessary if the frame is connected to a monitored grounding conductor from its power source.

5. The power transformer should be of the cast-core type with epoxy filler between the core and primary coil and between the primary and secondary coils; otherwise, there should be a grounded metallic shield between the primary and secondary windings (the Faraday shielding is preferred).

6. The power transformer should have transient overvoltage protection.

7. The power transformer secondary and all d-c components should be isolated from the system ground.

8. The charger should be equipped with a ground-check monitor which insures that the battery box remains at ground potential.

9. The d-c connection between the charger and battery box should consist of a single cable with appropriate ground and ground-check conductors.

10. The d-c couplers should be of the type which interrupt the ground-check circuit before the charging circuit.

11. Any semiconductor rectifier, charge rate control, or timer circuitry should be protected against transient overvoltages.

12. The power rectifiers should have protective overtemperature relays.

13. The charger should have overcurrent protection on both the input and output.

14. The charger should have a meter or similar device which indicates the state of battery charge.

15. The charger should contain circuitry which prevents a battery of the wrong voltage from being charged; otherwise, keyed battery couplers should be employed.

16. The charger should contain battery surface-leakage detection circuitry which prevents a leaky battery from being charged.

17. The charger time circuitry should operate in a failsafe manner to prevent battery overcharge.

Figure 3.1 is an one-line diagram of a typical solid-state-controlled taper-rate charger. All the desired electrical components specified by the above list are signified by the letters in parenthesis. The following description will cover each of these safety features; the outcome will be a specific way they can be included in the demonstration charger. It should be noted, however, that other practical methods of personnel protection might be available in some instances. These alternatives are discussed in the chapter section on electrocutions.

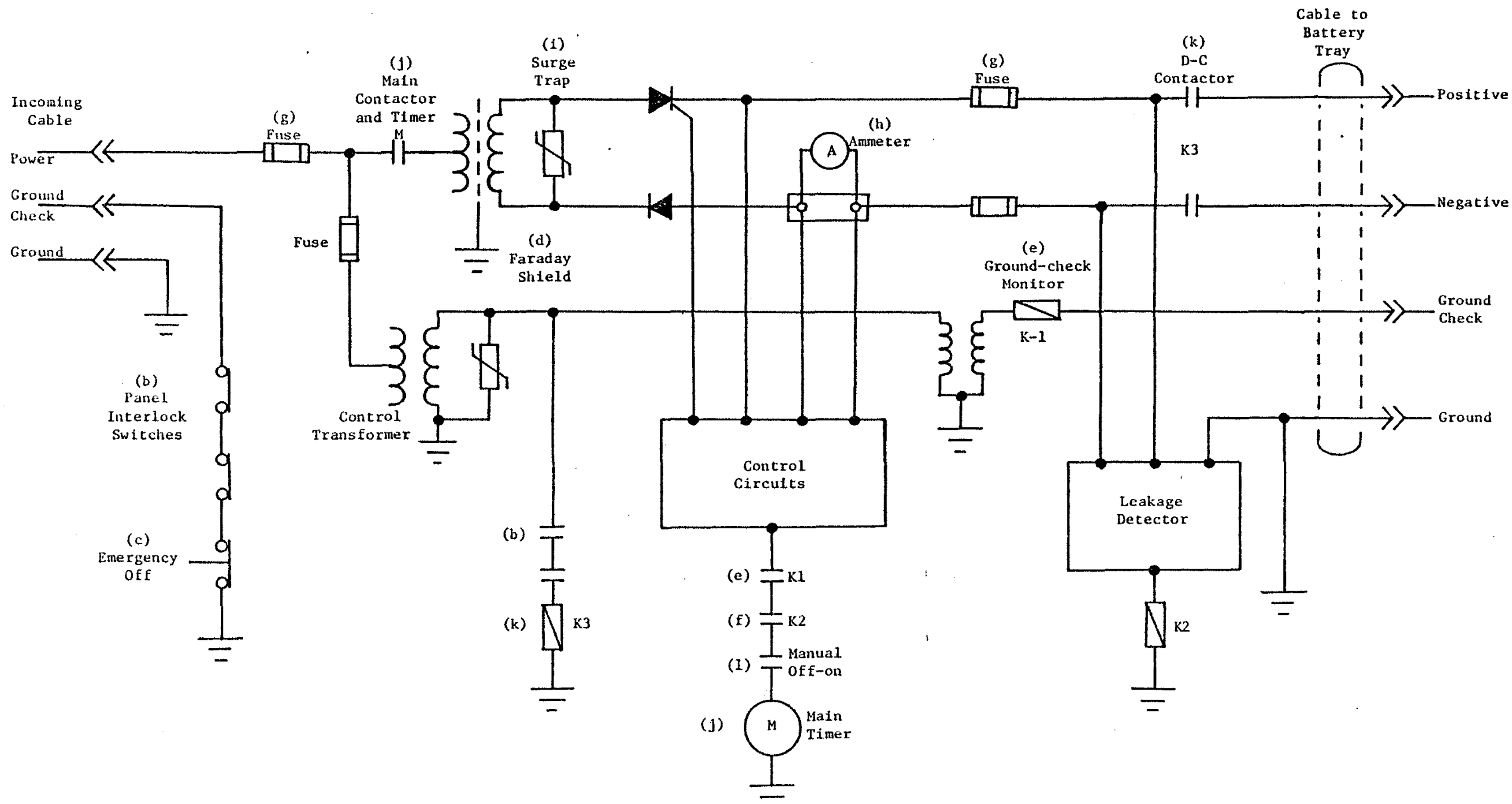

Figure 3.1. One-line diagram of desired charger features.

Items 1, 2, and 3. Because of the a-c to d-c application, the charger is considered portable electrical equipment, being fed by a resistance-grounded, low- or medium-voltage a-c system. Hence, under Title 30, Code of Federal Regulations, Sections 75.901 and 75.902, a grounding conductor and ground-check monitoring of this grounding conductor are required between the power source (usually a load center) and the charger frame (8). The portion of the ground-check circuit within the charger is indicated at (a). In series with the ground-check circuit are shown the panel interlock switches (b) and the emergency-off switch (c). Here, a pilot-type monitor is implied. If the circuit is opened in any manner, the circuit breaker at the source, through which source power is supplied, is tripped. Afterwhich, the circuit breaker must be manually reset at the source and cannot be reset until the ground-check circuit is restored.

The main reason behind the panel interlock switches is so unauthorized (or even authorized) personnel cannot unknowingly contact live parts inside the charger. The emergency stop, also termed "emergency off" or "panic button," can provide definite safety advantages. In case of an emergency, it provides a quick power stoppage at the charger. Without the switch, a miner must go back to the load center, which may be as far as 500 ft away. To assist use, the switch has a large red button; pushing the button breaks the outby ground-monitor circuit. The button must be manually pulled out before the outby circuit breaker can be reset. The switch thereby enables a double check on re-energization. This especially helps protect maintenance personnel from having their dangered-off power restored while they are still working.

Item 5. A Faraday shield is indicated at (d) and prevents primary-to-secondary (interwinding) faults in the power transformer. The shield also has a secondary benefit of isolating any high frequencies on the incoming power from the charger where they could interfere with the control circuitry. Additionally, if the amplitude is high enough, these can destroy solid-state devices. From an economic standpoint, the Faraday-shield transformer construction is preferable to the cast-coil construction. It provides, and likely exceeds, the desired safety feature of secondary-circuit isolation.

Items 9, 10, and 15. The cable(s) used to charge the batteries is a two-conductor type G-GC, containing grounding and ground-check conductors as well as the two charging power conductors. The battery-tray couplers have four pins to accommodate the cable and have grounded-metallic shells. The lengths of the coupler contacts are such that upon insertion into its receptacle, the ground connection is completed first, the charging conductors second, and the ground-check last. To prevent charging a battery with excessive voltage, the couplers are keyed with each battery voltage having its own distinctive key.

The grounding and ground-check conductors are grounded on separate welded studs inside the battery tray. If only one stud was used and knocked loose, the ground-check circuit could be intact but with the battery tray ungrounded.

Item 8. The ground-check circuit is designated by (e) and has the purpose of monitoring the grounding connections to the battery tray. One such circuit is provided for each battery on charge. The monitor shown is a simple current-sensing pilot-type (or loop). If the loop formed by the charger-cable grounding and ground-check conductors, the coupler contacts, and the battery-tray grounding studs is opened, relay K1 will be de-energized, tripping the charging power with contactor K3. A serious problem with ground-check monitoring on battery-charging systems is the abundant possibilities of parallel grounding paths. Thus, for this and other reasons, the monitor must be able to meet all MSHA guidelines for low-voltage power systems (27).

Item 16. The charging power is also being tripped if the leakage-detector circuit (f) senses surface-leakage or a ground-fault from the battery to the tray. Following work performed by Virr and Pearson (28) in the United Kingdom, a total battery-leakage resistance threshold of 1000 Ω has been selected. The value should not present nuisance-tripping problems caused by relaying which is too sensitive but should substantially reduce the gas-ignition and electrical-shock hazards created by such faulting.

Items 6 and 11. Transient-overvoltage conditions on mine power systems by switching or, in some cases, lightning apply large electrical stresses to power-transformer insulation. To protect the transformer, and thereby provide backup for the personnel protection given by the Faraday shield, the transformer insulation should be able to withstand peak of five times the nominal peak line voltage. Ventilated dry-type transformers designed to IEEE Standard 462-1973 (see reference 29) have a 10-kV, BIL, which is well within the transformer transient-protection needs. Accordingly, the voltage ratings of all other charger components are coordinated with the maximum anticipated overvoltage. The transformer secondary, and thus all circuits connected to it (rectifiers, charge-rate control, and timer circuitry) are further protected from transients by metal-oxide varistors (i).

Item 4. Electrocutions involving contact with the charger frame have taken place when grounding practices were unsatisfactory and a fault existed between the frame and some charger internal component. One idea of preventing this type of hazard would be to completely isolate the enclosure from possible contact with live circuits by using an insulation coating. This was the thinking behind the statement in Item 4.

There are several shortcomings of protection through isolation coatings of the charger enclosure. Most battery chargers, designed for underground use, are mounted on skids for practical mobility. In rough mine use, any insulation, especially on the skids, would be quickly worn off. Further, isolation coatings would be difficult to apply everywhere. Devices mounted to the cabinet would have to be coated for 100% protection. Such would create a problem of bonding all parts together and bonding components like timers and switches to the exposed panels. In addition, any insulating compound deteriorates with time.

Thus, any coating requirement might be unpractical and also could result in a false sense of security. Enforcement of present enclosure grounding regulations is a more effective safety approach.

Item 7. Completely isolating the transformer secondary and d-c charging circuitry from ground is mainly projected at preventing shock hazards caused by charger-battery grounding problems. With either polarity grounded, a low-impedance source of d-c voltage between the frame of the vehicle being charged and the ungrounded battery side is provided. A person touching the vehicle frame and any battery intercell connector could receive a d-c shock of, for instance, 80 V. The same would be true for anyone standing on a wet mine floor and touching any ungrounded terminal connected to the charging circuitry. Grounding the positive or negative charger terminal also promotes excessive corrosion of the battery tray.

Items 12 and 13. As indicated previously (1), the need for overtemperature relays (item 12) was projected at equipment protection, but the main objective was to insure that a failed diode did not create a personnel hazard. Frankly, if the charger is designed so a recifier failure does not cause a hazard, no such protection is necessary. For example, proper fusing (g) alone can provide this safety by removing the charger from the a-c line as well as blowing the d-c fuse if a power-rectifier device fails. Furthermore, the same fusing can protect against excessive currents (both overload and short circuit) which are outside the domain of the charger control circuitry.

Item 14. An ammeter (h) is provided so it can be determined, at a given time, what part of the charge cycle the system is operating in. Strictly speaking, this is not a safety feature, but having some idea of the status of the charge cycle is an aid to good operating procedures which in turn can contribute to safety.

Item 17. The last of the original desired features is a fail-safe means of preventing overcharge. The principal goal here is to protect against excessive battery gassing and, as a first line of defense, almost all manufacturers use timing circuitry to substantially reduce charging current through the last part of the charge cycle. However, there are common occurrences that call for additional protection. For instance, consider that during charging, the charge cycle is interrupted, say by a charger component failure, a power failure, or someone disconnecting the charger from the batteries and then reconnecting them. The bad component could cause the charger to continue the charge at the starting rate for an indefinite period. In the last two cases, the main timing circuitry could reset to zero, an unknowing individual might manually restart the charger for a full charge cycle. Considering the real world, a "fail-safe" timer would need to de-energize the charger with any failure mode that could lead to overcharge, many of which are perceivably beyond the control of practical timing circuits. Thus, a more reasonable safety requirement is that the charger time circuitry operate in a manner to minimize battery overcharge as much as practical.

One means of affording the necessary extra protection is to have a redundant timing device that overrides the main timing circuitry to shut the charger down after a set period. The timer (j) in the one-line diagram performs this function. Its d-c motor is tied to the charging power; having an automatic-reset capability, the timer de-energizes the charger (a maximum of) 11 operational hours after its initial setting.

Additional Features. When receiving all of the original features just discussed, some additional desires become apparent. One of these is a contactor (k) for both the positive and negative outgoing conductors, located near the point where charging power leaves the enclosure. The intent is to remove battery power from any uninsulated component within the enclosure if the charger is opened and the charging cable is still connected. Accordingly, the contactor is tripped anytime the a-c ground-check circuit is broken. Because the contactor load contacts might still be energized upon entry, the device should have a protective cover with a warning notice.

There have been many instances where charging couplers have been removed during the charge cycle, the charger not turned off, and the energized plug left on the mine floor, at times laying in water. The d-c ground-check circuit desired by Item 8 will prevent this condition as well as any arcing which might be encountered on plug removal. However, as a backup to power tripping, it would be advantageous to also have the manual on-off device simultaneously reset to off. This could be a simple switch tripped by the d-c ground-check monitor (component "l" in Figure 3.1) or a manual timer that is capable of being automatically reset to zero. Automatic resetting of either device type (for example, when the battery plug and receptacle are re-engaged) is unadvisable so manual resetting is required. Such necessitates a deliberate act by the user before the charger can be energized, as an automatic restart could pose a hazard to the unwary miner.

Unless prevented, another very serious (and quite obvious) hazard can occur if an energized charger is connected to a battery of wrong polarity. Therefore, control circuitry must be able to sense the wrong polarity condition and not allow energization of charging power.

3.2.3. In-mine Demonstration

Charger Specifications. After investigating chargers made by several manufacturers, selecting a mine for testing the charger, and considering the research time frame, it was decided that a modified Kersey Model SSC64-3-180 Dynacharger would meet the needs of the project. This manufacturer agreed to make all necessary changes in their standard charger at the unmodified price, thereby effectively underwriting the cost of the modifications. (It should be noted that reference to a specific manufacturer must not be interpreted as an endorsement by either the Department of Interior's Bureau of Mines or The Pennsylvania State University.)

The demonstration charger contained all of the desired safety features with just two exceptions. The first, however, was almost as originally perceived. The manufacturer's standard override timer acted both as a safety device to prevent excessive battery gassing but also as the charger off-on switch, being manually accessible from outside the charger enclosure. Hence, upon interruption of the charging cycle, its d-c timing (drive) motor would stop, restarting after the disturbance was corrected and automatically resuming the charging cycle. The timer was modified such that it would reset to zero upon charge-cycle interruption; manual resetting was required. This combined the action of components "j" and "l" of Figure 3.1. Practical overcharge protection was still available, as automatic charger shutdown would still occur after the manually preset time. (The manufacturer recommended one hour longer than the expected recharge time, 12 hours maximum for an equalizing charge.) The second exception was the battery leakage-detector circuitry. Prototypes were found to be in use in the United Kingdom (e.g., reference 28), but this development was in too early of a stage to obtain a device or even complete plans (25). However, an Australian device, similar to that described by Virr and Pearson (28), was found suitable and in use in their mines. A unit was ordered, yet delivery was not made during the project.

Charger Test Site. An Indiana County, Pennsylvania, underground coal mine was selected for the demonstration. The mining method was retreat longwall, and the vehicles to be serviced were two exceptionally large scoop-tractors, having 990-Ah capacity batteries.

The charging-station room was that previously used to charge the scoop batteries, and a sketch has been provided in Figure 3.2. Room dimensions were approximately 55-inches high, 14-feet wide, and 40-feet deep. A cinder-block wall sealed the room from the return airway, and room ventilation was provided by bleeding fresh air from the entry through a four-by-eight-inch hole in the wall about three feet above the floor. Corregated galvanized sheet was used to fireproof the ribs. The mine could be considered wet, leaving standing water in several haulage-entry areas, but the charging station had a dry floor.

Installation. The demonstration charger was delivered to the mine near the end of October, 1977. Shortly after delivery, the unit was examined by Pennsylvania Department of Environmental Resources, Office of Deep Mine Safety, inspectors, and all features met with their approval. (Note: this approval is required on all electrical equipment in Pennsylvania before it is allowed underground.) The charger was taken underground and placed in the charging station. At the time of installation, the location was about 4000 feet from the longwall, which was advancing toward the station. Three-phase, 440-V power was obtained from a belt transformer around 400 feet away.

The four-conductor charging couplers used (two pins for ground-check monitoring and grounding) were specially made by the charger manufacturer employing handmade parts and teflon insulation. These prototypes were certified permissible by MESA (now MSHA) Approval and

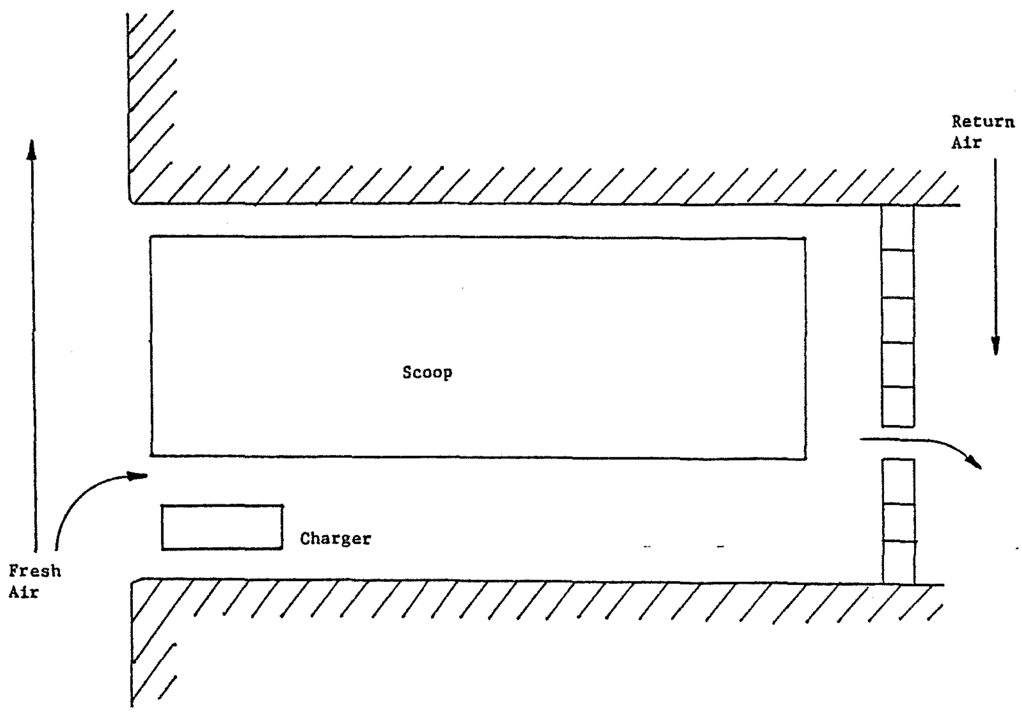

Figure 3.2. Plan View of Charging-Station Layout.

Certification and also accepted by Pennsylvania. Only two receptacle-plug combinations could be made and, as the scoop used two separate battery trays, this meant that just one scoop could be serviced.

Two grounding studs, one each for the grounding and ground-check conductors, were welded inside each tray of the scoop. After the couplers were installed in the tray dog houses and the conductors connected, the scoop was driven to the charging station, and the two charging cables were attached. An extensive series of tests were then performed to insure that all new safety as well as the manufacturer's original features were operating. Each was found to function properly.

The scoop batteries had 22% larger ampere-hour capacity than would normally be used with the charger. This was determined to be no problem in providing a proper charge because the charger was designed to stay on the 20% constant-current part of the charge cycle until the cell voltage reached 2.36 V regardless of the battery size.

Results. The charger received normal daily use for a period of about eight months, averaging one charge cycle per day. Two of these months were before the long UMWA strike in early 1978, through which the charger remained underground (idle), and the remainder (six months) after the strike was settled.

The only technical problem found during the test period did not involve the additional safety features and occurred immediately after the demonstration commenced. Here, routine use revealed erratic operation in the charge cycle. This was found to be caused by a loose knob on the override timer. Once it was tightened and the charging period extended to 9.5 hours to compensate for the oversized battery capacity, the charger functioned in an entirely satisfactory manner.

Periodic checks throughout the rest of the test period verified correct operation of all safety features. For one aspect the result was surprizing. The ground-check monitors for the d-c charging circuits were a simple loop type with potential relays. As mentioned earlier, generally, the correct operation of these can be easily negated by parallel grounding paths to the grounding conductor. Aware of the situation and realizing that parallel ground paths can be abundant in battery-charging systems, the researchers were ready, if problems occurred, to immediately change out the original monitors to a model sensitive to only the grounding conductors. As satisfactory operation continued, the change was not made. Perhaps, the only saving grace was that the batteries were always charged on the vehicle, and its rubber tires possibly blocked ground paths through the mine floor.

The demonstration success proves that a safer battery charger for underground coal-mine use is feasible. Considering the extent of necessary circuitry charges over what can be used now, this is very encouraging. The ramifications of the demonstration and the safety features which were used will be discussed in the next chapter section.

3.3. ELECTROCUTIONS

3.3.1. General

The effort under the Electrocutions Task was to clearly define what is required in underground coal mining to prevent electrocutions on battery-powered systems. As stated in the proposal, this work was intimately tied to the battery-charger effort just covered and would draw heavily on past findings (1) on hazard areas. The objective was to detail everything that is needed within a charging station or on battery-powered equipment. The principal direction was safety to personnel, but practicality was to be maintained.

Every safety feature that was originally recommended (1) has already received extensive discussion in the preceding section. Yet, considering the results of the in-mine demonstration, as well as safe electrical practice, some additional comments are necessary. This discussion follows. Afterwards, as all input will be covered, the final project recommendations will be listed.

3.3.2. Discussion of Original Features

Interlock Switches. Interlock switches were provided on all access doors, panels, and lids of the demonstration charger so personnel would not unknowingly contact live parts. A justifiable complaint against using these is that they must be defeated for maintenance and may be left in that condition, rendering the system dangerous from a false sense of security. However, experience on other mine power equipment that require panel interlocks has shown that these safety devices rarely remain in a defeated condition. The interlocks on the demonstration charger also presented no problem. Frankly, any protection system knowingly or unknowingly can be rendered useless, and it is the responsibility of training to make sure this is minimized. Notwithstanding, there are other available ways to discourage unauthorized entry. For example, barriers or partitions can separate energized components within the charger, and special opening tools and attachments can be used on many covers. However, even in these cases, panel interlocks would give an extra safety margin for any panel that is opened or removed for normal adjustments.

Transformers. Although Faraday shielding was preferred on transformers to prevent primary-to-secondary fault problems, the original recommendation suggested that potting transformer windings would also give the same level of protection. Yet, the primary and secondary windings on power transformers are wound in close proximity, and the rather viscous epoxy material likely would not penetrate the core-coil interface sufficiently to cause the desired isolation. Further, some transformer engineers consider such an isolation technique simply impractical on big industrial-type transformers. Thus, the process would not necessarily insure the desired feature and, whenever transformer windings are layered wrapped, the grounded Faraday shield is the only reasonable answer.

In place of the grounded shield, axial displacement of the secondary and primary windings on the transformer core plus separation of primary and secondary circuits would also be acceptable. Again, the goal is to accomplish electrical isolation of primary and battery circuits.

Charging Couplers and Cables. Hardly any comments have been made about the charging couplers other than the minimum number of required contacts and the engaging sequence of the plug-receptable combination. Obviously, the general safety requirements for any coupler should also be adhered to, such as employed on other low-voltage coupler applications. For example, each contact should be able to continuously carry the maximum current in the circuit for which it is designed; all exposed, uninsulated matallic parts should be grounded to the grounding conductor; and the coupler-cable interface should be so designed to prevent cable-insulation damage.

A logical safety item is insulated strain relief for all cables supplied with a charger. Unfortunately, however, one past battery-charger fatality could have been prevented if cable strain-relief had broke both charging conductors. To further protect against cable damage, insulated glands should be available for any cable passage through the charger frame. Beyond these, storage on the enclosure outside should be provided for all permanently attached cables. Such would help ease damage resulting from unstored charging cables and couplers that are left on the mine floor.

In a matter related to couplers, many maintenance personnel have received burns from battery-energized couplers, during repair, maintenance, or replacement. It is necessary, therefore, that the battery terminal connections should be constructed so power to the couplers can be removed.

3.3.3. Final Recommendations

The following is the final listing of safety features which should be included in all battery-powered systems. As should be obvious now, beyond the results of this research, input has also been received from operators, manufacturers, and state and federal regulatory agencies. The proper application of these should substantially reduce the probability of electrocutions on battery-powered mine equipment.

The recommendations scan five main areas: input circuitry, the charger enclosure, internal circuitry, outgoing cables, and battery-box connections. The "power source," referenced below, refers to the transformer from which the charger receives power. Clarification of some items is parenthetically stated within the list.

A. Input Circuitry. The necessary requirements for the incoming power and grounding from the power source are covered under Title 30, Code of Federal Regulations, Part 75 (30CFR75). The important paragraphs which must be followed include:

A.1. 75.900, specifies protective relaying for incoming circuitry;

A.2. 75.901, requires a grounding conductor between the load center and the charger;

A.3. 75.701-4, relates the size of the grounding conductor;

A.4. 75.902, mandates ground-check monitoring of this grounding conductor;

A.5. 75.902-4, requires that the grounding and appropriate ground-check conductors be attached to separate studs within the charger enclosure (these ground studs must not be on a removable panel); and

A.6. 75.514, states that these stud connections be mechanically and electrically effective (implies that the stud connection has the same ampacity as the largest conductor connected to it and the stud must be welded to the cabinet).

B. Emergency Stop or Panic Button.

B.1. An emergency-stop switch should be located in a conspicuous, convenient place on the outside of the charger enclosure.

B.2. The switch should open the ground-check circuitry between the charger and the power source.

B.3. The switch should be pushed to stop the source power to the charger and be manually reset (i.e., it should not be spring loaded).

B.4. The switch button should be large enough and placed so it is easily pushed in an emergency but not easily pushed accidently.

B.5. The button should be bright red to aid visibility.

C. Enclosure (or Charger Cabinet).

C.1. The charger cabinet should completely enclose all current-carrying components, except input and output cables.

C.2. The enclosure construction should minimize the possibility of adjustment or tampering by authorized personnel.

C.3. Enclosure doors, covers, or lids, providing access to uninsulated live parts, should be provided with means to discourage entry by unauthorized personnel. Otherwise, the charger should be equipped with interlocks on these panels that de-energizes the power at the outby source when access is attempted.

C.3.1. Any panel or barrier through which access to live parts can be obtained should have warning labels mounted on them in a conspicuous place.

C.4. All controls which are required for normal routine operation of the charger should be accessible from the outside of the charger.

C.5. All hinged panels, covers, or doors should be individually grounded (bonded) the charger main frame.

C.6. Drain holes should be provided to prevent standing water inside the enclosure.

C.7. All internal components should be securely mounted to the charger enclosure.

D. Internal Circuitry.

D.1. Power Transformer.

D.1.1. The power transformer should electrically isolate the battery being charged from the power source with primary and secondary windings being so arranged to eliminate hazardous interwinding faults.

D.1.2. The transformer windings may be inner and outer (or layered) wrapped only if a grounded metallic (or Faraday) shield is placed between the primary and secondary windings.

D.1.3. When used, an interwinding shield must be able to continuously carry the maximum ground-fault current available from the power source without damage to itself.

D.1.4. Failure of the transformer from a transient overvoltage must not create a personnel hazard. Otherwise, the power transformer should have transient overvoltage protection across its primaries, and the insulation of the transformer should be coordinated with such protection.

D.2. The power-transformer secondary and all d-c circuits and components should be isolated from the frame ground of the charger.

D.3. The charger circuits should be arranged to eliminate faults between the primary and the secondary circuits. (In other words, the circuit connected to the transformer primary must be physically separated (say, by a barrier) from those connected to the secondary so faulting between the two cannot occur.)

D.4. Control Power

D.4.1. The control voltage should not exceed a maximum of 120-V rms nominal.

D.4.2. The control circuitry should be ungrounded.

D.4.3. If the control-transformer primary is connected to the primary of the power transformer, it should electrically isolate the control circuitry from the power source and should be constrained by the same requirements as for power transformers.

D.5. The power rectifier should be designed such that a failed diode does not create a personnel hazard.

D.6. Overload and short-circuit protection should be provided for the charger output.

D.7. Protection should be included to prevent delivering power to a battery of wrong polarity.

D.8. Cicuitry should be provided to prevent charging a battery which has surface-leakage or ground-fault paths from a cell or cells to the battery tray such that the total path resistance is less than 1000 ohms.

D.9. Protection should be available to automatically disconnect all outgoing charging power conductors from the internal charging circuitry if the power source is removed.

D.9.1. The disconnect device of Item D.9 should be as close to the point where charging power leaves the enclosure as practical.

D.9.2. The disconnect device of Item D.9 should be provided with a protective cover and appropriate warning notice located in a conspicuous place.

D.10. Charge Timing Circuitry.

D.10.1. When the battery is connected, the charger off-on controls must be set manually; automatic resetting of such controls should not be permitted.

D.10.2. Any failure of the battery-box ground-check or grounding circuits, as specified in Item D.11, should cause the charger off-on controls to reset to zero.

D.10.3. The charger time circuitry should operate in a manner to minimize battery overcharge as much as practical.

D.11. A separate grounding conductor and ground-check-monitor circuit should be provided for each battery tray serviced by the charger.

D.11.1. Each battery tray should be frame grounded through the grounding conductor to the charger frame.

D.11.2. The ground-check-monitor circuit should trip the charging power to the appropriate battery if effective grounding to that battery tray is lost. In such cases, all power conductors should be de-energized.

D.11.3. The ground-check-monitor circuit should meet the requirements set forth in 30CFR Paragraphs 75.902, 75.901-2, and 75.902-2.

E. Output Cables (or Charging Cables).

E.1. The charging conductors and appropriate grounding and ground-check conductors should be contained in a single, flexible cable.

E.2. The charging conductors should be sized to safely carry the charger output current without exceeding the allowable temperature rise of the cable insulation.

E.3. Grounding and ground-check conductors, contained in the output cables, should meet the requirements of 30CFR Paragraph 75.906.

E.4. Insulated strain relief should be provided on all cables permanently attached to the charger.

E.5. Insulated glands should be available for any cable passage through the charger enclosure.

E.6. Convenient storage should be provided on the outside of the charger enclosure for all permanently attached cables.

F. Battery-box Charging Connector (Coupler) and Connections.

F.1. The charging cable should be connected to the batteries being charged through a single connector (coupler).

F.2. Such charging connectors should adhere to the coupler requirements of 30CFR Paragraph 75.902 so that the charging power is removed prior to charging-circuit contact separation.

F.3. The charging connector shall be keyed or sized such that a battery of fewer number of cells than that for which the charger is designed cannot be connected.

F.4. All exposed uninsulated metallic parts of the charging connector should be grounded to the grounding conductor.

F.5. Enough insulated contacts should be available in the charging connector for all appropriate positive, negative, grounding, and ground-check conductors.

F.5.1. Each contact should be able to continuously carry the maximum current in the circuit for which it is designed.

F.6. Grounding and ground-check connections on the battery tray should adhere to 30CFR Paragraphs 75.514 and 75.902-4 to insure mechanically and electrically effective grounding.

F.7. Battery terminal connections should be so constructed that power to the charging connectors can be removed.

3.4 CONCLUSIONS

All objectives under this project category of battery and battery-charging safety have been accomplished. The critical stresses involved or the withstand needs for traction-battery enclosures have been defined, or no less than clarified, so future research can arrive at test specifications. These included mechanical strength, insulation, ventilation, drainage, and electrical clearance. A battery charger containing all the necessary safety features to protect miners has been specified, constructed, and demonstrated. The successful routine use of this charger in an underground coal mine for an eight-month period has shown that safety battery chargers are practical. Finally, the battery-charging hazards that cause electrocutions have been delineated, and the requirements needed to prevent them have been documented.

Future Research. Even though this work has met the proposal objectives, there still remain some questions that justify future research.

1. Catalyst battery caps have proven advantages in other industrial and governmental applications. However, the advantages in light of underground mine employment need to be evaluated, including actual demonstrations.

2. The work described here concerns a-c to d-c battery chargers. An effort should also be extended on d-c to d-c chargers such as those which receive power from trolley lines.

3. A battery surface-leakage and ground-fault device could not be made available during the research. Such devices should be evaluated, designed, built, and tested in the underground mine environment. The 1000-Ω total resistance threshold referenced in this chapter should be verified.

3.5. REFERENCES

1. Morley, L. A., and J. A. Kiefer, "Battery and Battery-charging Safety," Annual Report on USBM Grant G0155003, Feb. 13, 1977.

2. U.S. Department of Interior, Bureau of Mines, "Electric Motor Driven Equipment and Accessories," Schedule 2G, March 1968.

3. National Fire Protection Association, National Electrical Code 1978, ANSI C1-1978.

4. American Society of Testing Materials, "Electrical Insulation - Test Methods: Solids and Solidifying Fluids," 1980 Annual Book of ASTM Standards, Part 39, June 1980.

5. Ray Knox, Kersey Mfg. Co., Bluefield, VA, personal communication, May 16, 1978.

6. Winters, K. D., G. R. Gaven, and J. C. Ault, "PLASTIC CANOPY - A Computer Program for the Structural Analysis of Protective Canopies," USBM IC8795, 1979.

7. Woodward Associates, Inc., "Design Criteria and Guidelines for Falling Object Protective Structures (FOPS)," Final Report on USBM Contract J0357110, Feb. 20, 1976.

8. Terzaghi, Karl, Rock Defects and Loads on Tunnel Supports, republished in Rock Tunnelling with Steel Supports, by R. V. Proctor and T. L. White, Commercial Sheaving, Inc., Youngstown, OH, 1977.

9. Bieniawski, Z. T., The Pennsylvania State University, personal communication, January 13, 1979.

10. Sawyer, S. G., and D. D. Brogan, "Elastic Plane Frame Analysis of Semisymmetric Cabs and Canopies Used on Underground Electric Face Equipment," USBM RI7799, 1973.

11. Sawyer, S. G., D. D. Brogan, J. L. Dahle, and G. J. Karabin, "Experimental Verification of the Computer Program CANOPY by the Static Testing of a Continuous Miner Canopy," MESA IR1004, 1974.

12. Code of Federal Regulations, Title 30, Part 75, as published in the Federal Register, December 31, 1972.

13. Robinson, H., "The Ventilation of the Battery Containers of Storage Batteries," SMRE Research Report No. 122, February, 1956.

14. Vinal, G. W., Storage Batteries: a General Treatise on the Physics and Chemistry of Secondary Batteries, Chapman and Hall, Ltd., London, 1924.

15. Ilsley, L. C., "Development and Safety of the Storage-battery Locomotive," USBM IC6068, May, 1928.

16. Director of Electrical Engineering, Admiralty Engineering Laboratory, West Drayton, England, as quoted by Robinson in reference 1.

17. Ministry of Fuel and Power (now Department of Energy), "Coal Mining: Report of the Technical Advisory Committee," Command Paper 6610, H.M.S.O., London, 1945.

18. Ministry of Fuel and Power, "Coal Industry: The Coal Mines (Locomotives) General Regulations," Statutory Instruments No. 530, H.M.S.O., London, 1949.

19. Ministry of Fuel and Power, "Tests and Specification for Storage Battery Locomotives for Use in Mines Under the Coal Mines Act, 1911," Testing Memorandum No. 11, H.M.S.O., London, 1949.

20. Burkle, B. J., "The Use of Traction Type Storage Batteries Under Ground in British Mines," Mining Technology, Vol. 53, Jan.-Feb. 1971.

21. Titman, H., "The Emission of Gas From Lead-acid Cells," SMRE Research Report No. 158, Feb. 1959.

22. Titman, H., "The Effect of Different Rates of Emission on the Accumulation of Hydrogen in a Vented Battery Container," SMRE Research Report No. 167, March, 1959.

23. Neill, A. G., "The Lead-acid Battery with Particular Reference to its Use in Mining," The Mining Electrical and Mechanical Engineer, Nov. 1965.

24. Sandford, James, "Plastic Caps Reconvert Battery Gases to Needed Water," Design News, November 3, 1975.

25. Virr, L. E., and F. K. Pearson, Safety in Mines Research Establishment, Harpur Hill, Buxton, Derbyshire, England, personal communication, April 29, 1976.

26. Mine Enforcement and Safety Administration (now MSHA), Reports of Fatal Coal Mine Electrical Accidents.

27. MSHA, Guidelines for Low-voltage Ground-check Monitors.

28. Virr, L. E., and F. K. Pearson, "Fail-safe Earth-fault-detection Device for Battery Supplies," Proceedings IEE, Vol. 212, No. 8, August 1974.

29. IEEE, "Recommended Practice for Electric Power Distribution in Industrial Plants,"IEEE Std. 141-1976, IEEE, New York, 1976.

CHAPTER IV

MINE-POWER-SYSTEM TRANSIENTS

4.0 BACKGROUND

4.0.1. General

Transient research, prior to the present reporting period, proceeded for approximately three years, actually commencing under USBM Grant G0133077. Much of the effort was devoted to the development of a transient recording system and measurement of transients on actual mine power systems. Conclusions and recommendations resulting from this work are available in references 1, 2, and 3.

4.0.2. Scope of Work

Even though there was good success in the preceding research, more was needed to be known about the duration, frequency, repetition, and amplitude of mine-power-system transients. More concrete information was required about destructive transient sources in relation to equipment failures and personnel safety. Based on these desires, the following research was proposed:

1. continue the development and testing of inexpensive transient detectors suitable for use by industry, MSHA, and researchers, and

2. continue collecting transient data on a-c and d-c mine power systems.

During the course of the effort, an additional task was added:

3. Delivery of two inexpensive transient detectors to the Bureau of Mines.

The overall objective was to gain substantial information about abnormal power-system transients in underground coal mines, both sources and effects, and a firm knowledge of worst-case events. Due to complimentary research at West Virginia University under USBM Grant G0144137, this research was coordinated through the Technical Project Officer with that organization.

4.0.3. Chapter Format

This chapter commences with a presentation of the transient-detector development effort. Transients on mine distribution systems are then covered, both from theoretical and practical points of view. Contained in that discussion are recommendations pertaining to reducing hazardous transient overvoltages on distribution systems. Afterwards, voltage transients observed on mine utilization systems are presented. The chapter ends with a summary of conclusions drawn form this research task.

4.1. INSTRUMENTATION

4.1.1. General

Precise knowledge of transient behavior on power systems is required before any safety hazard created by their presence can be ascertained then eliminated. The easiest way to access the occurrence of transient overvoltages is to measure various points within the power system. However, the desire to observe events on actual underground coal-mine systems places certain restrictions and precautions on the instrumentation used. Among these are:

1. the hostile mining environment, usually high humidity and dust;

2. portability and ruggedness;

3. ease and speed of instrumenting the power system, no loss in production can be caused; and

4. totally isolated power supply.

The conventional technique, used with good success by many researchers in utilities and other industries, employs a triggered single-sweep oscilloscope, the events being captured on film using a scope camera. For the first three restrictions above, the idea of oscilloscope-only instrumentation was discarded early in the research. Adding to the decision was the need for external scope triggering; to obtain a reliable trace, the trigger signal often must be supplied from an auxiliary component on the device under test, such as a trip coil on an interrupter. Such a connection is usually very difficult on operating mine power systems.

In order to overcome all precautions, two instrument packages were assembled during previous reporting periods (3). This instrumentation is summarized in the next section as background for the discussion of continued work on inexpensive transient-detector development.

4.1.2. Review of Past Work

Transient Recorder. The first system packaged is termed the "Transient Recorder." The main component is a Biomation Model 8100, basically a two-channel digitizer with memory, appropriate trigger controls, and various output options. Isolation from the power system (being studied) was first attempted with an isolation transformer but was found inadequate. Complete isolation is now provided through a battery-powered inverter.

The input signal to the transient recorder is the output from a capacitive-compensated resistive voltage divider. When a transient defined by setting the levels and controls on the recorder appears, it is "frozen" in a digital rotating memory. The event may then be viewed on an oscilloscope and a strip-chart recorder. If desired, the user can also store the transient waveform on a digital tape, which later can be analyzed by a computer. After displaying or recording, the user can re-arm the transient recorder for the next event. When a new transient is "captured," the procedure may be repeated according to the user's wishes. The instrument is extremely flexible, but the outstanding advantage of this system is its ability to provide an almost perfect digital record of any voltage disturbance.

The system was used in approximately 25 different mines to collect transient data. Even though a large amount of data was obtained, the system sometimes failed to operate and, when it did, constant user intervention was required. Furthermore, accuracy and reliability appeared to deteriorate with every in-mine trip. The poor reliability of the Transient Recorder was found to be caused by its sensitivity toward hostile environments. Although an excellent instrument, it was adversely affected by dust, temperature, moisture, or vibration.

Because of these problems, a search was made to find a more suitable field unit. The thought was not to abandon the Transient Recorder but to locate a simpler instrument which could be used on routine in-mine transient studies. When probable transient locations were found, if warranted, the Transient Recorder could then be employed to provide a thorough quantitative knowledge about the transients. After fruitless attempts to find an off-shelf detector, a decision was made to design and construct in-house equipment.

Some basic design criteria were established for the instrument from the past experience.

1. It must not be affected by the hostile mining environment.

2. It must be portable and contain its own power supply.

3. It must be inexpensive (less than $200).

4. The instrument should be constructed from readily available components; the construction should require only elementary skills in assembly.

5. The parameters measured must relate to power-system component specifications.

Peak Detector. The first circuit, resulting from this work, measures the crest voltage of a transient. It is composed of a resistive voltage divider, a precision detector, and an integrator, being designed around a 747 dual operational amplifier. The output from the detector is fed to a strip-chart recorder. The chart is easily calibrated, allowing the amplitude to the transient to be read directly. (For complete construction details see reference 3.)

This peak-detector circuit was successfully used to measure lightning transients on a strip-mine ground system and to measure d-c transient overvoltages on underground coal-mine trolley systems. The only circuit change was in the voltage-divider ratio. Although partially offset by the bulkiness of the strip-chart recorder, the small size and light weight of the detector were found convenient. For general application, however, more information about a transient than just amplitude must be known. Therefore, except for "ball-park" approximations, the Peak Detector was found of limited utility.

4.1.3. Transient Detector

Criteria. The experience gained with the Transient Recorder and Peak Detector provided the foundation for the development of a second-generation detector. In addition to the general criteria listed in the previous section, a couple of specific design requirements were added. Both were coupled to portability. The Peak Detector did function correctly in the mine environment, but the external strip-chart recorder made its use cumbersome. Thus, it was decided that the new design should incorporate a built-in printer. The portability aspect was further refined to restrict the unit's volume to less than one cubic foot and the weight to less than 25 pounds.

The peak-detector's output information falls way short of that which can be related to power-system component specifications. In order to meet this general design criterion (item 5 above), the measured quantities should correspond to dielectric withstand properties. Specifically, the detector should be designed to record the same quantities as the BIL impulse-wave test. These parameters, which are diagrammatically shown in Figure 4.1, are the peak value, rise time, and pulse width (4). The last value is defined as the time for the waveform to decline to 50% of the peak value. The quantities can easily be used to evaluate the transient severity and to select adequate transient-suppression devices and insulation coordination.

In order to maintain low cost and portability, some constraint of measured-parameter range is necessary. So that the detector is practical, the limits selected are set within those of transients known to occur on mine power systems (see reference 3 and also later sections of this chapter):

1. $0\ \mu s \leq$ rise time $\leq 99\ \mu s$,

2. $0\ \mu s \leq$ pulse width $\leq 99\ \mu s$, and

3. about $1.5\ V \leq$ pulse height $\leq 10\ V$.

The range of the detector allows recording transients up to 10 or 15 times line voltage, depending upon the construction of the voltage divider.

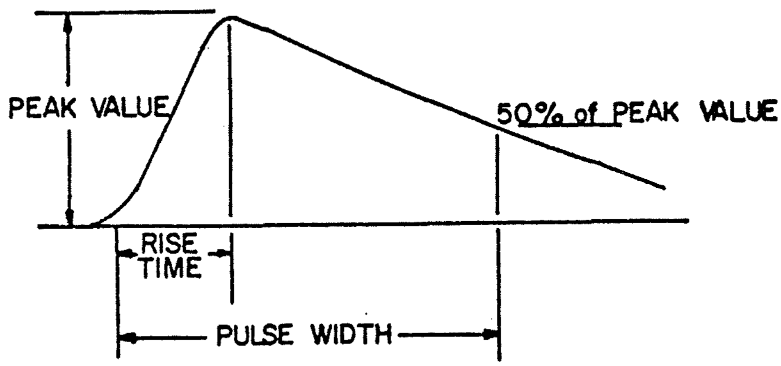

Figure 4.1. BIL Test Waveform.

Circuit Description. All of the desired characteristics have been incorporated into the final design, which is aptly called a Transient Detector. The block diagram is shown in Figure 4.2. The analog-input circuit accepts the analog signal and generates control signals to the input-control logic. The input-control logic contains a control-logic counter and analog-to-digital converter, from which the required parameters are extracted and computed. The output-control logic contains shift registers, decoders, and analog multiplexers to condition the data for the printer input. The clocks are generated with three inverters each. These blocks are described in detail in the following paragraphs.

Analog-input Circuit. The analog-input circuitry, illustrated in Figure 4.3, can accept voltages in the range from -10 to +10 V. The 318 op-amps and diodes are used to rectify the incoming pulse, and the rectified voltage is scaled (by one half with R1) before it reaches the input of the 306 comparator. (This comparator works well only in the $\pm$ 5 V range.)

The 306 comparator and the 3140 bifet op-amp are used for a high-speed analog peak detector. The output of the peak detector is fed to a non-inverting 3140 op-amp circuit to boost the voltage into the 0 to +10 voltage range for the analog-to-digital converter.

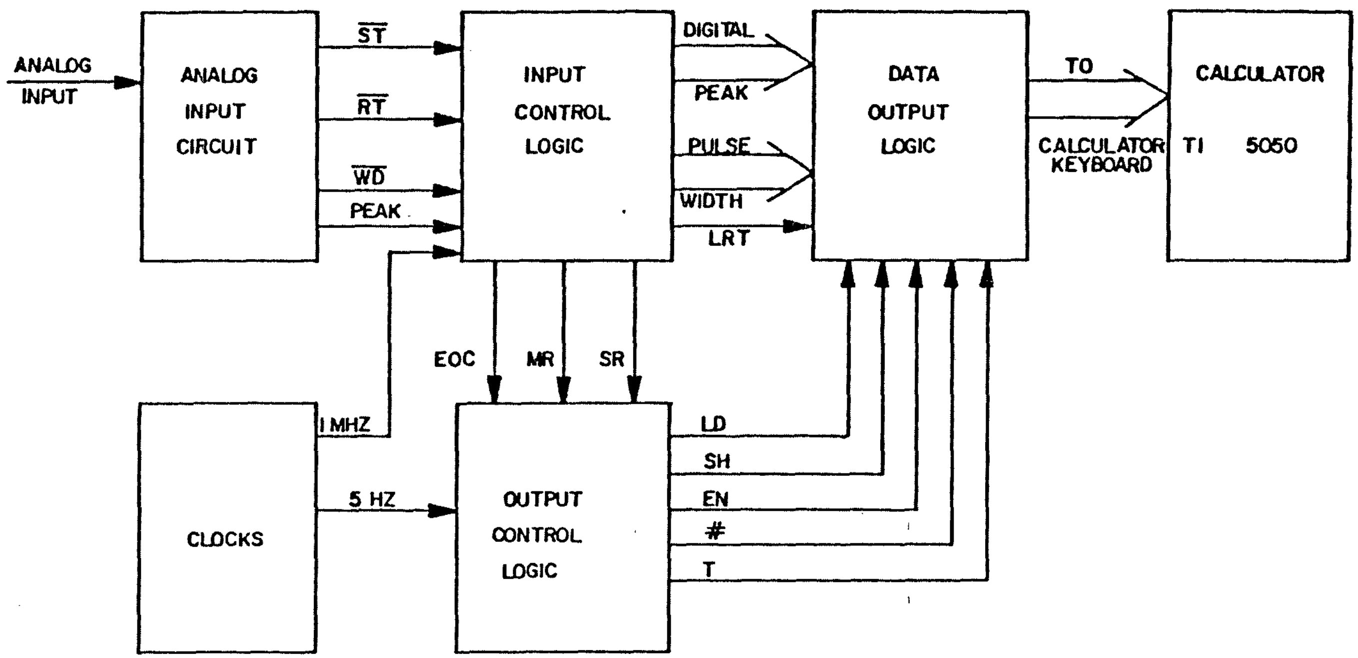

Figure 4.2. Transient-detector Block Diagram.

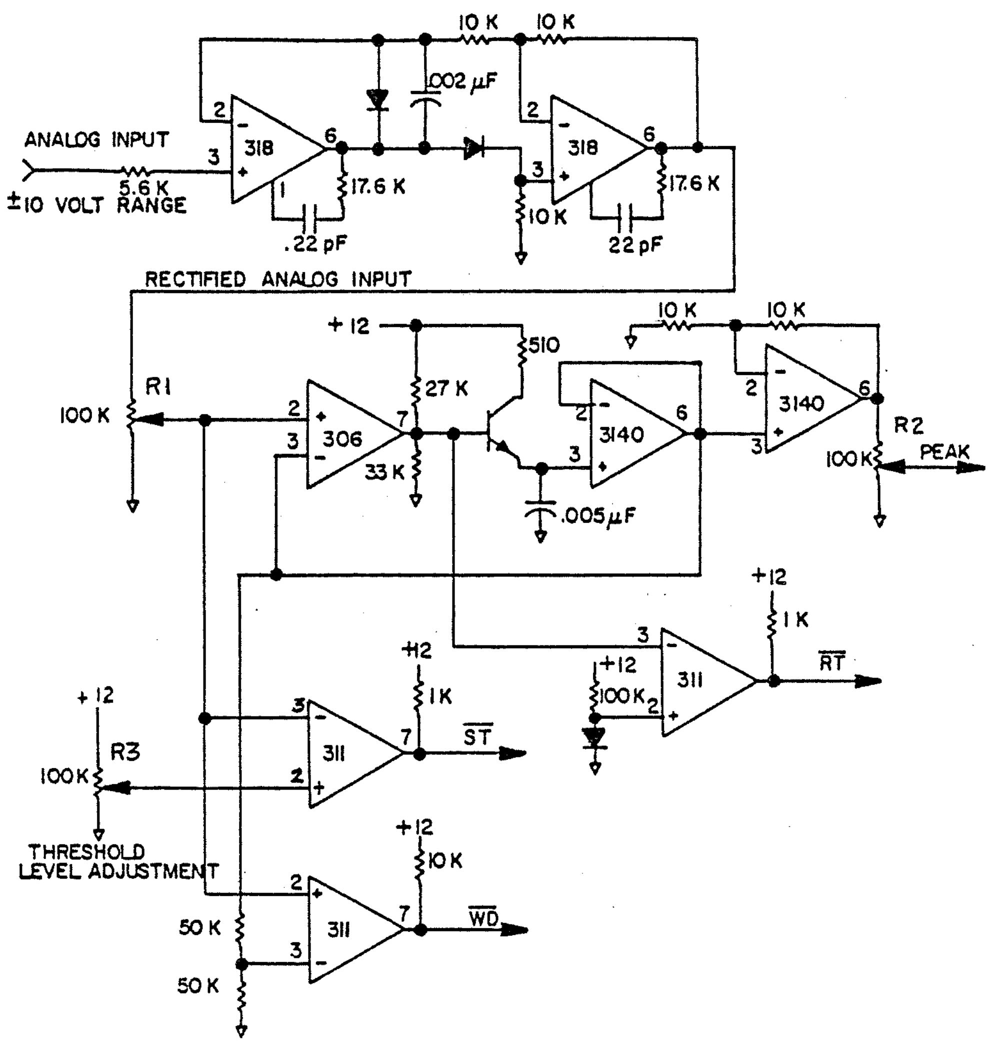

Figure 4.3. Analog-input Circuitry of the Transient Detector.

Three 311 comparators are used to drive the digital logic. The $\overline{ST}$ (start) output signal changes state when the threshold level is exceeded. The $\overline{WD}$ (width) output produces a 1 → 0 transition on the falling edge of the pulse at 50% of initial peak value. The $\overline{RT}$ (rise time) output produces negative pulses everytime the 306 comparator dumps more charge onto the holding capacitor during the period the analog pulse is rising. This signal can be used to measure rise time. Figure 4.4 contains typical timing diagrams for all these signals. (Note: the waveforms ST, RT, and WD in Figure 4.4 are the inverse of the actual waveforms $\overline{ST}$, $\overline{RT}$, and $\overline{WD}$.) Finally, the PEAK output signal is proportional to the peak of the analog pulse.

Input-control Logic. The Transient Detector is designed for functioning under battery power. Therefore, all digital logic uses CMOS circuits, and all integrated circuits (IC's) are the 4000 series unless specified otherwise. Most IC's in the following figures list only the last two or three digits, and the number within the circle represents the location of the IC (see Figure 4.11). The circuit for the input-control logic is given in Figure 4.5.

The inverters (4049), the D flip-flops (4013) and the AND gates (4073 and 4081) are the logic IC's which accept signals from the start ($\overline{ST}$), rise time ($\overline{RT}$), and width ($\overline{WD}$) input signals and generates control signals. The enable signal (EN) insures the 14518 dual decade counter counts during the appropriate range of the analog pulse. The master reset (MR) signal resets the entire system. The load rise time (LRT) loads the count from the dual decade counter into a shift register in the data-output circuit everytime a rise-time ($\overline{RT}$) pulse is generated. The start-of-conversion (SOC) signal is a pulse which will activate the analog-to-digital converter (MM5357). The end-of-conversion (EOC) signal enables the output-control logic. The typical timing diagram for these signals is also shown in Figure 4.4.

Data-output Logic. The data-output logic is illustrated in Figure 4.6. The circuit contains shift registers (4021's & 4013) which will serialize the data into four bits. The decoder (4128) controls the analog muliplexer switches (3-4016's) which simulate contact closures on the calculator keyboard. This output is in terms of the rows (R) and columns (C) of the keyboard key matrix; five rows and four columns are used.

Output-control Logic. The output-control logic is given in Figure 4.7 with the associated timing diagram in Figure 4.8. The output-control logic provides the appropriate control signals to the data-output logic (Figure 4.6) to serialize and print each character.

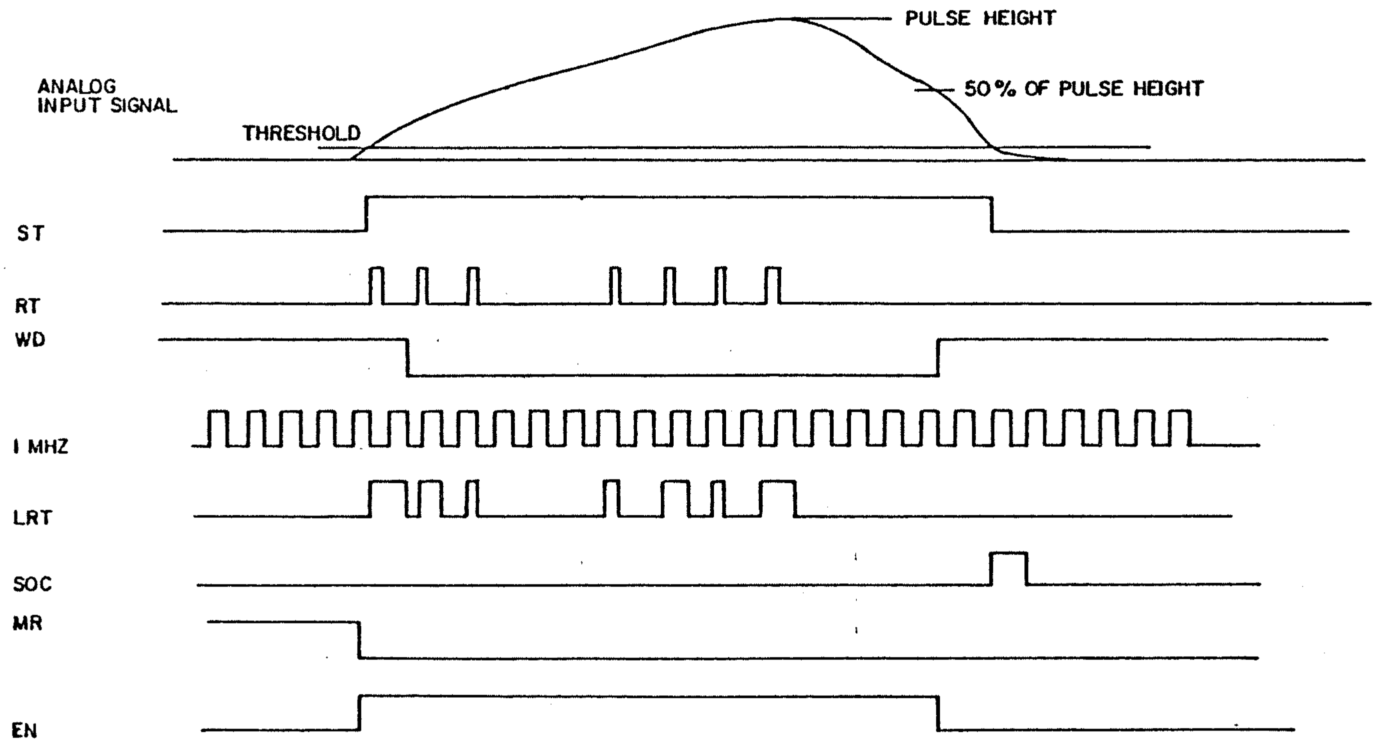

Figure 4.4. Digital-logic Typical Timing Diagrams.

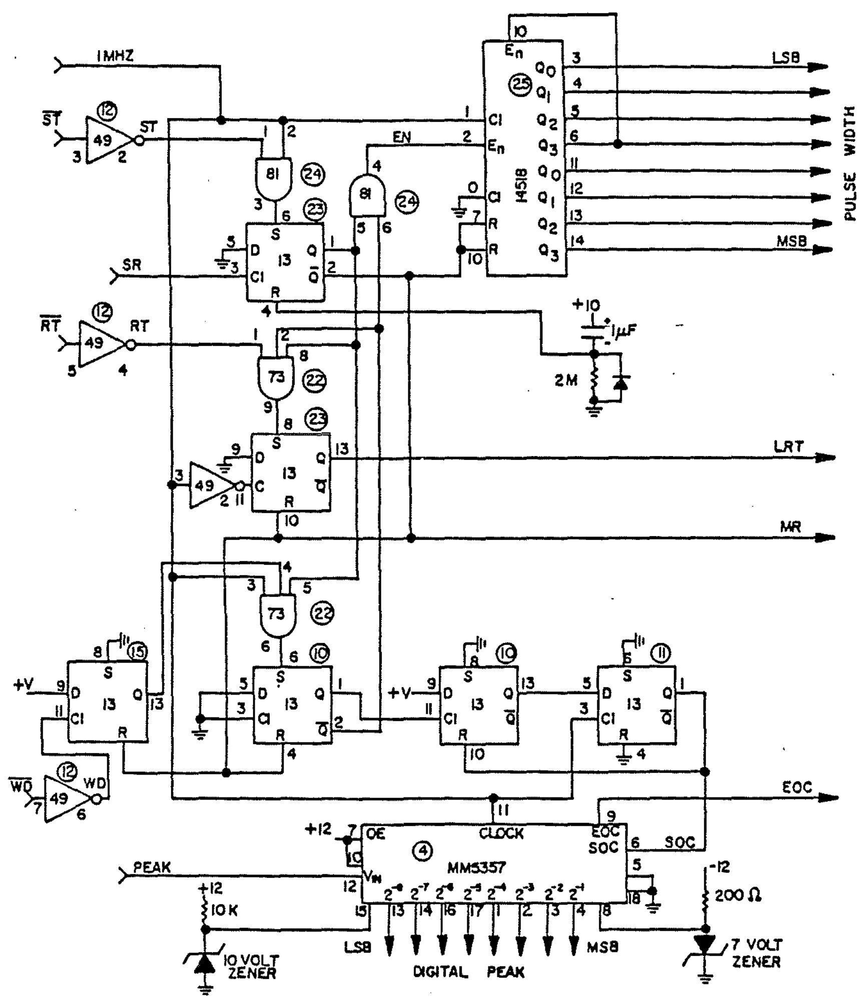

Figure 4.5. Input-control Circuit of the Transient Detector.

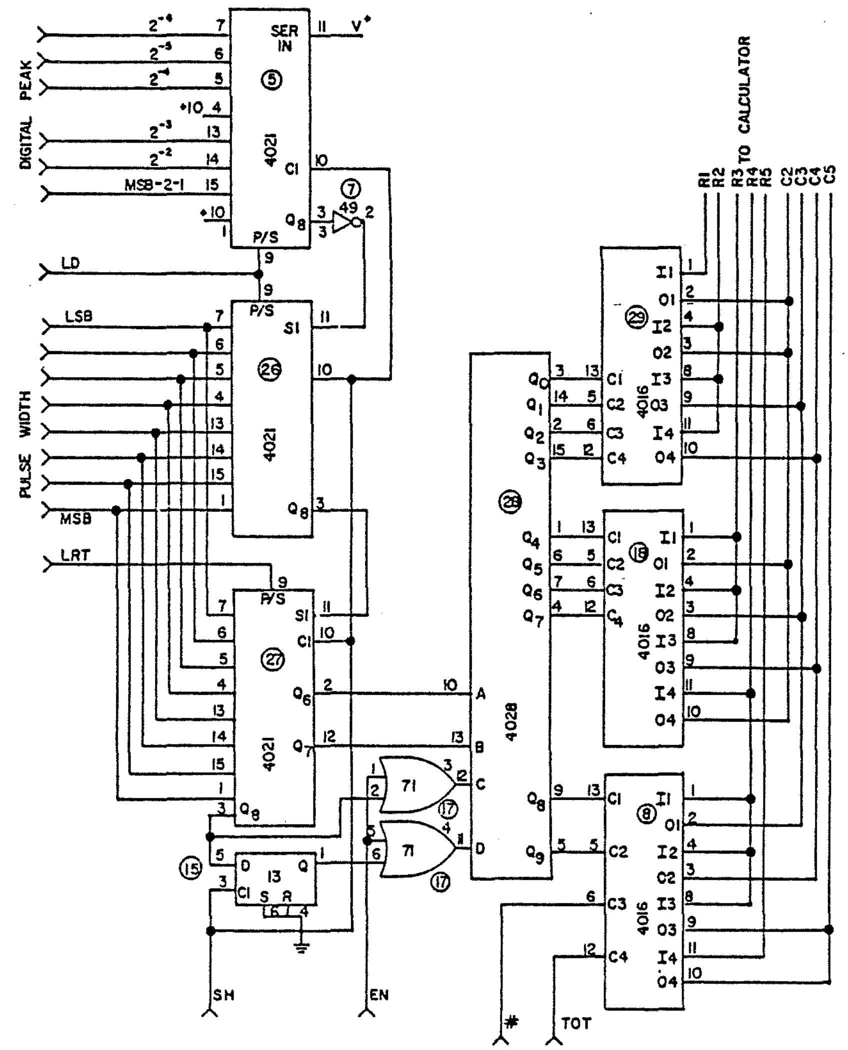

Figure 4.6. Data-output Logic of the Transient Detector.

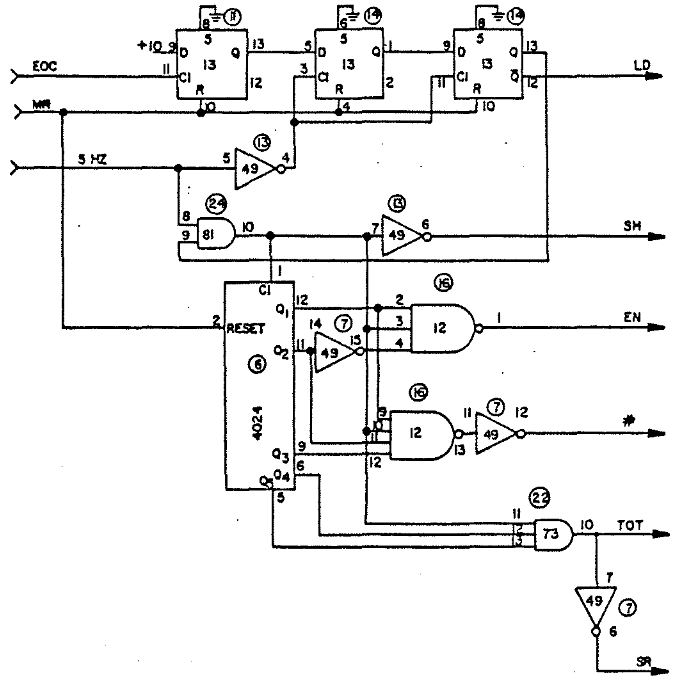

Figure 4.7. Output-control Logic of the Transient Detector.

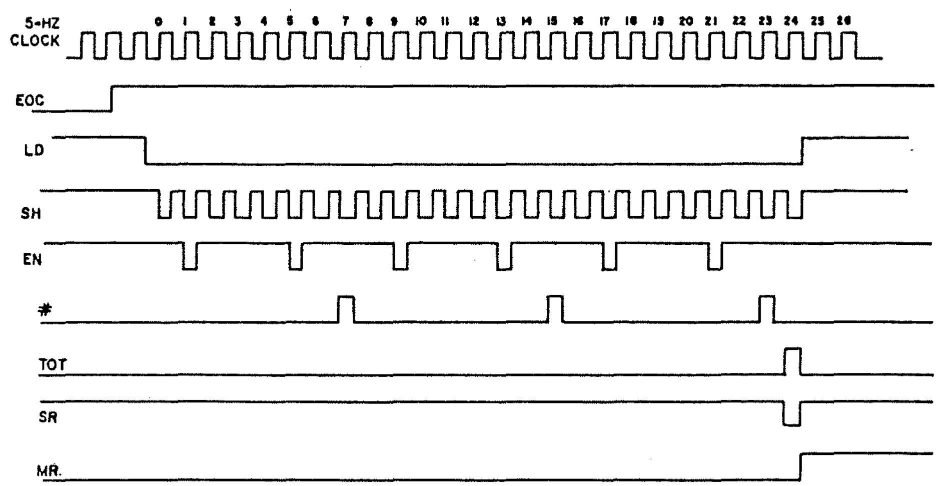

Figure 4.8. Associated Timing Diagram for Output Control Logic.

The D flip-flops (4013) are used to generate the load (LD) signal and enable the counter (4024) after the data conversion is complete in response to a 0 → 1 transition on end of conversion (EOC). The states of the counter are decoded to provide shift pulses (SH), enable pulses (EN), identifying pulses (#), and total pulses (TOT) in the proper time sequence.

The system-reset pulse (SR) resets a D flip-flop in the input-control logic which in turn resets the entire system via the master reset (MR). This insures no false resetting will occur. The Transient Detector will also ignore any new analog pulse until the Transient Detector is reset.

Calculator (TI5050). An inexpensive digital-printing device with low-power requirements is needed, and a thermal printer meets these requirements. Most thermal printers print each character one at a time with a 5 x 7 dot matrix. This requires a significant amount of logic to sequence all of these signals to control a thermal printer. Therefore, it was decided to use the logic which already existed in a small calculator to perform the printing task. A Texas Instruments Model 5050 is used, but perhaps any other thermal-printing calculator would work as well.

A general interface to a thermal printer would have allowed the printing of special heading and characters, but the interface directly to the calculator keyboard restricts the data format to the form which is indicated in Figure 4.9. It can be noted that rise time and pulse width are given in microseconds, while amplitude is presented in octal format.

As mentioned, the output of the 4016's in the data-output logic simulates calculator-keyboard contact closures. Thus, the rows and columns output of Figure 4.6 can be used to determine the connections between the 4016's and the calculator keyboard. Table 4.1, however, is presented to clarify these interconnections for the Texas Instruments circuitry.

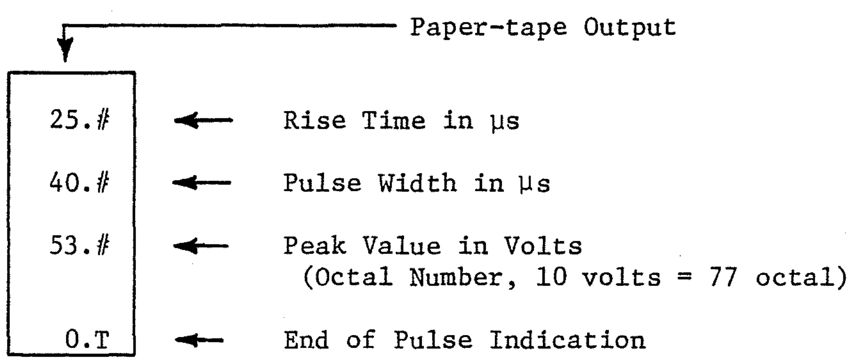

Figure 4.9. Data Output Format for the Transient Detector.

Table 4.1. Interconnections Between the Data-output Logic and the Calculator.

Row or Column Output of 4016's	Calculator Keyboard Output Conductor*	Notes
	1	not used
R2	2	
C2	3	
R1	4	
R3	5	
C3	6	
R4	7	
C4	8	
R5	9	
C5	0	

*Connections are numbered from left to right looking from the top of the TI 5050 calculator.

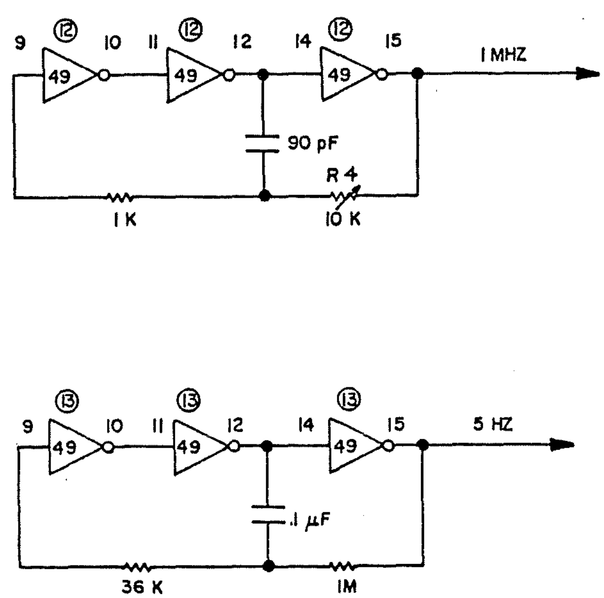

Figure 4.10. Transient-detector Clocks.

Clocks. Each clock (Figure 4.10) is built from three inverters plus resistors and capacitors. This design has been chosen because it is relatively immune to power-supply variations. A variable resistor is used to provide frequency adjustment on the 1-MHz clock.

Power Supply. Four rechargeable GEL cells (6 V each) in series are used to provide -12 V and +12 V requirements of the transient detector. Both are used to supply the transient-detector circuitry (+V, -V or +12, -12 on the preceding schematics); the +12 V also drives the calculator. A main power switch can be included using a double-pole double-throw (DPDT) unit. Power-supply decoupling should be available for all IC's in the analog-input circuitry (Figure 4.3) by 0.1-μF disk capacitors connected directly between each IC-socket positive and negative terminals and ground. Figure 4.11 illustrates typical power-supply wiring.

Under normal operating conditions (both circuitry and calculator on),

1. the -12 V source supplies 45 to 55 mA,

2. the +12 V have about 120 mA drains when idle, but

3. the +12 V supplies around 1.0A when a transient is detected and the calculator prints out.

From laboratory and in-mine experience with 4-Ah GEL cells under continuous transient monitoring, it was found that the +6-V battery required recharging each 24 hours, while the remaining three cells could last 72 hours.

Construction. Various construction techniques can be employed to assemble the transient detector. For the prototype and three subsequent units, practically all circuitry is mounted on one 4-1/2 by 10 inch board; connections between the IC's are wire wrapped. Board layout is given in Figure 4.12. The board, the calculator, and batteries easily fit into a 12-by-12-by-6-inch NEMA enclosure. The parts list available in Table 4.2 should greatly assist anyone desireous of duplicating the device.

Calibration. Calibration of the transient detector is very simple and requires only three adjustments. The 10-kΩ variable resistor (R4) in the clock circuitry (Figure 4.10) is used to obtain a 1-MHz squarewave output, observing the waveform at pin 15 of the 4049 IC. The amplitude of the squareware should be on the order of 10 V peak to peak. The adjustment of this clock should be performed with high precision (to the nearest 1000 Hz), as its output is used to directly measure pulse rise time and width. Next, two adjustments are made in the analog-input circuitry (Figure 4.3). First, the amplitude of a known incoming transient is measured. Then, the Amplitude Adjustment resistor (R1) is set so that the amplitude at the input (pin 2) to the 306 comparator is precisely one-half that of the incoming transient. Then, the Peak Calibration resistor (R2) is adjusted to provide a calculator printout in octal that is exactly the crest of an input transient. It is recommended that R1 and R2 be adjusted while simultaneously observing both the input transient and the 306-comparator input on a high-resolution dual-

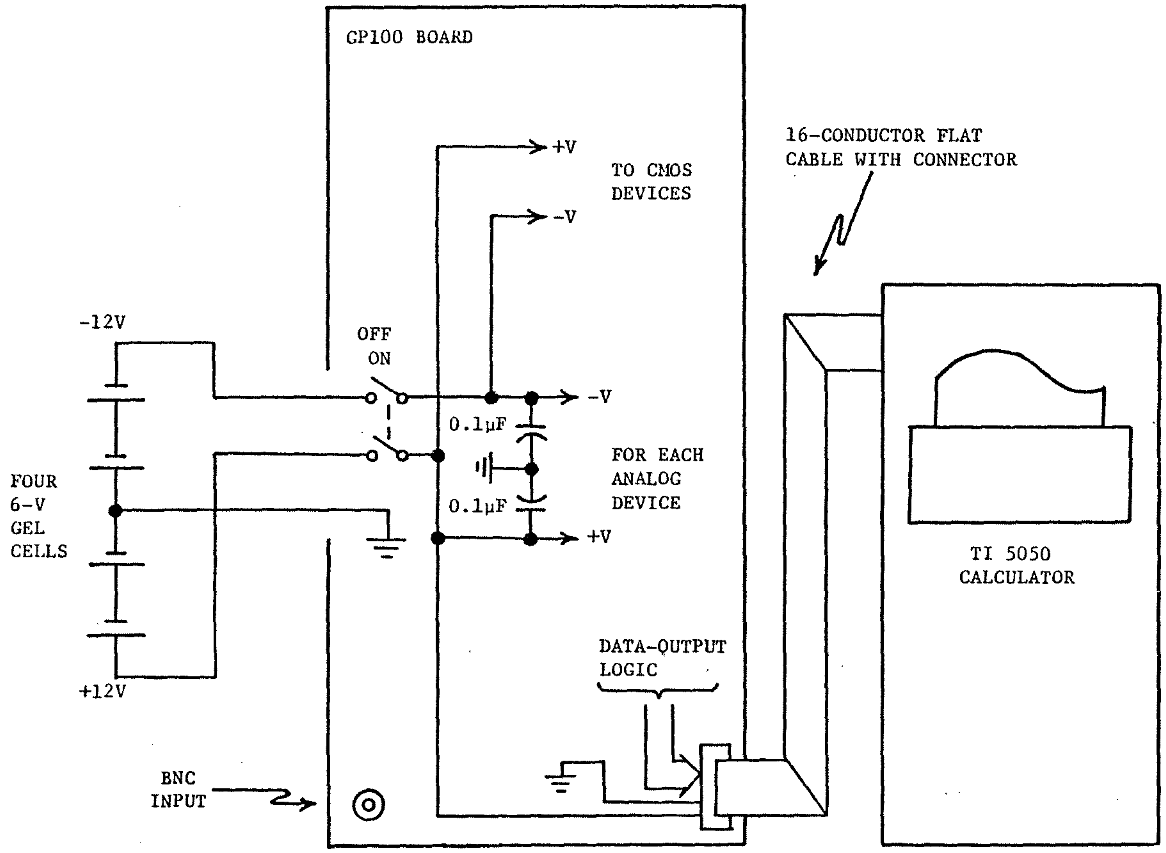

Figure 4.11. Typical Wiring Interconnections for Transient Detector.

channel oscilloscope (preferably with at least an 100-MHz bandwidth). Single-sweep scope triggering can use the input signal. Table 4.3 has been prepared to assist in octal-to-actual crest-voltage conversions, noting that 77 octal equals 63 decimal equals 10 V. Figure 4.13 contains an inexpensive pulse-generator circuit constructed and used in this project for calibration purposes with excellent results. As R1, R2, and R4 need be calibrated only one, all are multiturn PC-mount potentiometers.

Table 4.2. Parts List for the Transient Detector.

Integrated Circuits

1 - 306
3 - 311
2 - 318
2 - 3140
1 - 4012
5 - 4013
3 - 4016
3 - 4021
1 - 4024
1 - 4028
3 - 4049
1 - 4071
1 - 4073
1 - 4081
1 - 4518
1 - MM5357

Devices

1 - 2N3391 npn transistor
5 - 1N914 switching diode (must be high speed)*
1 - 6.8-V 1/2-W zener
1 - 10-V 1/2-W zener

Multiturn Resistors

1 - 100-kΩ panel mount
1 - 10-kΩ PC mount
2 - 100-kΩ PC mount

Fixed Resistors (all 5%, 1/4-W deposited)

1 - 220 Ω
1 - 510 Ω
3 - 1 kΩ
1 - 5.6 kΩ
7 - 10 kΩ
2 - 18 kΩ
1 - 23 kΩ
1 - 27 kΩ
1 - 30 kΩ
2 - 51 kΩ
1 - 91 kΩ
1 - 1 MΩ
1 - 2 MΩ

Capacitors

5%, Low drift:
2 - 22 pF
1 - 90 pF
1 - 0.0022 μF
1 - 0.0051 μF

Ceramic disk:
17 - 0.1 μF

Tantalum:
1 - 2.2 μF

Miscellaneous

1 - Dial 10 turn
1 - Female BNC Connector
1 - DPDT Switch
26 - 16-pin WW-terminal DIP sockets
1 - 18-pin WW-terminal DIP socket
40 - WW Terminals
1 - 16-wire flat-parallel cable with 16-pin DIP connector
1 - GP100 Board (Artec Electronics, San Carlos, CA 94070)
1 - TI5050M Calculator
4 - 6-V 4-Ah GEL cells
1 - GEL Cell Charger
1 - 12 x 12 x 6" NEMA Enclosure
Misc. - Wire Standoffs, Nuts, Bolts, lockwashers

*Hewlett-Packard 5082- diodes were used in the analog-input-circuit rectifier.

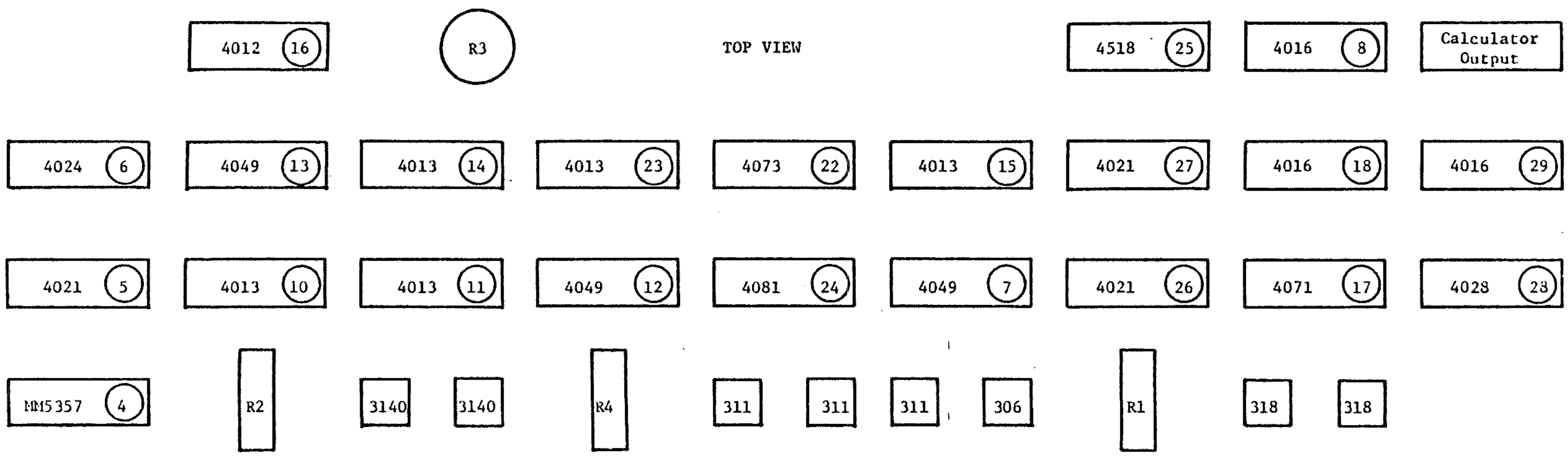

Figure 4.12. Device Layout of Main Circuit Board for the Transient Detector.

Table 4.3. Octal-printout to Actual-crest-voltage Conversions.

Octal	Actual Voltage	Octal	Actual Voltage	Octal	Actual Voltage
77	10.0 V	52	6.7 V	25	3.3 V
76	9.8	51	6.5	24	3.2
75	9.7	50	6.4	23	3.0
74	9.5	47	6.2	22	2.9
73	9.4	46	6.0	21	2.7
72	9.2	45	5.9	20	2.5
71	9.1	44	5.7	17	2.4
70	8.9	43	5.6	16	2.2
67	8.7	42	5.4	15	2.1
66	8.6	41	5.2	14	1.9
65	8.4	40	5.1	13	1.8
64	8.3	37	4.9	12	1.6
63	8.1	36	4.8	11	1.4
62	7.9	35	4.6	10	1.3
61	7.8	34	4.4	7	1.1
60	7.6	33	4.3	6	1.0
57	7.5	32	4.1	5	0.8
56	7.3	31	4.0	4	0.6
55	7.1	30	3.8	3	0.5
54	7.0	27	3.7	2	0.3
53	6.8	26	3.5	1	0.2
				0	0.0

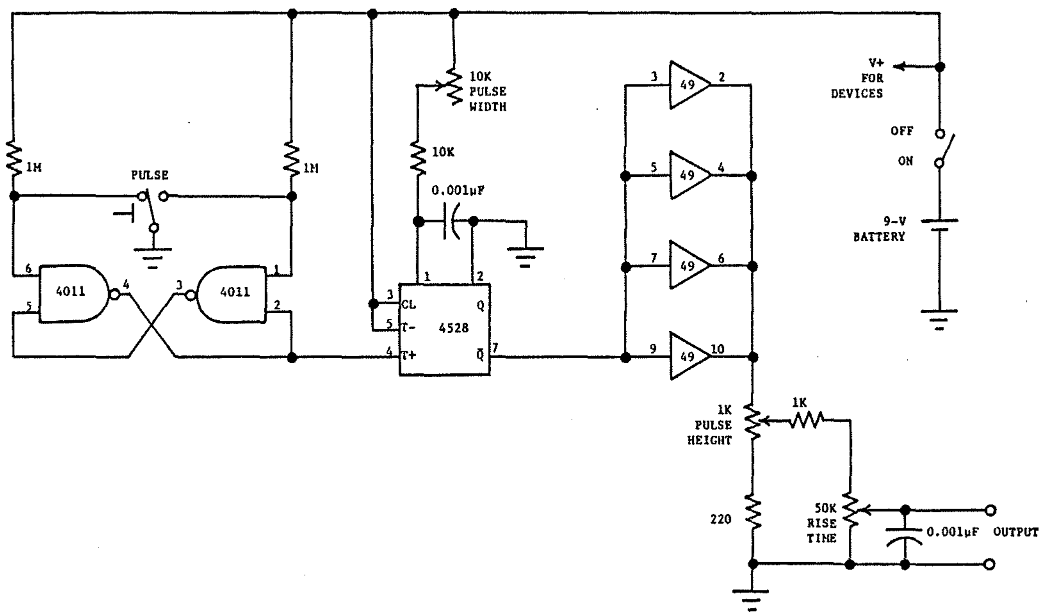

a. Schematic.

b. Parts List.

<u>Printed Circuits</u>

1 - 4011*

1 - 4528*

1 - 4049†

* only 1/2 used.
† only 4 inverters used.

<u>Potentiometers</u>

1 - 1 kΩ

1 - 50 kΩ

1 - 100 kΩ

<u>Resistors (all 5%, 1/4 W deposited)</u>

1 - 220 Ω

1 - 1 kΩ

1 - 10 kΩ

2 - 1 MΩ

<u>Capacitors (Ceramic Disk)</u>

2 - 0.001 μF

<u>Miscellaneous</u>

1 - 9-V Battery (e.g., MN1604 Mallory)

1 - SPDT Push-button Switch

1 - SPST Toggle Switch.

1 - Box

Misc. - Perf board, wire, knobs, nuts, bolts, etc.

Figure 4.13. Pulse Generator Used in Transient-detector Calibration.

Finally, the Threshold Level Adjustment resistor (R3) can be set so only those transients with crests greater that a desired value are recorded. Because easy readjustment is desireable, a ten-turn panel-mount potentiometer with lockable indicating dial was selected, mounting it on the main circuit board. Again, known transients can be used for this adjustment.

Application. The transient detector can be assembled and packaged by any electrical technician. It can be used to measure events on either a-c or d-c systems. Because of portability, the instrument can be placed and left inside a switchhouse, load center, or wherever required. At some later time, the detector can be recovered along with the paper tape listing the parameters of all detected transients. The only caution for operation would be in the recharge time of the batteries. If more than 24-hours continuous operation is desired, a simple modification to the batteries is all that is necessary, for instance, using a separate higher capacity battery for the calculator. The only other assembly required for use of this or most other transient instruments is a voltage divider.

The measured signal on a mine power system may range from a few hundred volts up to 14,000 V, under normal conditions. Under transient conditions, the signal may be as high as 120,000 V. Obviously, the amplitude of this signal must be reduced before it is supplied to the instrumentation. For this research, a resistive voltage divider with a ratio of 10,000:1 has been used for measurements on distribution systems. Thus, a 50,000 V transient would cause 5.0 V to appear on the instrumentation input.

If care is exercised in construction, the inexpensive divider discussed in reference 3, and again shown in Figure 4.14, can be used with minimal problems. More sophisticated versions, with capacitors which cancel the stray capacitance, can be built if desired. Where size is a factor, a more compact divider can be constructed by mounting the resistors, in a straight line, on a piece of "perf board." The resistor-lead lengths should also be minimized, and the assembly should be mounted in a non-metallic box. The divider should then be tested to insure that the division ratio is the same at 60 Hz as it is at 1.0 MHz.

The construction and use of voltage dividers are fairly simple, as indicated here. However, there are pitfalls to their use. Although this type of divider is constructed from only resistors, capacitive coupling creates problems. The capacitance of the lead terminals and stray capacitance, form a low-impedance path around the divider. Consequently, high-frequency transients can be recorded at an incorrectly higher value. Other problems, such as "ringing," may also occur. Thus, a reference, such as reference 5, should be reviewed before attempting operation.

4.1.4. Summary

In-mine transient measurements are a worthwhile endeavor at any mine. The Peak Detector or the Transient Detector developed during this research can be easily and economically constructed. The choice of which one to use depends upon the information desired.

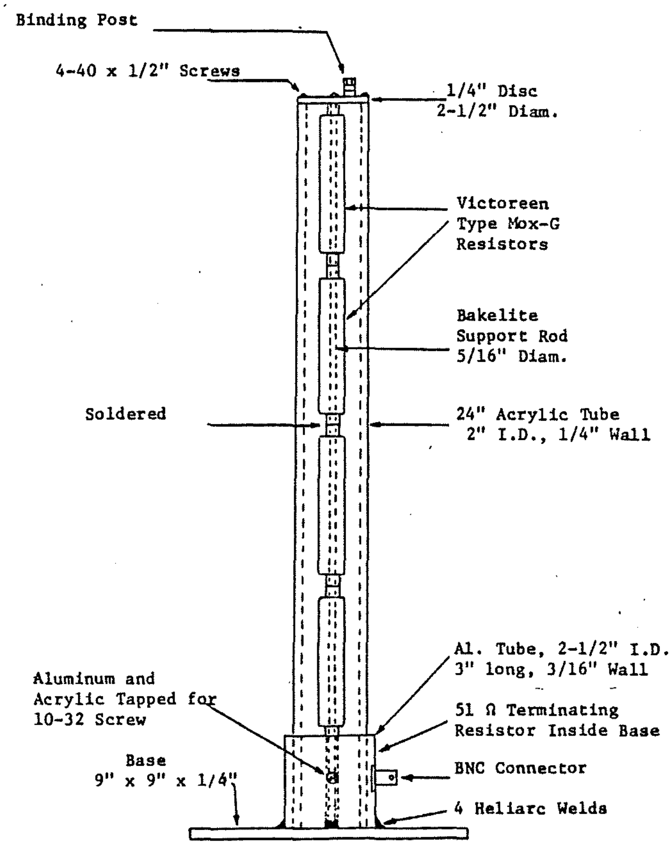

Figure 4.14. A Voltage Divider for Transient Measurements.

The utility of the Transient Detector is in collecting sufficient data to enable the selection of appropriate transient protection. According, its measured-parameter precision is less than 20% for the worst case of an almost square wave, and less than 10% for the typical waveform case. Field experience with this device has demonstrated its ability to collect useful data with minimum effort. However, it should be mentioned that the Transient Detector described here is a prototype. Anyone desirous of producing this device should thoroughly investigate its circuitry.

4.2. TRANSIENTS ON MINE SYSTEMS

4.2.1. Previous Effort

Previous to this last reporting period, an extensive series of transient measurements were made by project personnel on underground coal-mine electrical systems. Emphasis was primarily pointed at high-voltage distribution systems, but some utilization-system recordings were performed. The work was enhanced by an extensive literature survey which, because of availability, only covered similar industrial applications other than mining. The results of all research were presented in previous reports (1,3).

Subsequent to the formulation of reference 3, it was found that more information was required about transient sources in relation to equipment failures and personnel safety. The desires were twofold. First, the preceding results on distribution systems needed additional verification. Here, it was hoped that additional comparison of theory with the previous findings would provide the confirmation; if not, further measurements would be required. Next, because of time constraints, the past effort on utilization systems was minimal; thus, more research of these systems was necessary. In this case, the development of the Transient Detector could allow extensive routine measurements. Through both efforts, the goal was to gain a satisfactory knowledge of mine-power-system transients, the principal objective being the definition of worst-case events. The following will discuss the findings of the research and the information is divided into two major sections: Distribution Systems and Utilization Systems.

4.2.2. Transients on Mine Distribution Systems

General. Transient overvoltages are created by several sources, and a discussion of these in light of underground coal-mine power systems has already been presented (3). However, because of the succeeding arguments, a summary of possible sources is beneficial here.

When investigating transients on these mine systems, three important facts should always be considered.

1. The a-c distribution system is resistance grounded with extensive ground-fault protection.

2. Three-phase conductors extending underground are in (SHD) shielded-cable configurations.

3. Direct lightning strokes can only occur on the surface.

Accordingly, events caused by line-to-ground faults, restriking ground faults, and contact with higher voltage systems are rare. From typical system resistance, inductance, and capacitance combinations, resonant-created transients are also uncommon.

In terms of direct lightning strokes on the surface to a power conductor, the penetration of any traveling wave into the underground phase conductors has a substantial voltage-magnitude reduction. For instance, the refracted wave underground, assuming energy conservation, would have a crest value (6):

$$v_3 = \frac{2Z_2}{Z_2 + Z_1} v_1 \tag{4.1}$$

where

v_3 = the crest voltage of the wave propagating underground, V

v_1 = the crest voltage of the incident wave from the surface, V

Z_1 = the characteristic impedance of the surface phase conductor, Ω

Z_2 = the characteristic impedance of the underground phase conductor, Ω.

A representative characteristic impedance for a surface overhead phase conductor is about 400 Ω, while that for a typical shielded feeder or borehole cable is 50 Ω (sometimes as low as 40 Ω). Thus, using the above equation, the surge penetrating the cable would only have around 22% of the surface voltage magnitude.

Of all transient overvoltage sources on coal-mine distribution, by far the majority of all events (perhaps as much as 99%) are caused by lightning and switching. Considering the thought of traveling-wave refraction, switching operations must then account for the majority of all transient phenomena on underground systems. The previous in-mine measurements (3) have substantiated this statement and have also shown that switching transients are the most destructive. (Except for direct lightning strokes, these findings can also be applied to surface-mine distribution.)

Switching events can be categorized into three basic types: capacitance switching, current chopping, and prestrike. Each will be reviewed in the following paragraphs.

Capacitance Switching ("Restrike"). From the extensive use of cables, surge capacitors, and power-factor-correction capacitors, capacitance plays a major role in most mine electrical systems. Abnormal transients can occur when current to capacitance is interrupted (5,6). The problem is that current leads voltage by nearly 90°. Capacitive currents are usually rather small so there is a good chance that current flow is stopped at a very early current zero. For a circuit breaker, such could occur shortly after contact separation with the contact gap being small. Thus, the load-side capacitance would be charged to the peak voltage of the system, and this energy becomes trapped.

Obviously, the source-side voltage at the breaker continues to alternate at the normal system frequency. Because early current interruption is possible, the circuit-breaker recovery voltage (that between the contacts) may attain two times the system peak when the contact gap is very small. Hence, the arc may reignite or "restrike." With restrike, an inductance-capacitance circuit is formed with a resonant frequency

$$f_o = \frac{\omega_o}{2\pi} = \frac{1}{2\pi (LC)^{1/2}} \tag{4.2}$$

where

f_o = the resonant or "natural frequency" of the system, Hz

L = the system inductance, H

C = the system capacitance, F.

The transient voltage per phase for the load-side capacitance is (on worst case):

$$v_c = V_M - 2V_M\cos(\omega_o t) \tag{4.3}$$

in which

v_c = load-side voltage, V

V_M = the peak source voltage, V

This equation is of special interest as the transient voltage can obtain three times the peak system voltage. The transient voltage waveform does decay with time due to damping by system resistance. However, if the capacitor voltage is around $3V_M$ when circuit-breaker current again becomes zero, another current interruption will trap $3V_M$ across the load-side capacitance. Now, the recovery voltage may approach $4V_M$, causing a second restrike and a capacitance voltage near $-5V_M$. Such a "multiple-restrike" process can continue, developing higher voltages. For instance, the transient overvoltage could theoretically attain $7V_M$ with a third restrike.

The problem here is large capacitance as seen by the switching apparatus, with a very small impedance between the load-side contact and that capacitance. Situation examples could include the charging current to an unloaded cable or distribution line. Yet, perhaps the most drastic instance would be interrupting current to a load-side static capacitor bank, involving either one phase of a grounded bank or two phases of an ungrounded bank.

Current Chopping. "Current chopping" is the phenomenon of forcing current to zero before a natural current zero. The effect can trap magnetic energy in the inductance (mainly transformers) on the load-side of the switching apparatus. This energy can then be transferred to the load-side capacitance, and the crest of the resulting transient voltage can reach (accounting for normal system losses):

$$V_p = 0.63I\left(\frac{L}{C}\right)^{1/2} = 0.63IZ_o \tag{4.4}$$

where

V_p = the peak transient voltage, V

C = load-side capacitance, F

L = load-side inductance, H

I = the magnitude of chopped current, A

Z_o = the "characteristic impedance" or "surge impedance" of the system, Ω.

The level of overvoltage created is independent of the system voltage but is inversely proportional to the square root of the load-side capacitance. Thus, increasing this capacitance decreases the maximum voltage possible by chopping, and adding surge capacitors is an approach to controlling these events. The energy transferral, back and forth from inductance to capacitance, will cause oscillations at the natural frequency of the power system (again, equation 4.2). The transient waveform will decay through damping by system resistance.

A likely arrangement, which would promote current-chopping transients in mining distribution, would be a switchhouse connected to an energized, but unloaded, transformer through a short feeder cable. Thus, load-side capacitance would be small and the surge impedance high. Here, transformer magnetizing current will be about 0.03 to 0.05 pu of rated current. If this current is chopped by the switching apparatus, transient crest voltages up to $7V_M$ on a per-phase basis may be expected.

Transients created through current chopping have received the most concern in recent years. The worry has been connected with the increased use of vacuum circuit breakers, perhaps to the point where current-chopping transients have become associated with VCB's. These interrupters, through their high-efficiency arc environment, can easily chop "small" currents (e.g., transformer magnetizing). However, all circuit breakers can cause chopping, as well as certain fuses, especially current-limiting types.

Prestrike. As implied, added system capacitance can reduce the effects of chopping, but large capacitance may not only cause severe transients upon de-energizing through restrike but also upon energizing. Researchers (7, 8, 9) have shown that during energizing of system capacitance, an arc ignition or "prestriking" may occur across the contacts of a circuit breaker, prior to (final) mechanical closure. The phenomenon appears to be enhanced when the load-side capacitance is "considerably" in excess of the source-side capacitance. However, these events seem dependent upon the capacitive inrush current, and the magnitude of inrush current is controlled by the amount of load-side capacitance. Prestrike transients have usually been associated with vacuum interrupters, and overvoltages have been found to reach substantial levels if the initial inrush current caused by the prestrike is momentarily stopped then followed by a subsequent prestrike or contact closure. Situations can involve energizing one phase of grounded capacitance or two phases of ungrounded capacitance.

Hypotheses accounting for prestriking include the following (9):

1. Contact "whiskers." When exposed to high electrostatic stress in a vacuum, extremely fine filaments can grow from the surface of metals. Such filaments could cause an arc ignition.

2. High electric-field strength. Stress created by a high electric-field strength could cause breakdown of the dielectric.

3. Contact bounce. Contact bounce is deflection of the moving contact after impact with the fixed. Considered being caused primarily by a weak operating mechanism, the resulting separation could allow arc extinction.

Whatever the source, if the load-side capacitance is uncharged and a prestrike occurs, the voltage on the immediate load side of the breaker will collapse to zero. This can cause voltage and current traveling waves to radiate on cables and lines. The waves can reflect and refract at discontinuities of the system characteristic impedance, and the typical frequencies of the resultant waveforms can be 60, 600, 6000, 60,000, and 600,000 Hz, all superimposed. The combination of the harmonics obviously has many current zeros and, when these zeros occur between the prestrike and the mechanical-pole closing, the circuit breaker can easily interrupt the inrush current flow. In the same manner as capacitance switching, energy can be trapped on the capacitance being energized. Subsequent arc reignitions then interruptions can create an unusually rapid escalation of high overvoltage. Pflantz (9) has found that prestrike transients can have crest voltages up to 7.0 pu of system peak with an oscillating frequency band that spans from 60 Hz into the megahertz region.

Switching-transient Summary. The combination of capacitance switching, chopping, and prestrike is very perplexing for high-voltage system design. If capacitance on the downstream side of an interrupter is small, destructive voltage transients can occur from current chopping. However, when this load-side capacitance is large, overvoltages may result from capacitance switching or prestrike events. Consequently, the placement of capacitance within the system is critical, and this will be discussed later.

It is interesting to note from the foregoing discussion that the resulting overvoltage in each switching-transient case can crest in the neighborhood of 7.0 pu of the system peak ($7V_M$) or more. However, a way to distinguish among the types is from the oscillation frequency: the system natural frequency for capacitance switching or chopping (generally less than 10 kHz) and much higher for prestrike (often these have frequency components greater than 100 kHz).

Previous Research Comparison. A summary of the previous research findings on distribution systems follows. The conclusions were based on measurements involving both in-mine on existing systems and on-the-surface using actual underground power equipment. For the most part, these involved recording transients on unloaded and loaded systems created by chopping or capacitance switching (tripping the interrupter) and by prestrike (engaging the interrupter). The system segment in every instance consisted of a VCB-equipped switchhouse with various lengths of feeder cable supplying a load center. Low-sparkover, distribution-class surge arresters, connected across transformer primaries, afforded transient protection during all testing. Transformer capacities were 600, 750, and 1000 kVA. System voltages were 7200 and 12,470 Vac. Voltage-divider connections were at both the immediate downstream side of the circuit breaker and the immediate upstream side of the power transformer. The system characteristic impedance at the measurement points was around 40 to 50 Ω.

From the measurements, chopping transients were found to be substantially reduced whenever load-side capacitance was significant (e.g., 1000 ft of SH-D cable yielding about 0.1 μF per phase) or when surge capacitors (0.25 μF per phase) were on the load-side. Without surge capacitors and with cable capacitance minimized (50 ft of SH-D, approximately 5000 pF per phase, excluding transformer capacitance), chopping transients were frequent, but the maximum per-phase value was about 4.5 pu of system crest voltage. Oscillation frequencies in these cases were 10 kHz and less, with a minimum rise time of about 100 μs.

When the interrupter load-side capacitance was maximized (surge capacitors on line and the feeder-cable length at 1000 ft or greater), severe high-frequency transients were often observed on interrupter engaging. Typical recorded maximum per-phase voltages were about 7.0 pu of system crest, approaching the sparkover voltage of the surge arresters. Maximum oscillation frequencies were 1.0 MHz with minimum rise times bordering on 1.0 μs. The duration of events like these extended for around 5.0 μs. Although severe events were frequent regardless of surge-capacitor location, the worst-case situations were associated with capacitors located on the immediate downstream side of the interrupter. Yet, because of interrupter engaging, all these transients were thought to be from prestrike. On a couple of observations, voltage transients up to 9.0 pu were measured, but these occurrences were believed suspicious because the values were above what was considered normal transient suppression. No abnormal capacitance-switching transients were observed during interrupter tripping.

These findings are in close agreement with switching-transient theory. The high frequencies observed on the worst-case events definitely point to their being a result of prestrike. Consequently, it is the researcher's opinion that no additional field measurements are necessary on distribution. Assuming that the 9.0 pu values were a result of measurement problems, the worst-case distribution event that could be expected is:

1. magnitude of 7.0 pu of system crest,

2. minimum rise time of 1.0 μs, and

3. maximum duration of 5.0 μs.

(Note: From measurement data, events caused by other phenomena could have longer rise times and durations by usually reduced magnitudes. For instance, the worst chopping event observed had a 4.5 pu crest with 0.1 ms rise time and about 0.5 ms duration.)

Protection. Conventional methods of suppression appear to be adequate in protecting the underground-mine distribution system (and what is directly connected to it) against energies resulting from such events. Much has been written about the application of surge protection devices (e.g., references 4, 5, 10, 11, 12, and 13), but only a couple of articles (14, 15) have been produced on the unique properties of mine systems. Hence, it would be beneficial to examine how protection can be applied in this application. The next section will cover this subject. The information is actually beyond the task scope of work but is included for report completeness.

4.2.3. Transient Protection on Mine Distribution

General. It was stated in an earlier report (3) that elimination of transient-voltage problems is best started with an excellent power-system design applying time-tested principles. The basic thought is to avoid the situations covered previously. However, such an effort often can only address normal conditions, and the unpredictable abnormal conditions can still arise, producing destructive transient overvoltages (5). Accordingly, additional overvoltage control must be placed in the mine power system. The traditional methods that afford this protection on distribution fall into two categories: surge arresters and surge capacitors. The role of these protective devices is to ensure that equipment dielectric strengths are not exceeded. In other words, if a transient attempts to raise the voltage above an insulation withstand level, the protective device must exert a clamp or restraint to maintain voltage within acceptable limits (5). Effective transient voltage suppression is, thus, basically the dissipation of transient energy.

Surge Arresters. The most simple form of overvoltage device is the spark gap, essentially two conductors separated by air. Direct application of this device has one main disadvantage. Once an arc occurs, it creates a fault on the system which remains until the gap is deionized. The attendant current flow or "follow current" often can only be interrupted by a circuit breaker or a fuse. Surge arresters, formerly called "lightning arresters," use this spark-gap principle to clip the peak of the voltage and divert the excess current to ground; they also contain a device to interrupt the follow current (13). The most important surge arrester type for use in mine power distribution systems is the valve surge arrester.

In valve surge arresters, the spark gap is in series with a non-linear resistor or valve block. The block, commonly made of silicon carbide, has the property that the resistance diminishes sharply as the voltage across it increases. To increase spark-gap efficiency, a number of short gaps are used; these sparkover more consistently and in less time than the one long gap. Therefore, the gaps spark over on an overvoltage, and the valve block operates in its highest conductance mode to safely pass the surge current to ground. After the surge voltage diminishes, the block then changes to a low-conductance mode to limit the follow current, such that the gaps can provide an arc interruption.

Four important parameters are connected with the proper application of surge arresters (13).

1. Voltage rating. The "power frequency sparkover voltage" is the lowest rms 60-Hz a-c voltage across the arrester at which it will perform the operating cycle. This level is 1.5 times the arrester voltage rating (for arresters rated at 60 kV and below).

2. Sparkover voltage. The highest crest voltage at which the arcs will form across the gap electrodes, initiating the operating cycle.

3. Discharge current. This is the current through the arrester created by the overvoltage immediately after the sparkover.

4. IR-discharge voltage. This is the voltage across the arrester during the discharge of surge current.

Ideally, gap sparkovers should occur on any dangerous system overvoltage, ignoring all minor and harmless transients. After sparkover, the IR-discharge voltage occurs, being equal to the product of the discharge current and the arrester-discharge-path resistance. As discharge current may be very large, the discharge voltage may equal or exceed the sparkover voltage. Thus, protected equipment are exposed to both the sparkover and IR-discharge voltages, and the system insulation withstand ability or BIL must be safely above both.

To establish an IR-discharge voltage, it is important to realize the possible discharge current. Field measurement have shown that discharge current (13);

1. typically ranges from 1000 to 2000 A,

2. that 5.0% exceed 9000 A, and

3. that only 1.0% exceed 20,000 A.

Even though 20,000 A is rare, it is often used to estimate the discharge voltage, justifying a worst case.

There are three classes of valve-type arresters available; station class, intermediate class, distribution class. The factors to consider when selecting a class for an application are the degree of transient exposure and the importance of the equipment being protected. This is basically an economic question but, in general, intermediate or station arresters are justifiable for surface substations, with distribution-class arresters being suitable for distribution and normal utilization-equipment protection. The latter type is therefore applicable to this discussion.

Typical voltage ratings of distribution-class arresters range from 1000 V to 18 kV, and they can withstand a 65 kA current surge (surge arresters are actually available as low as 50 V). When protecting rotating machinery and dry-type transformers, because of commonly low BIL's, they must be the low-sparkover rotating-machinery (RM) type.

An arrester voltage rating has associated sparkover and IR-discharge voltages. System voltage, as well as the method of system grounding, affects the voltage that the protective device is exposed to and, therefore, the selection of the arrester voltage rating. Consequently, once an arrester voltage rating is set, the system BIL must be coordinated.

Arrester application versus system grounding refers to two categories: effectively grounded and non-effectively grounded. The "coefficient of grounding" can be employed to find catagory is being used and is defined as the percent ratio of the highest rms line-to-ground voltage existing during a line-to-ground fault to the nominal line-to-line voltage (13). If the ratio does not exceed 80%, the system is called "effectively grounded." Solidly grounded and typically low-resistance-grounded systems (current limits of 200 to 400 A) are in this class. (The neutral potential remains rather constant in these systems during a phase-to-neutral fault.) However, for high-resistance and ungrounded systems, the occurrence of phase-to-neutral fault can shift the neutral to near the faulted phase, with the potential to ground of the other two phases approaching the phase-to-phase system voltage. The coefficient of grounding here can be from 80 to 100%. Thus, these systems are termed "non-effectively grounded," and resistance-grounded mine power systems serving portable and mobile equipment are included. In either grounding case, the arrester voltage rating should be above the exposed crest voltage. If not, a disruptive discharge might occur.

Therefore, on effectively grounded systems, the arrester is sized to maximum expected line-to-ground voltage, whereas maximum line-to-line voltage is used for non-effectively grounded systems (11). To allow for the expected increase due to voltage-regulation compensation, the voltage rating should be five to ten percent above these values (references 11, 12, 13, and 15 can be consulted for typical application tables).

With a selected arrester, equipment protection from voltage surges can be verified. Full coordination requires checking arrester performance over a full line range for an expected surge (11). However, the following quick guidelines will ensure safe protection (17, 18).

1. The insulation BIL ratings of the equipment should be at least 20% greater than the arrester sparkover voltage.

2. The BIL rating should be above the IR-discharge voltage of the arrester.

As mentioned earlier, a discharge current of 20,000 A to establish IR-discharge voltage is a good approximation of worst-case conditions. However, this value is more applicable to surface portions of distribution, and discharge currents of not more than 3000 A can be assumed within the underground system (19). (Manufacturer catalog values should be consulted for actual applications as differences among manufacturers' products exist.)

An additional important point about maximum exposed surge voltage concerns the arrester connections from line and ground. These conductors extend from each ungrounded power conductor to an arrester and from the arrester to ground (in three-phase systems, a minimum of three arresters are needed). For stationary equipment on the surface, an arrester ground bed, such as a substation (station) ground bed, can serve as the grounding medium; on portable equipment, the frame would be the ground. As the connections exhibit inductance, they should be as short as possible and of No. 6 AWG solid-copper conductor or larger. Otherwise, the inductance of too long a conductor can render an arrester ineffective (5). Sharp bends should also be avoided, because a bend substantially increases effective inductance. The inductance of connections, which adhere to these requirements, is estimated at 0.4 H/ft. A good estimate of a voltage drop produced during a surge is 1.6 kV/ft, using a current wavefront of 4000 A/s (13). Whichever value is used, the resulting extra voltage should be added to sparkover and IR-discharge voltages to assess protective margins.

As a general rule, all arresters should be located as close as possible to the equipment they are to protect. Ideally, they should be across the protected equipment terminals, the connections for three-phase systems being a wye configuration with the common arrester connection grounded. First of all, this location minimizes the possibility of a destructive surge entering the circuit between the protecting and protected devices (5). Secondly, close proximity also reduces the chance of surge-voltage amplification through reflection of a traveling wave. The problem is that surge-arrester locations, other than directly across the equipment terminals, can lead to higher surge voltages at the protected apparatus than the arrester sparkover voltage. (Note: With the wavefront rise time no greater than 0.5 s, a maximum distance of 25 ft is perhaps allowable, but shorter distances always afford greater protection (4).)

A further point should be stated about selecting minimum BIL's for the system. The foregoing criteria assumes correct arrester operation and only applies to protected equipment. For system portions which cannot be protected, a better criterion might be to base BIL's on the maximum anticipated transient crest voltage with the traditional 20% safety factor. Using the 7.0-pu value stated earlier, the minimum of 95-kV BIL would be acceptable for 15-kV class systems, 60-kV BIL for 8.7-kV class, and 35-kV for 5-kV equipment. Considering that protection can fail, these are perhaps the desirous minimums for underground-coal-mine distribution systems. (Note: IEEE (4) does recommend slightly different values for distribution-class equipment: 60-kV BIL for 15-kV class insulation, 45-kV BIL for 8.7 kV, and 30-kV for 5 kV. Past NEMA recommendations have only specified 50-kV, 35-kV, 25-kV BIL's, respectively for these insulation classes (12).)

Surge capacitors. Surge capacitors, also termed "rotating machinery (RM) capacitors," are special units with low internal inductance that are used extensively to protect rotating machinery and dry-insulated transformers (4). These equipment are very susceptible to line-end turn-to-turn failures caused by fast rise-time wavefronts. The faster the rise time, the greater is the probability for damage. Connected across the equipment in a grounded-wye configuration, the capacitors serve to limit the transient-voltage rate of rise. Simply, the capacitor has to be charged before the overvoltage can be impressed on the system dielectric; transient rise time is then largely determined by the capacitor charging rate. Coupled with the system inductance, the limiting criterion is that at least 10 μs is needed before the crest value of the equipment nameplate voltage is reached (4). Low internal inductance of the capacitor is important, because the presence of series inductance in the capacitor circuit deteriorates the wave-sloping action. Obviously, the capacitors must be located as close as possible to the protected equipment with very short connections to insure protection.

The following capacitors have been standardized for protection by wave sloping (4):

1. 1.0 μF for 650 V or less rated equipment,

2. 0.5 μF for 2400 to 6900 V rated equipment,

3. 0.25 μF for 11,500 V or higher rated equipment.

With these in combination with the recommended low-sparkover distribution-class surge arresters, the crest voltage of transients is considered restricted to harmless values for utilization equipment (13).

Surge capacitors can also be used to control transient overvoltages by reducing the system characteristic impedance. An increase of system capacitance, as exhibited by equation 4.4, can lower surge impedance and therefore the peak transient voltage resulting from possible current chopping. However, a fine line exists here. As shown earlier, too much capacitance on the load side of the switching apparatus can cause capacitive switching or pre-strike transients. System capacitance is therefore a critical factor in transient protection.

Hence, the problem of characteristic-impedance reduction is mainly pointed at how much capacitance is necessary to limit transient overvoltages caused by current chopping. Actually, any magnitude safely below the minimum insulation withstand level or if used, the surge-arrester sparkover, can be considered adequate, yet perhaps the most conservative approach would be to limit any chopping event to two times the peak system voltage. The most critical portion of the mine power system would be where capacitance is minimum, such as the case with the switchhouse connected to a distribution transformer or rotating machinery.

Equation 4.4 can be used to select a value of capacitance, which will include that inherent to the distribution system (i.e., the equivalent phase-to-neutral capacitance of all devices on the load side of the switching apparatus). Considering a three-phase transformer as the load, the procedure can be as follows (20).

1. Determine the allowable peak voltage, V_p.
2. Find the exciting current and assume interruption is at peak level, I_m.
3. Determine the transformer exciting inductance, L_m.
4. Assume all transient energy is absorbed by the capacitance, C.
5. The necessary per-phase capacitance in farads, referred to the transformer primary circuit, is then

$$C = \frac{I_m^2 L_m}{V_p^2} \qquad (4.5)$$

The value resulting from equation 4.5 is total system capacitance per phase. If the level is above that supplied to the system, additional capacitance might need to be added.

For three-phase systems the common surge-capacitor connection is in a wye configuration with the center being connected to ground. Two advantages are gained through the ground connection: transient energy is shunted to ground and, in comparison to delta connections, a lesser voltage rating is necessary. The capacitor working voltage rating (WVDC) should be at least three times the exposed rms system voltage, usually phase-to-neutral for wye grounded, phase-to-phase for delta connections (20). For the same reasons given for surge arresters, it is perphaps best to rate surge capacitors in resistance-grounded systems to phase-to-phase voltages.

The typical capacitor location, be it for wave-sloping or characteristic-impedance-reduction applications, is directly across the protected equipment terminals. Another popular location, which recently has been used in the industry, is immediately downstream of the switching-apparatus terminals. The philosophy here is that the interrupter directly sees the increased system capacitance and, therefore, chopping transients are limited more effectively. In other words, transients are best elminated at their source. Furthermore, it is a belief that the entire system downstream of the capacitor location would receive protection. However, surge capacitors have an extremely low internal series impedance. Thus, at an interrupter load terminals, they can be a significant source of capacitive inrush current, as well as having the ability to efficiently exchange transient energy to and from the system. This is a likely reason why the worst-case transients, which resulted from prestrike, were associated with switchhouse-located surge capacitors. Consequently, it is the authors' opinion that the best location for applying surge capacitors (when they are needed) is at the protected equipment terminals. If such is not practical, a series-impedance should exist between the interrupter and the capacitors. The determination of the minimum impedance value is beyond the scope of work. Yet, from the research results, a safe empirical valve should be the equivalent of 50 ft of 1/0 SH-D cable.

It is interesting to note the previous research (3) conclusion that surge arresters alone were considered sufficient transient protection for underground-coal-mine power systems. Furthermore, surge capacitors were at least unnecessary redundant protection, and their general use could result in more severe transients than those they were installed to correct. As long as surge arresters protect each distribution load, it was found that vacuum circuit breakers can be employed on any mine power distribution system without a need to add surge capacitors. However, without surge capacitors, a significant length of cable should be installed between switchhouses and loads to limit chopping events to safe levels. For general mining applications, 500 ft of SH-D cable was recommended, although 100 ft would probably be satisfactory.

Recent work under this grant has not changed these recommendations. Yet, an additional benefit for the above use of cable should be stated. Beyond overall surge impedance reduction (if lumped circuit elements are considered), the normally lower characteristic impedance of the cable, as compared to that of the switchhouse circuits, provides a reduction to the crest of the voltage traveling waves through refraction.

Even with these findings for underground-mine distribution systems, some installations could benefit from the wave-sloping action of surge capacitors. One instance would be in surface mines, where there is a high incident of lightning and the distribution loads are rotating machines (e.g., excavators) or dry-insulated transformers.

4.2.4. Transients on Mine Utilization Systems

General. The discussion thus far has concerned only transients on high-voltage distribution. This section's application is not direct utilization from mine distribution, as such would be classed with the foregoing, but is low- and medium-voltage underground-mine systems. The implication is that a power transformer exists between the distribution system and the utilization equipment. Therefore, of interest here are face low- and medium-voltage (a-c and d-c) systems and trolley systems.

The theory behind transients on these systems was provided in a preceding report (3) and will not be presented here. Protection against utilization events has been the responsibility of West Virginia University under Grant G0144137. Their results are available in reference 21.

Results. Measurements for these events were taken with Transient Recorder and the Transient Detector (the latter instrument was used much more extensively). For face equipment, the a-c measurement points were between the low-voltage a-c bus bars and frame ground, likewise for d-c work, between the positive and negative d-c bus bars. On trolley systems, several different instruments sites were tried, but worst-case events were observed at the center of rectifier blocks (equidistant between the rectifiers) or at the end of dead-ended trolley lines (i.e., rectifier feed from one end only). The voltage divider ratio was 1000:1 for all measurements.

The worst-case events for the above conditions are presented in Table 4.4. These were observed on the following actual face situations:

1. a-c, 750-kVA 7200/600-V load center,

2. d-c, 150-kW 480-Vac/300-Vdc rectifier.

The trolley system events were recorded on a 300-Vdc trolley line. Here, a 60-ton locomotive was located at the center of a 2000-ft block. The brakes were locked, and the locomotive contactors were dropped at a full-load current.

4.3. CONCLUSIONS

All objectives as specified in the scope of work for this task have been accomplished. Through the instrumentation effort, an inexpensive transient detector was developed, capable of capturing power-system voltage transients and recording their peak voltage, rise time, and duration. Two of these devices were delivered to the Technical Project Officer. From the detailed analysis of switching transients, the previous research findings on distribution systems were confirmed. Finally, from the collection of additional transient data, knowledge of typical worse-case voltage transients existing on mine low- and medium-voltage utilization systems was gained. As a result of all these efforts, a satisfactory knowledge of mine-power-system transients has been uncovered.

Table 4.4. Worst-case Voltage Transients Observed on Underground-coal-Mining Utilization.

Application	Crest Voltage per System Nominal	Rise Time	Duration
a-c face	5 pu	1 ms	5 ms
d-c face	4 pu	10 μs	2 ms
trolley	14 pu	0.5 ms	5 ms

4.4. REFERENCES

1. Stefanko, R., L. A. Morley, and W. R. Chubb, "Mine Electrical Systems Evaluation - Transient Analysis," Final report for USBM Grant G0133077, NTIS PB 245929/AS, July 18, 1974.

2. Morley, L. A., F. C. Trutt, and J. L. Kohler, "Evaluation of Coal Mine Electrical System Safety," Annual report for USBM Grant G0155003, NTIS PB 80-119514, December 1977.

3. Morley, L. A., J. L. Kohler, and W. R. Chubb, "Coal Mine Electrical Systems Evaluation - Volume II - Transient Analysis," Annual report on USBM Grant G0155003, NTIS PB 283491/AS, May 15, 1977.

4. IEEE, Standard 141-1981, IEEE Recommended Practice for Electric Power Distribution for Industrial Plants, IEEE, New York, 1981.

5. Greenwood, A. N., Electrical Transients in Power Systems, John Wiley and Sons, Inc., New York, 1971.

6. Beehler, J. E., "Capacitance Switching with Power Circuit Breakers," A paper presented at the IEEE Symposium on Capacitance Switching Capability, New York, January 31, 1968.

7. Pflantz, H. M., "Analysis of Multiple Prestrike and Interruption Phenomena in Capacitive Circuits," A paper presented at the IEEE Summer Meeting of the Power Engineering Society, San Francisco, July 12, 1972.

8. Pflantz, H. M. and G. N. Leaster, "Control of Overvoltages on Energizing Capacitor Banks," A paper presented at the IEEE Summer Meeting of the Power Engineering Society, San Francisco, July 12, 1972.

9. Boehne, E. W., "Energization Surges in Capacitive Circuits," IEEE Conference Paper 70CP235-PWR, Presented at the IEEE Winter Power Meeting, 1970.

10. ANSI, Standard C62.1-1975 (also IEEE Standard 28-1974), IEEE Standard for Surge Arresters for Alternating Current Power Circuits, ANSI, New York, 1975.

11. ANSI, Standard C62.2-1969, U.S.A. Standard Guide for Application of Value Type Lightning Arresters for Alternating Current Systems, ANSI, New York, 1969.

12. ANSI, Standard C57.12.00-1973 (also IEEE Standard 462-1973), IEEE Standard General Requirements for Distribution, Power, and Regulating Transformers, ANSI, New York, 1973.

13. Ohio Brass, "How Does a Distribution Class Surge Arrester Work?," Technical Booklet 2470-H, The Ohio Brass Company, Mansfield, Ohio.

14. Smith, E. P., "Lightning Arrester Applications for Mine Power Systems," Conf. Record of the 1976 IEEE-IAS Annual, Chicago, IL, Oct. 11-14, 1976.

15. Morley, L. A., "Mine Power Systems - Chapter 10 - Transients and Overvoltages," Final report for USBM Contract J0155009, July 31, 1980.

16. McGraw-Edison Company, Distribution-System Protection Manual, Bulletin No. 71022, McGraw-Edison Company, Power Systems Division, Canonsburg, PA.

17. Westinghouse, Electrical Transmission and Distribution Reference Book, Westinghouse Electric Corporation, Central Station Engineers, East Pittsburgh, PA, 1964.

18. Morley, L. A., Mine Power Systems, Volumes I and II, final report on USBM Contract J0155009, August, 1981.

19. IEEE, IEEE Recommended Practice for Underground Mine Power Centers, a standard now in preparation under an IEEE Working Group for Project P 685.

20. Stanek, E. K., Professor and Head of Electrical Engineering, Michigan Technological Univ., Personal Communication, August, 1977.

21. Stanek, E. K., "Transients Protection, Reliability Investigation, and Safety Testing of Mine Electrical Power Systems - Volume I - Transients in Mine Electrical Power Systems," Final report for USBM Grant G0144137, August 1979.

APPENDIX I

ABSTRACTS OF REPORTS AND THESES PRODUCED UNDER USBM GRANT G0155003

I.0. GENERAL

This appendix abstracts all the preceding reports and theses that have been produced under USBM Grant G0155003. There have been twelve major reports and six theses. Each document will be presented by its formal title, followed by a description of its contents.

I.1. REPORTS

1. Morley, L. A., "Evaluation of Coal Mine Electrical System Safety," Annual Report to the USBM, Grant G0155003, USBM OFR, August 1975, 172 p.

This document was the first annual report under the subject grant, detailing research accomplishments during the period July 8, 1974 through July 7, 1975. The effort covered four main interest areas and, accordingly, a report chapter presented each research effort.

The first chapter detailed the first phase of the Electrical Power Safety Monitoring Task. The purpose of this research was to develop a prediction system in which abnormalities are found by continuously monitoring electrical power parameters. The nature of the problem necessitated a study of both system deterioration and techniques to detect and thereby predict incipient failure points. The chapter covered a feasibility study of the monitoring system and its projected structure. The significant parameters and hardware received in-depth coverage. The chapter concluded with statements about a needed experimental program.

The second chapter described the Mine Power System Transient research. The work was a continuation of effort commenced under USBM Grant G0133077: the measurement of coal-mine power-system transients. The chapter contained information on instrumentation, field work, and transient sources.

Mine Cables and Cable Splices was presented in the third chapter. Primary purposes of the work were to evaluate (1) the affects of using shielding in low-voltage trailing cables and (2) a-c trailing cable splices. The chapter commenced with a presentation of the literature which was pointed at shield theory, construction, and underground usage. Low-voltage shielded-cable advantages and disadvantages then received in-depth coverage. Included in this section was a thorough description of proper shielded trailing cable splicing methods. Afterwards, fficacy of shielding and percent coverage was entertained. The chapter concluded with statements concerning a-c non-shielded splices and shielded-cable conclusions.

Direct-current offsets existing in grounding systems was covered in the fourth chapter. The purpose of this research was to investigate these currents in mixed a-c/d-c systems for three specific areas: the source of the currents, their effects on electrical equipment, and competent methods to eliminate them. The chapter first reviewed mixed a-c/d-c underground-coal-mine ground systems followed by discussion of d-c offset problems. A description of the field testing program, conclusions to date, and projected future work closed the chapter.

(Note: The project was without funding from July 8, 1975 through November 4, 1975. Research continued during the period but only quarter reports were supplied to the technical project officer.)

2. Morley, L. A., F. C. Trutt, R. A. Rivell, "Coal Mine Electrical System Evaluation - Computer Modeling," Annual Report to USBM, Grant G0155003, NTIS PB 283496/AS, December, 1976, 163 p.

Research performed on computer modeling of mine power systems during the period November 1975 through November 1976 was described in this report. Results presented were interim in nature, and future research was planned to integrate the simulations which have been developed.

The thrust of this research was divided into three main areas.

1. Modification of a previously developed model (Mine Power System Simulation or MPSS) to include interactive operation and the use of default (average) load data.
2. Development of a dynamic simulation of interdependent mine power system induction motors.
3. Development of an approach to modeling of motor shaft loading of induction machines for mining operations.

During the course of that year's research, significant results were achieved in all areas. Construction of an interactive MPSS model was completed and checked. This simulation was written in APL code and was fully interactive. In addition, default data representing 158 different pieces of mining equipment were developed for use with the interactive model. Additional work described included the construction of a dynamic simulation of interdependent continuous-miner induction motors and the development of an approach for motor-shaft load-torque computation from experimental data.

3. Morley, L. A., R. H. King, P. A. Sopko, "Coal Mine Electrical System Evaluation - Shielded Cables," Annual Report to USBM, Grant G0155003, NTIS PB 283492/AS, January 1977, 170 p.

This report detailed the shielded-cable research during November 5, 1975 through November 4, 1976. Proposed advantages and disadvantages of low-voltage shielded trailing cables were formulated utilizing the literature and industry sources. A partial analysis of these proposed advantages and disadvantages was completed through a review of the literature. Cable costs were assembled from mine operators, cable and splice manufacturers, and actual cable purchases. To confirm each advantage and disadvantage, an underground test site was established, and testing was performed there and in the laboratory. All testing procedures were completely described. The results of this investigation were reported and used to formulate recommendations attendant to low-voltage shielded cables. Suggestions for installation, handling, and maintenance were presented.

4. Morley, L. A., J. L. Kohler, "Coal Mine Electrical System Evaluation - Continuous Monitoring," Annual Report to USBM, Grant G0155003, NTIS PB 283490/AS, January 1977, 270 p.

The second year of the Continuous Electrical Power Safety Monitoring research was detailed in this report. A concept was presented to improve underground-coal-mine electrical-system safety and availability, and the proposed technique was based upon the ability to predict incipient failures in the mine power system. Prediction was made by a new method, developed during this research, which used a minicomputer to implement pattern-recognition algorithms. The theoretical basis of the prediction system was discussed, along with the synthesis of the hardware and software sections. The deterioration modes which could be detected were examined, and an evaluation of the system's ability to predict incipient failure was presented. Typical results of the system's performance during laboratory simulation of power-system deterioration were given.

5. Morley, L. A., J. A. Kiefer, "Coal Mine Electrical System Evaluation - Battery and Battery-Charging Safety," Annual Report to USBM, Grant G0155003, NTIS PB 283494/AS, February 1977, 65 p.

The primary goal of this research report was to discuss safety considerations involved in the use of lead-acid batteries for traction purposes in underground coal mines. This was a new research task added to the project on November 5, 1975.

In order to arrive at the objective, the topic of battery safety was divided into two specific areas. The first dealt with the fact that batteries emit hydrogen gas during and after the charge cycle. The second major topic dealt with the electrical nature of the battery and battery-charging systems, which also provides a source of mine fires as well as electrocution hazards.

In addition to the discussion on battery safety, a literature review was undertaken to acquaint the reader with some basic concepts inherent to the battery-usage process.

The result of this research was a proposed set of design specifications and procedural recommendations directed at improving the safety factors inherent in any underground battery-usage scheme.

6. Morley, L. A., F. C. Trutt, R. A. Rivell, "APL Mine Electrical System Load-Flow Program," Task Completion Report to USBM, Grant G0155003, NTIS PB 283496/AS, April 1977, 136 p.

A guide to the development and use of an APL computer program for the analysis of load-flow problems was presented here. The research (an additional task to the original grant scope of work) was performed from October 4, 1976 through March 4, 1977. The program was designed to provide an interactive method of load-flow study to improve underground-coal-mine electrical-system design and safety.

The theoretical basis for load-flow analysis was discussed, along with per-unit calculations which facilitate computation. Specific input/output, execution, and network modification procedures were presented for using the APL program. In addition, typical results were given for examples taken from power-system-analysis literature.

7. Morley, L. A., J. L. Kohler, W. R. Chubb, "Coal Mine Electrical System Evaluation - Transient Analysis," Annual Report to USBM, Grant G0155003, NTIS PB 283491/AS, May 1977, 68 p.

This report detailed the continuation of mine-power-systems transient research under USBM Grant G0155003. The work period spanned November 4, 1975 through November 3, 1976. The purpose of the work, which commenced under Grant G0133077, was the elimination of safety hazards created by transients, and the objective was to provide knowledge about transients existing in a-c and d-c coal-mine power systems.

The report chapters covered theoretical background, instrumentation, and experimental investigations. The instrumentation discussion scanned measurement problems and considerations plus the development of a low-cost peak detector. Transient data from in-mine measurements were presented and included high-voltage distribution and d-c trolley systems. Extremely unique field exercises were described and used actual power equipment connected on the surface to duplicate typical underground coal-mine system arrangements. Here, transients on high-voltage distribution resulting from vacuum-circuit-breaker operations could be observed under controlled conditions, and work centered around how surge capacitors effect transients. Using the in-mine and staged transient data, specific conclusions and recommendations were made with emphasis on high-voltage distribution.

8. Morley, L. A., "Coal Mine Electrical System Evaluation - Executive Summary," Annual Report to USBM, Grant G0155003, NTIS PB 283495/AS, May 1977, 17 p.

This report abstracted project work performed under USBM Grant G0155003 during the period November 4, 1975 to November 3, 1976. Abstracts comprised the balanced of the document with one exception. The task "d-c offset currents," did not fall under the scope of the other report volumes and, further, the material to be presented did not justify a separate report.

9. Morley, L. A., F. C. Trutt, R. A. Rivell, "Extended APL Mine Electrical System Load-Flow Program," Task Completion Report to USBM, Grant G0155003, NTIS PB 283497/AS, September 1977, 100 p.

The work contained in this report was a continuation of that started with report 6 (above) and was performed from June 1, 1977 through September 30, 1977. Here, a guide to the utilization and development of modifications to the APL Mine-electrical-system Load-flow Program was presented. These modifications included program enhancements in execution time, situation/error checking, and user convenience. In addition, the capability to simulate balanced faults and combined a-c/d-c systems was included.

To test the generality of the algorithms and APL programs, the computing facilities at West Virginia University and Virginia Polytechnic and State University were used in addition to those at The Pennsylvania State University.

10. Morley, L. A., F. C. Trutt, S. A. Thomas, "Dynamic Simulation of Coal Mine Electrical Power Systems," Task Completion Report to USBM, Grant G0155003, NTIS PB 292333/AS, January 1978, 169 p.

Two mine electrical power system simulations were presented in this report. The first was a batch-processed procedure capable of modeling a single mining machine consisting of a number of motors operating under various loads. These loads are the mechanical torque loads present at the motor shaft.

The second simulation was a more flexible tool for modeling entire mine electrical power systems. Detailed analyses of bus voltages, transmissionline power flows, and machine behavior were possible. This simulation operated interactively, and the power system was configured as the user responds to program generated questions and requests.

Development of the theory behind the programming, as well as detailed explanations of the models, was presented. Examples were provided to demonstrate simulation capabilities.

11. Morley, L. A., F. C. Trutt, R. C. Jamison, "Load Modeling of Continuous Induction Motors," Task Completion Report to USBM, Grant G0155003, NTIS PB 292462/AS, January 1978, 138 p.

Two methods were presented in the document to determine the mechanical shaft torque as a function of time for an induction motor. The methods were based on the motor equivalent circuit and used as input variables of the motor terminal voltage, line current, input power, and power factor. One method used all four variables, and the other used only voltage and current. The test data dealt specifically with continuous miners, but the theory could be applied to other mining machines driven by multiple induction motors. Results were given for the tramming, maneuvering, cutting, and cutting with loading operations and are in the form of a minimum, a maximum, and an average of the shaft-torque time function. The theoretical development and computer implementation were discussed for both methods.

12. Morley, L. A., F. C. Trutt, J. L. Kohler, "Evaluation of Coal Mine Electrical System Safety," Annual Report to USBM, Grant G0155003. NTIS PB 80-119514, January 1978, 43 p.

This annual report detailed progress under USBM Grant G0155003 during the projected period of January 1, 1977 through December 31, 1977. The report contained four principal chapters covering accomplishments in the mine electrical safety research areas of continuous monitoring, battery and battery-charging safety, and computer modeling. Highlights of the work were summarized in the last report chapter.

I.2. THESES

1. Kohler, J. L., "A Tentative Method for the Prediction of Mine Power System Component Failures by Pattern Recognition Techniques," An Unpublished M.S. Thesis, The Pennsylvania State University, March 1977, 227 p.

This thesis was basic input to Report 4. A concept was presented to improve underground coal-mine electrical-system safety and availability. This proposed technique was based upon the ability to predict incipient failures in the mine power system. Prediction was made possible by a new method, developed during this research, which used a minicomputer to implement pattern-recognition algorithms.

Theoretical basis of the prediction system was discussed, along with synthesis of the hardware and software sections. The deterioration modes which could be detected were examined, and an evaluation of the system's ability to predict incipient failure was presented. Typical results of the system's performance during laboratory simulation of power-system deterioration were given.

2. Sopko, P. A., "Shielded Low-Voltage Trailing Cables for Underground Coal Mines," An Unpublished M.S. Thesis, The Pennsylvania State University, March 1977, 161 p.

This thesis was the principal input to Report 3 above. Proposed advantages and disadvantages of low-voltage shielded trailing cables were formulated utilizing the literature and industry sources. A partial analysis of these proposed advantages and disadvantages was completed through a review of the literature. Cable costs were assembled from mine operators, cable and splice manufacturers, and actual cable purchases.

To confirm each advantage and disadvantage, an underground test site was established, and testing was performed here and in the laboratory. Testing procedures were completely described. The results of this investigation were reported and used to formulate recommendations attendant to low-voltage shielded cables. Suggestions for installation, handling, and maintenance were presented.

3. Jamison, R. C., "Load-modeling Continuous Miner Induction Motors," An Unpublished M.S. Thesis, The Pennsylvania State University, November 1977, 130 p.

This thesis was the principal input to Report 11 above. Two methods were presented to determine the mechanical shaft torque as a function of time for an induction motor. The methods were based on the motor equivalent circuit and used as input variables the motor terminal voltage, line current, input power, and power factor. One method used all four variables, and the other used only voltage and current. The test data dealt specifically with continuous miners, but the theory could be applied to other mining machines driven by multiple induction motors. Results were given for the tramming, manuevering, cutting, and cutting with loading operations and were in the form of a minimum, a maximum, and an average of the shaft-torque time function. The theoretical development and computer implementation were discussed for both methods.

4. Thomas, S. A., "Dynamic Simulation of Coal Mine Electrical Power Systems," An Unpublished M.S. Thesis, The Pennsylvania State University, November 1977, 161 p.

Report 10 above used this as a major input. Two mine electrical power simulations were presented. The first was a batch-processed procedure capable of modeling a single mining machine consisting of a number of motors operating under various loads. These loads were the mechanical torque loads at the motor shaft.

The second simulation was a more flexible tool for modeling entire mine-electrical-power systems. Detailed analyses of bus voltages, transmission-line power flows, and machine behavior were possible. This simulation operated interactively, and the power system was configured as the user responds to program-generated questions and requests.

Development of the theory behind the programming, as well as detailed explanations of the models, was presented. Examples were provided to demonstrate simulation capabilities.

5. Tylavsky, D. J., " A Microprocessor Based Implementation of the Sequential Events Detections, Analysis, and Prediction System," An Unpublished M.S. Thesis, The Pennsylvania State University, August 1978, 350 p.

This thesis was input to Chapter II of this report where a synopsis has been presented.

A study was presented in the thesis to show the feasibility of using a microprocessor-based system to predict incipient failures in an underground coal-mine power system. The microprocessor-based system was designed to perform many of the functions of a mincomputer-based system, which was currently being used as the failure-prediction system.

The maximum allowable signal-processing time and desired arithmetic accuracy of the proposed system were the two main constraints which governed the selection of a microprocessor and the overall system design. An analysis of the proposed system with respect to these constraints was presented to conclusively show feasibility.

6. Keifer, J. A., "An Assessment of Direct-current Mine-Power-System Failure Parameters," An Unpublished M.S. Thesis, The Pennsylvania State University, March 1979, 86 p.

This thesis was also input to Chapter II of this report where a synopsis has been presented.

Electrical system safety related to the use of d-c haulage equipment in underground coal mines was discussed in this thesis from both theoretical and practical viewpoints. The main objective of the research was to determine if the voltage and current waveforms supplying d-c equipment contained any information which could be used to detect electrical deterioration in the power system.

One result of the investigation showed that harmonics on the d-c waveforms can be used to indicate the presence of electrical faults on the d-c system. An application of the findings was a method for detecting illegitimate loads on trolley-haulage systems.

APPENDIX II

DESCRIPTION OF PREDICTION-SYSTEM SOFTWARE

II.0. GENERAL

The following report appendix contains an in-depth description of the last version of the prediction-system software, titled SEDAPS 2.4. Program-module relationships and principal data structures are presented first. Then, construction of the input/output (I/O) files, measured-data unit conversions, and spectral-component normalization are covered. Afterwards, detailed descriptions of each major program module are given in separate appendix sections. The appendix then concludes with definitions of all major variables.

II.1. PROGRAM MODULE RELATIONSHIPS

II.1.1. Module Name: SEDAPS

Language: FORTRAN

Is an Entry Point In: None

Is called By: None (Main Program)

Calls: INPUT, RDFT, SYCOMP, POLAR, TIMER, CABLE, EVINIT, EVRSET, EVCALC, EVPRNT, EVREFS, DSKDTA, DISKW, DISKR

Brief Description:
This is the primary module of the SEDAPS package. As such, it reads measurements from the environment via an analog-digital converter (ADC), optionally displays this data to the user, optionally stores this data in a measured data I/O file, calculates and optionally displays features of this data, and links to a module which tracks the features for excursions outside of certain limits (error-vector monitoring).

II.1.2. Module Name: ANALGP

Language: FORTRAN

Is an Entry Point In: None

Is Called By: None (Main Program)

Calls: None

Brief Description:
This module builds the analysis-group definition file from information supplied by the user.

II.1.3. Module Name: CPYMRG

Language: FORTRAN

Is an Entry Point In: None

Is Called By: None (Main Program)

Calls: SYSIO (part of the Interdata extended FORTRAN library for binary file manipulation)

Brief Description:
This module provides for copying and merging measured-data files.

II.1.4. Module Name: SYCOMP

Language: FORTRAN

Is an Entry Point In: None

Is Called By: SEDAPS, PLOT

Calls: None

Brief Description:
This subroutine takes three vectors corresponding to phases A, B, and C and computes their symmetrical components; namely, the positive, negative, and zero sequence.

II.1.5. Module Name: PUNCH

Language: FORTRAN

Is an Entry Point In: None

Is Called By: None (Main Program)

Calls: SYSIO (part of the Interdata extended FORTRAN library for binary file manipulation)

Brief Description:
This module converts the measured-data file from a binary format to an ASCII file suitable for intercomputer transfer.

II.1.6. Module Name: INPUT

Language: FORTRAN

Is an Entry Point In: None

Is Called By: SEDAPS

Calls: ADCSET, ADCGET, TIMER, DISKW, DISKR

Brief Description:
This module acquires the measured data either from the ADC or from a measured data I/O file. It also optionally generates a measured data I/O file if the measured data is being acquired from the ADC.

II.1.7. Module Name: DSKDTA

Language: FORTRAN

Is an Entry Point In: INPUT

Is Called By: SEDAPS

Calls: DISKW

Brief Description:
This module transfers previously acquired measured data to a measured data I/O file.

II.1.8. Module Name: POLAR

Language: FORTRAN

Is an Entry Point In: None

Is Called By: SEDAPS, CABLE, & PLOT

Calls: None

Brief Description:
This module converts a complex number from rectangular format to polar format.

II.1.9. Module Name: TIMER

Language: FORTRAN

Is an Entry Point In: None

Is Called By: SEDAPS

Calls: TIMSET & TIMGET

Brief Description:
This module performs timing services for the calling routines. It reports elapsed time and wall-clock time.

II.1.10. Module Name: RDFT

Language: FORTRAN

Is an Entry Point In: None

Is Called By: SEDAPS, PLOT

Calls: None

Brief Description:
This module calculates the real discrete Fourier transform of a sequence of measured data from one channel.

II.1.11. Module Name: CABLE

Language: FORTRAN

Is an Entry Point In: None

Is Called By: SEDAPS & PLOT

Calls: POLAR

Brief Description:
This module calculates and displays features associated with power cables (e.g., voltage drop, impedance, phase shift, etc.).

II.1.12. Module Name: EVINIT

Language: FORTRAN

Is an Entry Point In: None

Is Called By: SEDAPS

Calls: None

Brief Description:
This module allows the user to enter parameters associated with the error-vector calculations via the error-vector menu.

II.1.13. Module Name: EVRSET

Language: FORTRAN

Is an Entry Point In: EVINIT

Is Called By: SEDAPS

Calls: None

Brief Description:
This module, at the user's request, resets the error vector in the sense that a new zero region and new reference values will be sought.

II.1.14. Module Name: EVCALC

Language: FORTRAN

Is an Entry Point In: EVINIT

Is Called By: SEDAPS

Calls: EVDIFF & CLASS

Brief Description:
This module arranges for the calculation of the error vector via EVDIFF, arranges for classification of threshold overruns via CLASS, and monitors "zero" regions and cycles.

II.1.15. Module Name: EVREFS

Language: FORTRAN

Is an Entry Point In: EVINIT

Is Called By: SEDAPS

Calls: None

Brief Description:
This module establishes the reference values that are used in the error-vector calculations.

II.1.16. Module Name: EVPRNT

Language: FORTRAN

Is an Entry Point In: EVINIT

Is Called By: SEDAPS

Calls: None

Brief Description:
This module displays the error vectors to the user in a numerical format.

II.1.17. Module Name: EVDIPF

Language: FORTRAN

Is an Entry Point In: None

Is Called By: EVCALC

Calls: None

Brief Description:
This module calculates an error vector (the value is the difference between a current feature value and a reference value that was selected at the beginning of a cycle), optionally performs a phase transform on a grouping of three (corresponding to the three phases), and determines whether the error vector has exceeded user-selected thresholds.

II.1.18. Module Name: CLASS

Language: FORTRAN

Is an Entry Point In: None

Is Called By: EVCALC

Calls: None

Brief Description:
This is a skeleton module whose purpose will be to classify error-vector threshold overruns.

II.1.19. Module Name: PLOT

Language: FORTRAN

Is an Entry Point In: None

Is Called By: None (Main Program)

Calls: TIMELT, SYCOMP, POLAR, RDFT, GRAPH, & CABLE

Brief Description:
This module reads previously recorded data from the measured-data I/O file, calculates certain features of this data as requested by the user, and arranges for these features to be displayed in graphical form on a printer via Subroutine GRAPH.

II.1.20. Module Name: TIMELT

Language: FORTRAN

Is an Entry Point In: None

Is Called By: PLOT

Calls: None

Brief Description:
This routine determines whether one time is less than a second time. The times are in the wall-clock format (month, day, year, hour (24-hour format), minute, and second).

II.1.21. Module Name: GRAPH

Language: FORTRAN

Is an Entry Point In: None

Is Called By: PLOT

Calls: None

Brief Description:
This module is a general-purpose line-printer graphical-display subroutine. It can plot several variables at one time; and it includes axis generation, annotation, and windowing of the data.

II.1.22. Module Name: ADCSET

Language: Interdata Assembler

Is an Entry Point In: None

Is Called By: INPUT

Calls: None

Brief Description:
This module initializes the ADC hardware by transferring to it the sampling-rate and channel-polling schedule.

IMPORTANT NOTE:
Two versions of this module and its associated entry points have been developed. The first controls an ADC system that was developed in house. A second version controls the Interdata mini-I/O system.

II.1.23. Module Name: ADCGET

Language: Interdata Assembler

Is an Entry Point In: ADCSET

Is Called By: INPUT

Calls: None

Brief Description:
This module obtains the measured data from the ADC as set up by ADCSET. If the remote trigger option is being used, sampling of the data is delayed until an external event occurs.

II.1.24. Module Name: TIMSET

Language: Interdata Assembler

Is an Entry Point In: ADCSET

Is Called By: TIMER

Calls: None

Brief Description:
This module sets up the line-frequency interrupt in the clock hardware associated with Interdata's mini-I/O system.

II.1.25. Module Name: TIMGET

Language: Interdata Assembler

Is an Entry Point In: ADCSET

Is Called By: TIMER

Calls: None

Brief Description:
This module retrieves the current value of the 6-s counter associated with the hardware clock circuitry.

II.1.26. Module Name: BREAK

Language: Interdata Assembler

Is an Entry Point In: ADCSET

Is Called By: SEDAPS

Calls: None

Brief Description:
This module returns the status of the console-teletype break key (either depressed or not depressed).

II.1.27. Module Name: DISKR

Language: Interdata Assembler

Is an Entry Point In: ADCSET

Is Called By: SEDAPS & INPUT

Calls: None

Brief Description:
This module is a high-speed binary read-and-file positioning subroutine which is used to read the measured-data I/O file.

II.1.28. Module Name: DISKW

Language: Interdata Assembler

Is an Entry Point In: ADCSET

Is Called By: SEDAPS & INPUT

Calls: None

Brief Description:

This module is a high-speed binary write-and-file positioning subroutine which is used to write the measured-data I/O file.

II.2. PRINCIPAL DATA STRUCTURES

There are two principal data structures in the SEDAPS 2.4 program. One reflects the way in which a user would naturally think the computer would handle the data, and the other one is an "inversion" of this natural structure to permit fast processing and reduce computer-storage requirements. A mechanism exists for mapping the first structure into the second one.

The first structure is divided into three levels. On the first level are concepts and variables that pertain to the entire program such as the date, run title, and the concept of analysis groups. The second level contains the structure of the analysis-group concept. It contains such variables as the analysis-group title, voltage/current type indicator, the concept of a phase group, and the concept of a symmetrical-component group.

Two third-level structures exist for the phase-group and symmetrical-component concepts. The phase-group structure contains such items as the channel which contains the corresponding data, a map into the inverted structure, conversion information, the measured data, and most features and error vectors. The symmetrical-component structure contains the symmetrical-component features and the symmetrical-component error vectors.

The accompanying chart shows this natural structure in diagrammatical form. Items in capital letters represent actual variables or stand for actual variables in the program. Items in small letters are logical concepts or variables that are implemented only in the inverted structure. The chart does not attempt to categorize all variables used in the program, only the major ones and some others to serve as examples.

Items in brackets indicate that the corresponding concept or variable is actually an array of structures or an array of data elements ranging over the variable in the brackets. The concept of a sequence number used as an index refers to the fact that over time, those associated variables logically act as multidimensional arrays when in fact they are not. That is, one sequence of data is taken from the environment, processed, and displayed. Then, over the next interval of time, another sequence of data is acquired and processed in those same arrays. Note that the sequence index when referring to positive, negative, or zero symmetrical component is not the same as the sequence number just discussed.

The "inversion" of the natural structure refers to turning it upside down. Those variables at the lowest level of the uninverted structure can now be directly accessed.

This inverted structure is used in the SEDAPS 2.4 program for three reasons. First, the execution speed of the program can be increased since the data is directly available. Although most of the

Table II.1. Natural Data Structure Chart.

01 TITLE

01 DATE

01 NAG

01 NSAM

01 NFQ

01 XFMR

01 RMTRIG

01 Analysis group [ANALYSIS GROUP NUMBER]

  02 AGTI

  02 REF

  02 TYPE

  02 GROUP

  02 MOST ERROR VECTOR THRESHOLDS

  02 phase group [PHASE INDEX (i.e., A, B, or C)]

    03 PTR

    03 CHNL

    03 CONVERSION (i.e., SCALE & OFFSET)

    03 MOST ERROR VECTOR THRESHOLD OVERRUN INDICATORS [sequence no.]

    03 measured data [ELEMENT INDEX, sequence no.]

    03 most features [sequence no.]

    03 most error vectors [sequence no.]

  02 symmetrical component group [SEQUENCE INDEX (i.e., POSITIVE NEGATIVE or ZERO]

    03 PTR

    03 symmetrical component features [sequence no.]

    03 symmetrical component error vectors [sequence no.]

    03 symmetrical component error vector thresholds

    03 SYMMETRICAL COMPONENT ERROR VECTOR THRESHOLD OVERRUN INDICATORS [sequence no.]

program accesses the data through the natural structure using a map into the inverted structure, two time-consuming areas use the inverted structure directly. Those are the data acquisition and discrete Fourier transform.

Secondly, the inverted structure saves computer storage due to the fact that not all of the phase-group structures will contain three elements (there can be single element a-c and d-c phase groups). Thus, the phase-group structure will have "holes" in it for these cases. Finally, the FORTRAN language does not have the facilities to conveniently process structures.

The inverted structure contains the measured data, features, and error vectors. These arrays are indexed by the sequence number and a new index called the channel index. This index is built up from the analysis-group number and phase index such that there is a one-to-one correspondence between it and each channel that will be measured.

The following chart, Table II.2, similar to the previous one, diagrammatically shows the form of the inverted structure.

Table II.2. Chart Showing Inverted Structure.

01 A [CHANNEL INDEX] } { Conversion variables
01 B [CHANNEL INDEX] } { derived from SCALE & OFFSET

01 CH [CHANNEL INDEX] derived from CHNL

01 DATA [ELEMENT INDEX, CHANNEL INDEX, sequence no.]

01 CFFT [ELEMENT INDEX, CHANNEL INDEX, sequence no.]

01 SS [CHANNEL INDEX, sequence no.]

01 POWER [CHANNEL INDEX, sequence no.]

01 Z [CHANNEL INDEX, sequence no.]

01 SYCMP [CHANNEL INDEX, sequence no.]

01 SCZ [CHANNEL INDEX, sequence no.]

01 ERROR VECTORS [CHANNEL INDEX, sequence no.]

01 ERROR VECTOR REFERENCES [CHANNEL INDEX, sequence no.]

Most of the SEDAPS 2.4 program must access the measured data, features, and error vectors by using the natural structure. This is always because some control information is needed that can only be obtained by "going down through" the natural structure. Some examples follow.

In order to compute the power or impedance, it must first be determined that this analysis group is used to measure current. Secondly, the associated analysis group measuring a voltage must be determined. In order to compute a symmetrical-component group, it must be determined that this is a three-phase analysis group along with which three channels comprise the phase group.

To avoid the extra time and computer storage that would be needed to duplicate the measured data, features, etc., into the natural data structure, a mapping technique is used to logically link the inverted structure to it. This technique uses a two-dimensional array to map the analysis-group number and phase index of the natural structure into the channel index of the inverted structure as shown in Table II.3. For example, the content of row 3, column 1, is the channel index corresponding to analysis group 1, phase C.

Table II.3. Channel Index of Inverted Structure.

	Analysis Group No. 1	2	...	16
Phase Index 1				
Phase Index 2				
Phase Index 3				

PTR array whose contents is the mapping set of channel indexes

II.3. INPUT/OUTPUT FILES

SEDAPS 2.4 uses two I/O files for intermodule communication and preservation of the measured transducer data.

II.3.1. Analysis-group-definition File.

This file contains data describing the structure and composition of each analysis group in an ASCII-character format. The first record contains a two-digit integer giving the number of analysis groups (maximum of 16). Each succeeding record contains information about one analysis group as follows.

CARD IMAGE NO.	COLUMNS	DESCRIPTION
1	1-60	Up to 60 characters of identification.
	61-63	Phase-group definition: 1 Three-phase a-c (Phase A, Phase B, Phase C) 2 Single-phase a-c 3 Direct Current.
	64-66	Voltage or current measurement: 1 Voltage 2 Current.
	67-69	Reference-analysis group (must be voltage type) to be used in impedance and power calculation (equal to zero for voltage type analysis groups).
2	1-2	Channel number used to measure phase A, single-phase a-c, or d-c.
	3-13	A scale factor used to convert the value measured by the ADC on the above channel from volts as seen by the ADC to volts or amps as it exists in the measured equipment.
	14-24	An offset (in volts or amps) to accompany the above conversion.
	25-26	Channel number used to measure phase B (zero if not used).
	27-37	Scale factor for phase B (zero if not used).

CARD IMAGE NO.	COLUMNS	DESCRIPTION
2 (cont'd)	38-48	Offset for phase B (zero if not used).
	49-50	Channel number used to measure phase C (zero if not used).
	51-61	Scale factor for phase C (zero if not used).
	62-72	Offset for phase C (zero if not used).

This file is generated in the ANALGP module and used in the SEDAPS module. Since it is also part of the measured-data file, it is implicitly used whenever that file is referenced.

II.3.2. Measured Data File.

This file is used to preserve the measured electrical data along with the information needed to extract the features from it. The file is organized as a binary file composed of a sequence of blocks. The first block is a file header and contains the analysis-group-file definition information. Each succeeding block contains a block header followed by the measured data for one time sequence.

The characterization of the file is as follows.

FIRST BLOCK (length is 1344 bytes)

ITEM NO.	BYTE NO.	DATA TYPE	DESCRIPTION
1	1-52	Character	The title of the experiment (up to 52 characters).
2	53-54	Integer	Number of analysis groups.
3	55-56	Integer	Number of used channels.
4	57-58	Integer	The number of times any given channel is sampled during one time sequence.
5	59-60	Integer	The number of frequencies that can be uniquely discerned during one time sequence.
6	61-62	Integer	Frequency Spacing (Hz).
7	63-64	Integer	60-Hz component (d-c component = 1).
8	65-124	Character	Identification for Analysis-group 1.

FIRST BLOCK (length is 1344 bytes)

ITEM NO.	BYTE NO.	DATA TYPE	DESCRIPTION
9	125-184	Character	Identification for Analysis-group 2.
			⋮
23	965-1024	Character	Identification for Analysis-group 16.
(Note: Only the first NAG Groups have valid information.)			
24	1025-1026	Integer	Phase-group definition for Analysis-group 1.
25	1027-1028	Integer	Phase-group definition for Analysis-group 2.
			⋮
39	1055-1056	Integer	Phase-group definition for Analysis-group 16.
40	1057-1058	Integer	Measurement Characteristic (voltage/current) for Analysis-group 1.
41	1059-1060	Integer	Measurement Characteristic (voltage/current) for Analysis-group 2.
			⋮
55	1087-1088	Integer	Measurement Characteristic (voltage/current) for Analysis-group 16.
56	1089-1090	Integer	Impedance and power reference for Analysis-group 1.
57	1091-1092	Integer	Impedance and power reference for Analysis-group 2.
			⋮
71	1119-1120	Integer	Impedance and power reference for Analysis-group 16.
72	1121-1122	Integer	IPTR (1,1).
73	1123-1124	Integer	IPTR (2,1) This array, given the phase index (A=1, B=2,
74	1125-1126	Integer	IPTR (3,1) C=3) as the row index and the analysis group number
75	1127-1128	Integer	IPTR (1,2) as the column index, gives the channel index.
			⋮

FIRST BLOCK (length is 1344 bytes)

ITEM NO.	BYTE NO.	DATA TYPE	DESCRIPTION
119	1215-1216	Integer	IPTR (3,16).
120	1217-1220	Floating Point	Scale factor * $\frac{10}{1024}$ for channel whose index is 1.
121	1221-1224	Floating Point	Scale factor * $\frac{10}{1024}$ for channel whose index is 2.
			⋮
135	1277-1280	Floating Point	Scale factor * $\frac{10}{1024}$ for channel whose index is 16.
136	1281-1284	Floating Point	Negative offset for channel whose index is 1.
137	1285-1288	Floating Point	Negative offset for channel whose index is 2.
			⋮
151	1341-1344	Floating Point	Negative offset for channel whose index is 16.

SUCCEEDING BLOCKS (length is variable = 2 (c.s + 16) BYTES where "c" is item no. 3 above and "s" is no. 4)

ITEM NO.	BYTE NO.	DATA TYPE	DESCRIPTION
152	1-2	Integer	Month in which this data sequence was measured.
153	3-4	Integer	Day in which this data sequence was measured.
154	5-6	Integer	Year in which this data sequence was measured.
155	7-8	Integer	Hour (24-hour clock) in which this data sequence was measured.
156	9-10	Integer	Minute in which this data sequence was measured.
157	11-12	Integer	Second at which this data sequence was measured.
158	13-32	Character	User identification for this sequence of data (may be set to blanks for certain data collection options).

SUCCEEDING BLOCKS (length is variable = 2 (c.s + 16) BYTES where "c" is item no. 3 above and "s" is no. 4)

ITEM NO.	BYTE NO.	DATA TYPE	DESCRIPTION
159	33-34	Integer	Measured-data sample for channel index 1 at time t_1.
160	35-36	Integer	Measured-data sample for channel index 2 at time t_1.
⋮		⋮	
158+c	2•c+31 thru 2•c+32	Integer	Measured data sample for channel index "c" at time t_1.
159+c	2c+33 thru 2c+34	Integer	Measured data sample for channel index 1 at time t_2.
			⋮
158+cs	2cs+31 thru 2cs+32	Integer	Measured data sample for channel index "c" at time t_s.

(Note: The measured data samples are recorded in "ADC units." To connect them to natural units (i.e., volts, amps), the following equation is used:

$$a \cdot \text{value} + b$$

Where "a" is Item Nos. 120 thru 135 and "b" is Item Nos. 136 thru 151.)

The Measured-data file can be converted to an ASCII-character file suitable for intercomputer transfer by using the SEDAPS 2.4 module PUNCH. The format of this file using the item numbers above is as follows.

Record No.	Character Locations	Item Reference No.
1	1-52	1
2	1-2	2
	3-4	3
	5-6	4
	7-8	5
	9-10	6

Record No.	Character Locations	Item Reference No.
	11-12	7
	13	24
	14	25
	⋮	
	28	39
	29	40
	30	41
	⋮	
	44	55
	45-46	56
	47-48	57
	⋮	
	75-76	71
3	1-2	72
	3-4	73
	⋮	
	47-48	95
4	1-2	96
	3-4	97
	⋮	
	47-48	119
5	1-10	120 (in FORTRAN "E" format)
	11-20	121
	⋮	
	71-80	127 (in FORTRAN "E" format)
6	1-10	128 (in FORTRAN "E" format)
	⋮	
	71-80	135 (in FORTRAN "E" format)

Record No.	Character Locations	Item Reference No.
7	1-10	136 (in FORTRAN "E" format)
	⋮	
	71-80	143 (in FORTRAN "E" format)
8	1-10	144 (in FORTRAN "E" format)
	⋮	
	71-80	151 (in FORTRAN "E" format)
9	1-60	8
10	1-60	9
	⋮	
8+η		7+η

(Note: η is the value of Item No. 2)

Record No.	Character Locations	Item Reference No.
9+η	1-2	152
	3	The Character "/"
	4-5	153
	6	The Character "/"
	7-8	154
	9	The Space Character
	10-11	155
	12	The Character ":"
	13-14	156
	15	The Character ":"
	16-17	157
	18-37	158
10+η	1-4	159
	5-8	160
	⋮	
	77-80	178

Record No.	Character Locations	Item Reference No.
$11+\eta$	1-4	179
	⋮	
	77-80	198
$12+\eta$	1-4	199
$10+\eta+\frac{c\cdot s-1}{20}$	$4[(c\cdot s-1)\bmod 20]+1$ thru $4[(c\cdot s-1)\bmod 20]+4$	$158+c\cdot s$

II.4. MEASURED-DATA UNIT CONVERSIONS

The data as measured by the analog-to-digital converter is initially seen by the program as an integer ranging in value from -512 through 511. In order to convert these values to volts and amperes (as the user thinks of the data units that are being measured, termed natural units,) it is necessary to supply the program with conversion information.

The conversion information can be derived with referral to the following diagram.

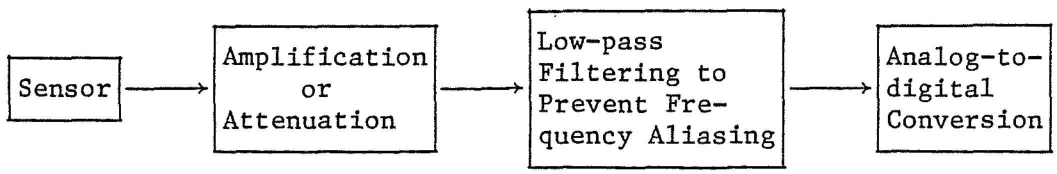

Each of the blocks will have a sensitivity associated with it. For example, a current sensor's sensitivity might be 1.2 mV/10 A; the amplifier, 2 V/10 mV; the filter, unity; and ADC, 1 count/9.77 mV.

Since the sensitivity of the ADC is constant, it can be automatically accounted for within the program. The composite sensitivity is arrived at by multiplying the individual sensitivities up to but not including the ADC. In the above example the composite sensitivity would be 2.4 V/100 A.

The first piece of conversion information that is given to the program for each channel, called the scale, is the reciprocal of the composite sensitivity.

The second piece of conversion information is a d-c offset correction. The signal that the sensor is measuring is adjusted so the ADC output is exactly zero. The value of the signal at this point is the d-c offset.

The scale and the offset are entered into the analysis-group-definition file via the ANALGP program module. This information must be given for each phase of each phase group and of each analysis group.

The SEDAPS program module converts this information and stores it in two inverted structures (see principal data structures) called A and B which are defined over the channel index. Structure A is the scale item augmented to include the ADC sensitivity, and B is simply the negative of the offset.

Thus, for each channel the equation

$$A \cdot X + B$$

(where X is the ADC output integer)

can be used to perform the conversion to natural units.

II.5. SPECTRAL-COMPONENT NORMALIZATION

Spectral-component normalization is used in SEDAPS to allow comparison of the components over several sequences of data. The normalization consists of three parts: magnitude normalization, phase normalization, and correction for sampling offset.

The magnitude-normalization factor is a function of phase-group type. If the phase group is an a-c type, then the magnitude-normalization factor for the phase group is chosen such that the 60-Hz spectral component of phase A (or the only phase if this is a single channel a-c group) will have a magnitude of unity. If the phase group is of a d-c type, then the normalization factor is chosen such that the d-c spectral component will have a magnitude of unity. In all of the above cases, if the magnitude of the 60-Hz component (or the d-c component for a d-c phase group) is less than one volt or ampere, then no magnitude normalization is performed.

Phase normalization is necessary because the time at which a sequence of data is started to be measured is not controlled. Therefore, the phases of all spectral components which are 60 Hz and above for all channels being measured are adjusted so the phase of the 60-Hz component of the first channel in the first analysis group is zero. This adjustment is made by multiplying the complex spectral elements greater than or equal to 60 Hz by $e^{-jk\Theta}$ where $j = \sqrt{-1}$, Θ is the required phase connection in radians, and k is the spectral-component index.

A second adjustment to the phase of the spectral component is needed to correct for the sampling offset. Since the ADC hardware has only one sample and hold unit, it is necessary to time multiplex this unit across all the channels being measured. The resulting time skew can be corrected by using the following procedure.

The direct Fourier transform is defined as:

$$f(k\omega) = \sum_{n=0}^{n-1} x(nT)e^{-jnTk\omega}, \quad k = 0, 1 ---, N-1$$

where,

x = the time ordered sequence of measured data
n = time ordered sequence index
T = the sampling period in seconds
f = the resulting spectral components
k = the spectral component sequence index
ω = the frequency separation of the spectral components in radians = $\frac{2\pi}{NT}$
N = the number of elements in the time ordered sequence
$j = \sqrt{-1}$

Now suppose that the time-ordered sequence is displaced in time by an amount τ. Then the DFT would be

$$f(k\omega) = \sum_{n=0}^{N-1} x(NT+\tau)e^{-j(nT+\tau)k\omega}, \quad k = 0,\ 1\ ---,\ N-1$$

$$= e^{-j\tau k\omega}\sum_{n=0}^{N-1} x(nT+\tau)e^{-jnTk\omega}, \quad k = 0,\ 1\ ---,\ N-1$$

$$= e^{-j\tau k\omega} \cdot \mathrm{DFT}[x(nT+\tau)], \quad k = 0,\ 1,\ ---,\ N-1$$

Thus to correct for the sampling offset, it is sufficient to multiply the spectral components of the measured-data sequence by a complex exponential involving τ and the spectral-component index.

Because of the way in which the channels are time multiplexed in this application, τ can be removed from the above complex exponential. Within the time period T, the sampling point of each of the channels is equally distributed. Thus,

$$\tau = \frac{mT}{M}, \quad M = 0,\ 1,\ \ldots,\ M-1$$

where,

T = the sampling period in seconds
M = the number of channels being sampled
m = the channel index.

Substituting this expression for τ and a previous expression for ω reduces the complex exponential to

$$e^{-j2\pi mk/MN}.$$

Note that this exponential for sampling offset correction can be combined with the one for phase normalization along with the magnitude normalization factor to give

$$\frac{1}{X} \cdot e^{-jk\left(\frac{2\pi m}{MN} + \Theta\right)}$$

where X is the magnitude normalization factor selected as previously discussed.

II.6. DETAILED DESCRIPTION OF THE SEDAPS 2.4 MODULE

For discussion purposes the SEDAPS 2.4 module can be subdivided as follows:

```
1.  Assign default values, Initial readings
2.     Main Menu Processing
3.        Looping Menu Processing
3.           Initial looping control
4.           Data Processing and Display
3.           Ending looping control
3.        END
2.     END
1.  END
```

The numbers to the left refer to the four major blocks that will be subsequently described.

As can be seen from this structure, the program control centers around menu usage. A menu can be defined as a list of parameters that a user can selectively modify. The selectivity is an important element in interactive-program usage.

II.6.1. Assign Default Values, Initial Readings.

This section of the program can be subdivided as follows:

1.1 Assign default values for menu parameters;
1.2 Read the date, title, and analysis-group-definition file;
1.3 Set up the inverted-file structure;
1.4 See blocks 2, 3 and 4;
1.5 Termination control.

1.1. Assign Default Values for Menu Parameters.

GLOBAL VARIABLES REFERENCED: None

GLOBAL VARIABLES MODIFIED: OREAD (2, 3, & 4), NFQ, SRT, XFMR, VLOW, PBASE, VBASE, IBASE, ZBASE, FQPRT, RMTRIG, ETRIP, QRAW, QFFT, QPU, QSS, QSYC, GROUP, TYPE, REF, A, B, PTR

LOCAL VARIABLES: None

DESCRIPTION: Since menus are used, it is necessary to give the parameters in them initial or default values. As will be seen later, certain variables dependent on the menu parameters are computed as part of the menu processing and thus must be initialized here (e.g., VBASE and IBASE).

Since the analysis-group-definition file is only defined for those analysis groups being used, its components must be initialized because all 16 groups are made part of the measured-data file.

1.2. Read the Date, Title, and Analysis-group-definition File.

GLOBAL VARIABLES REFERENCED: CNTL

GLOBAL VARIABLES MODIFIED: TIME, TITLE, IFAULT, AGF, NAG, AGTI, GROUP, TYPE, REF, CHNL, SCALE, OFFSET

LOCAL VARIABLES: I, J

MODULES CALLED: TIMER

DESCRIPTION: The user enters a title for the processing to be performed and the wall-clock time. The wall-clock time (including date) is passed to subroutine TIMER in order to synchronize it with an internal hardware timer. The user then enters a value called "fault" which is used to detect malfunctions in the ADC.

The user then enters the I/O unit where the analysis-group-definition file is located, and the program next reads this file.

1.3. Set Up the Inverted-file Structure.

GLOBAL VARIABLES REFERENCED: NAG, SCALE, OFFSET

GLOBAL VARIABLES MODIFIED: NCH, PTR, CH, A, B

LOCAL VARIABLES: I, J, M

DESCRIPTION: The inverted structure is started in this block by the creation of the PTR array and arrays CH, A, and B.

The PTR array is assigned successive channel index values as the array subscripts naturally move over the analysis-group numbers and the phase indexes. The variable M which is derived from GROUP (I) is the number of phases in a phase group. If GROUP (I) = 1, M = 3, GROUP (I) = 2, M = 1, and GROUP (I) = 3, M = 1

The array CH is in the inverted structure and is the ADC channel address which is one less than the address as known by the user. Arrays A and B are also in the inverted structure and are used to scale the data from the ADC to natural units (see Measured-data Unit Conversions).

1.5. Termination Control.

GLOBAL VARIABLES REFERENCED: CNTL

GLOBAL VARIABLES MODIFIED: None

LOCAL VARIABLES: OREAD (3) & OREAD (4)

DESCRIPTION: At this level in the termination of this module, the user can either have the program execution terminated, or control can be transferred to the very beginning of the program so that a new run title and new analysis-group-definition file can be entered.

II.6.2. Main-menu Processing.

This section of the program can be subdivided as follows:

```
2.1   Derived spectral parameter initialization;
2.2   Menu-item selection:
         CASE
2.2.1       Spectral-parameter modification,
2.2.2       Special-subroutine initialization,
2.2.3       Per-unit normalization parameters,
2.2.4       Error-vector initialization,
2.2.5       Spectral-component display threshold,
2.2.6       Remote-trigger usage,
2.2.7       Data-display control,
2.2.8       Display main menu,
         END;
2.3   Blocks 3 and 4;
2.4   Termination control.
```

2.1. Derived Spectral Parameter Initialization.

GLOBAL VARIABLES REFERENCED: NFQ, SRT, CNTL

GLOBAL VARIABLES MODIFIED: NSAM, IDELFQ, K60, KOUNT

LOCAL VARIABLES: NFQ2, TEMP

DESCRIPTION: This block uses most of section 2.2.1 to perform the initialization of the derived spectral parameters.

2.2. Main-menu-item Selection.

GLOBAL VARIABLES REFERENCED: CNTL, NAG

GLOBAL VARIABLES MODIFIED: None

LOCAL VARIABLES: I, J

DESCRIPTION: The user is requested to enter an integer indicating which parameters are to be modified. This integer is chosen by referring to a display of the main menu (see section 2.2.8). The program then transfers control to the block of code which will allow that parameter to be changed.

One of the items that can be selected from the menu transfers control to block 2.3.

2.2.1. Spectral Parameter Modification.

GLOBAL VARIABLES REFERENCED: CNTL

GLOBAL VARIABLES MODIFIED: NFQ, SRT, NSAM, IDELFQ, K60, KOUNT

LOCAL VARIABLES: NFQ2, TEMP

DESCRIPTION: This block first requests the user to enter the number of spectral components (NFQ) and the channel sampling rate (SRT). The program then determines the length of the sequence of measured data that is needed for any one channel (NSAM), the frequency separation of the spectral components (IDELFQ), the index of the 60-Hz spectral component (K60), and an ADC-hardware sampling-rate control word (KOUNT).

Only certain values are allowed for NFQ and SRT because of two factors. First, the DFT used in this program is based on a radix 2 FFT algorithm. Secondly, there is an upper limit as to how fast the ADC can be made to operate. Table II.4 shows the allowed values of NFQ and SRT as well as the values for some of the derived parameters.

The ADC-hardware sampling-rate control-word calculation is based on the sampling rate and the number of channels being sampled (NCH). Since the ADC must be time multiplexed among all the channels, the ADC sampling rate is NCH•SRT. The actual timing of the sampling point is controlled by a six-megahertz clock which is used to count down a loadable counter. A value of zero placed into this counter causes the ADC to sample at the six-megahertz rate; a value of 1, three megahertz; etc. Thus, the expression for the initial value of this counter is

$$\frac{6000000}{NCH \cdot SRT} - 1.$$

A complication arises in that this counter is a 16-bit unsigned integer while FORTRAN only supports 16-bit twos-complement integers. Therefore, it is necessary for values greater than 32767 to create a negative integer whose bit pattern is the same as the unsigned integer. This is accomplished by using floating point and subtracting 65,536.5 from any value greater than 32767. The 0.5 is included to insure proper rounding when the resulting floating point value is converted to integer.

2.2.2. Special-subroutine Initialization.

GLOBAL VARIABLES REFERENCED: None

GLOBAL VARIABLES MODIFIED: None

LOCAL VARIABLES: None

MODULES CALLED: CABLE

DESCRIPTION: At this point, calls are made to initialize subroutines which calculate special-purpose features. The only subroutine implemented so far is one which calculates electrical features of power cables.

Table II.4. Allowable Samping Rates and Number of Harmonics.

Rate	No.	Frequency Corresponding to Bin																
HZ	HAR	1	2	3	4	5	6	7	8	9	10	11	12	13	14	15	16	17
480	5	0	60	120	180	240												
240	5	0	30	60	90	120												
160	5	0	20	40	60	80												
120	5	0	15	30	45	60												
960	9	0	60	120	180	240	300	360	420	480								
480	9	0	30	60	90	120	150	180	210	240								
320	9	0	20	40	60	80	100	120	140	160								
240	9	0	15	30	45	60	74	90	105	120								
192	9	0	12	24	36	48	60	72	84	96								
160	9	0	10	20	30	40	50	60	70	80								
1920	17	0	60	120	180	240	300	360	420	480	540	600	660	720	780	840	900	960
960	17	0	30	60	90	120	150	180	210	240	270	300	330	360	390	420	450	480
640	17	0	20	40	60	80	100	120	140	160	180	200	220	240	260	280	300	320
480	17	0	15	30	45	60	75	90	105	120	135	150	165	180	195	210	225	240
384	17	0	12	24	36	48	60	72	84	96	108	120	132	144	156	168	180	192
320	17	0	10	20	30	40	50	60	70	80	90	100	110	120	130	140	150	160
192	17	0	6	12	18	24	30	36	42	48	54	60	66	72	78	84	90	96
160	17	0	5	10	15	20	25	30	35	40	45	50	55	60	65	70	75	80
128	17	0	4	8	12	16	20	24	28	32	36	40	44	48	52	56	60	64

The initialization will, of course, depend on the nature of the special-feature calculations. In general, it should include a capability to include or exclude the calculations for this particular run, and it should request from the user information that it needs to set up the calculations.

2.2.3. Per-unit Normalization Parameter.

GLOBAL VARIABLES REFERENCED: CNTL

GLOBAL VARIABLES MODIFIED: XFMR, VLOW, PBASE, VBASE, IBASE, ZBASE

LOCAL VARIABLES: None

DESCRIPTION: In order to perform per-unit normalization, the user must enter the transformer rating in VA and the low-side voltage in volts. From these two values, normalization factors are derived for the voltage, current, power, and impedance.

The analysis groups to which per-unit normalization is applied is controlled by array QPU which is set up by the user in block 2.2.7 (Data-display Control).

2.2.4. Error-vector Initialization.

GLOBAL VARIABLES REFERENCED: None

GLOBAL VARIABLES MODIFIED: None

LOCAL VARIABLES: None

MODULES CALLED: EVINIT

DESCRIPTION: All initialization for the error vectors is performed in subroutine EVINIT. In this module a submenu is used to set up such parameters as thresholds, select the error-vector phase transformation, and to request error vector processing or not.

2.2.5. Spectral-component Display Threshold.

GLOBAL VARIABLES REFERENCED: CNTL

GLOBAL VARIABLES MODIFIED: FQPRT

LOCAL VARIABLES: None

DESCRIPTION: The user enters the spectral component display threshold. Only those components whose magnitudes are larger than this value are displayed.

Since the magnitudes of all spectral components are normalized to the 60-Hz level (d-c if this is a d-c type phase group), a single threshold can be used to effectively control display of all components. The largest normalized magnitude will normally be 1.0, so a threshold of 0.1 will inhibit display of all components less than 10% of the maximum value.

2.2.6. Remote-trigger Usage.

GLOBAL VARIABLES REFERENCED: CNTL

GLOBAL VARIABLES MODIFIED: RMTRIG

LOCAL VARIABLES: None

DESCRIPTION: In order to synchronize the time at which a sequence of measured data is taken, a hardware facility called a remote trigger is used. Whether this facility is to be used is determined by the user at this point.

If the user enters "true," then the remote trigger facility will be used; "false," it will not.

2.2.7. Data-display Control.

GLOBAL VARIABLES REFERENCED: CNTL

GLOBAL VARIABLES MODIFIED: I, QRAW, QFFT, QPU, QSS, QSYC

LOCAL VARIABLES: None

DESCRIPTION: Normally the user is only interested in seeing a display of a subset of all the data that has been calculated. This block allows him to select which data is to be displayed as a function of both analysis group and data type.

Menu Items 9 through (8 + NAG) are used to set up this option for analysis group numbers 1 through NAG. For each analysis group, the user can choose to display or not (depending on whether he enters "true" or "false") the raw data, the spectral components, the steady-state features, and the symmetrical-component features.

Along with the above four control parameters, the user can also choose whether to have the calculations performed on a per-unit normalization basis. An entry of "true" causes per-unit normalization, and "false" results in calculations in natural units.

2.2.8. Display Main Menu.

GLOBAL VARIABLES REFERENCED: OUT, NFQ, SRT, IDELFQ, XFMR, VLOW, PBASE, VBASE, IBASE, ZBASE, FQPRT, RMTRIG, NAG, QRAW, QFFT, QPU, QSS, QSYC, AGTI

GLOBAL VARIABLES MODIFIED: None

LOCAL VARIABLES: I, J, K

DESCRIPTION: The main menu is displayed on the FORTRAN I/O unit "OUT" in a form that briefly describes each parameter that can be changed along with its current value, possibly some derived parameters, and an item number. The user in block 2.2 enters the item number of the parameter to be changed and on the next line enters the new value for that parameter.

2.4. Termination Control for Section 2.

GLOBAL VARIABLES REFERENCED: None

GLOBAL VARIABLES MODIFIED: OREAD (1)

LOCAL VARIABLES: None

DESCRIPTION: At this level in the termination control, the user can have the program control transferred to select an item on the main menu or to transfer control as explained in block 1.5, "Termination Control."

II.6.3. Looping Menu Processing.

```
DO until terminated

3.1  Menu-item selection;
3.2  CASE:
3.2.1   Display looping menu,
3.2.2   Open measured-data file (writing only),
3.2.3   Spool measured data to the measured-data file,
3.2.4   Acquire and process data continuously,
3.2.5   Same as 3.2.4 with the addition of transferring the
        measured data to the measured-data file,
3.2.6   Acquire and process one sequence of measured data,
3.2.7   Acquire data from the measured-data file and process it,
3.2.8   Close measured-data file (after writing only),
3.2.9   Terminate looping menu.
     END
END
```

The name, looping menu, could be considered a misnomer, since the program development has progressed beyond simple looping. It should really be called a task menu because it allows a user to select which of several tasks are to be performed in a specific instance of use of the program.

3.1. Looping Item Menu Selection.

GLOBAL VARIABLES REFERENCED: CNTL

GLOBAL VARIABLES MODIFIED: None

LOCAL VARIABLES: CASE

DESCRIPTION: The user is requested to enter an integer indicating which task is to be performed. This integer is chosen by referring to a display of the looping menu (see section 3.2.1). The program then transfers control to a block of code which will perform the indicated task.

3.2.1. Display Looping Menu.

GLOBAL VARIABLES REFERENCED: OUT

GLOBAL VARIABLES MODIFIED: None

LOCAL VARIABLES: None

DESCRIPTION: The looping menu is displayed on the FORTRAN I/O unit "OUT" in a form that briefly describes each task that can be performed by the program. The user in block 3.1 enters the item number of the task he wants to run.

3.2.2. Open Measured Data File (WRITE ONLY).

GLOBAL VARIABLES REFERENCED: KOMMON

GLOBAL VARIABLES MODIFIED: None

LOCAL VARIABLES: REWIND

MODULES CALLED: DISKW

DESCRIPTION: The measured-data file is rewound, and the entire analysis-group-definition file plus variables PTR, A, B, and those related to the spectrum attributes are written to it forming the first record. All variables in the first record are equivalent to the KOMMON array to facilitate writing of this record.

3.2.3. Spool Measured Data to the Measured-data File.

GLOBAL VARIABLES REFERENCED: IDELFQ, CNTL

GLOBAL VARIABLES MODIFIED: None

LOCAL VARIABLES: COLECT

MODULES CALLED: INPUT

DESCRIPTION: The user first enters the amount of data (in seconds) that he wants to spool. He can also specify that only a subsequence of the data be spooled (e.g., every third block).

The program then computes the number of blocks of data which must be transferred. A block of data as used here is synonymous with a sequence of data needed to compute one spectrum. Since the length of one block (in sec.) is equal to the reciprocal of the frequency resolution (IDELFQ), this computation can be performed by multiplying the total collection time by IDELFQ. Subroutine INPUT is used to actually perform the spooling. A small amount of data will be lost between each block since only one I/O operation can be performed at a time.

3.2.4. Acquire and Process Data Continuously.

GLOBAL VARIABLES REFERENCED: CNTL, CASE

GLOBAL VARIABLES MODIFIED: OREAD

LOCAL VARIABLES: BRK, I, TIMPRT, ITIMPR, TIME, ITIME, ITEMRF

MODULES CALLED: TIMER, INPUT, EVRSET

DESCRIPTION: This particular block can be further broken down as follows:

3.2.4.1 Setup,
3.2.4.2 DO Until a User Interrupt:
3.2.4.2.1 Acquire Data,
3.2.4.2.2 Perform Block 4,
END;
3.2.4.3 Termination Control.

The setup section begins by initializing the BLOKID array to blanks since the user will never have a chance to enter his identification for each block with this case. The user then enters the time interval (in minutes) at which he wants mandatory displays of the data to appear. This value is then converted to a number of six-second intervals and added to the current time to form the time at which the first mandatory display should occur.

The program then goes into a loop of acquiring data, processing it, and possibly displaying it until terminated by a user interrupt (the break key on the teletype is depressed). The data is acquired with subroutine INPUT, and the processing and displaying are described in block 4.

The termination section allows the user to repeat this case, transfer control to the looping menu item selection, or to go to the termination control for block 2 (see section 2.4). Before control is transferred and if error vector processing is being used, the user is queried via subroutine EVRSET as to whether the error vector status should be reset to search for a new "zero" region.

3.2.5. Acquire, Transfer to Measured-data File, and Process Data Continuously.

DESCRIPTION: This block is identical to block 3.2.4 with the addition of transferring the measured data to the measured data file. The transfer takes place in subroutine INPUT.

The user must realize that the file needs to be opened (see block 3.2.2) prior to running this task and closed (see block 3.2.8) following it. If this task is to be performed several times with the data all going to the same file, then the file should be only opened before the first time and only closed following the last time.

3.2.6. Acquire and Process Only One Sequence of Measured Data.

GLOBAL VARIABLES REFERENCED: CNTL, CASE

GLOBAL VARIABLES MODIFIED: OREAD

LOCAL VARIABLES: HP

MODULES CALLED: INPUT, DSKDTA

DESCRIPTION: This particular block can be further broken down as follows:

3.2.6.1 Acquire the Measured Data;
3.2.6.2 Perform Block 4;
3.2.6.3 Optionally Transfer the Measured Data to the Measured-data File;
3.2.6.4 Termination Control.

The measured data is acquired via subroutine INPUT or in previous blocks. After performing block 4, the user, who has reviewed the displayed data, is queried as to whether the measured data should be transferred to the measured-data file for future reference. If it is, subroutine DSKDTA is used for the transfer. The remarks made in section 3.2.5 concerning opening and closing of this file also apply here.

The termination control is the same as in section 3.2.4.3.

3.2.7. Acquire Data from the Measured-data File.

GLOBAL VARIABLES REFERENCED: CASE

GLOBAL VARIABLES MODIFIED: KOMMON

LOCAL VARIABLES: BRK, REWIND

MODULES CALLED: DISKW, DISKR, INPUT

DESCRIPTION: This particular block can be further broken down as follows:

```
3.2.7.1   Setup
3.2.7.2   DO UNTIL end-of-file OR user interrupt
3.2.7.2.1   Acquire data from the Measured Data File
3.2.7.2.2   Perform Block 4
          END
3.2.7.3   Termination Control
```

During the setup phase, the measured-data file is rewound, and the initial record is read. It must be noted that this read destroys the existing analysis-group-definition file and the spectrum attributes variables.

The program then goes into a loop of acquiring data, processing it, and displaying it until terminated by an end-of-file or a user interrupt (the break key on the teletype is depressed). The measured data is acquired from the measured-data file via subroutine INPUT, and the processing and displaying are described in block 4.

The termination section is similar to that in section 3.2.4.3.

3.2.8. Close Measured Data File (WRITE ONLY).

GLOBAL VARIABLES REFERENCED: None

GLOBAL VARIABLES MODIFIED: None

LOCAL VARIABLES: EOF, REWIND

MODULES CALLED: DISKW

DESCRIPTION: An end-of-file is placed after the last record written to the measured-data file. The file is then rewound.

3.2.9. Terminate Looping Menu.

GLOBAL VARIABLES REFERENCED: None

GLOBAL VARIABLES MODIFIED: None

LOCAL VARIABLES: None

DESCRIPTION: Control is transferred to the main-menu-item selection block (see section 2.2).

II.6.4. Data Processing and Display.

The sequence for data processing and display can be divided into:

4.1 DFT computation;
4.2 Spectral-component normalization;
4.3 Feature calculation;
4.4 Error-vector calculation (Module EVCALC);
4.5 Data display;
4.6 Conditionally set the error-vector references (Module EVREFS)
(Note: The error vector calculation and the setting of the error-vector references is described in the EVINIT module. As a result, sections 4.4 and 4.6 will not be presented here.)

4.1. DFT Calculation.

GLOBAL VARIABLES REFERENCED: DATA, NCH, NSAM

GLOBAL VARIABLES MODIFIED: FFT, CFFT

LOCAL VARIABLES: I and J

MODULES CALLED: RDFT

DESCRIPTION: The measured data is first copied from the DATA array into the FFT array. This action is necessary because the DFT algorithm performs its calculations in place thus destroying the original values. The measured data needs to be preserved for possible later display.

The DFT is performed for each channel of measured data by subroutine RDFT. The FFT and CFFT arrays are equivalenced. Even though the DFT calculations are performed in place, the input data is real while the output is complex.

4.2. Spectral Component Normalization.

GLOBAL VARIABLES REFERENCED: K60, NAG, GROUP, QPU, IBASE, VBASE, NFQ, TWOPI, NCH, NSAM

GLOBAL VARIABLES MODIFIED: CFFT, SS

LOCAL VARIABLES: THETA, J, L, M, I1, XNORM, PUN, K, ARG

DESCRIPTION: Determine the phase normalization factor (THETA):

```
     DO for each analysis group
          •    Based on the analysis-group types (e.g., AC, DC,
               Voltage, current) select the magnitude normalization
               factor (XNORM) and the per-unit normalization factor
               (PUN). PUN is set to 1.0 if per-unit normalization
               is not wanted.
          •    DO for each phase
          •    •    DO for each spectral component
          •    •    •    Determine the sampling offset correction.
                         Normalize each spectral component for phase
                            and magnitude.
                         Also correct it for sampling offset.
          •    •    END
          •    •    Define the steady state component by selecting
                    the correct spectral element and reintroducing
                    the magnitude. Convert to per unit if wanted.
          •    END
     END
```

The spectral-component normalization theory is discussed as a separate topic under a heading of the same name.

The usual method of getting to the inverted structures of CFFT and SS by using the PTR array to perform the mapping from the natural structure is not used in this section. Because of the method used to correct for the sampling offset, the program must sequentially move over the channel indexes (variable J) while at the same time move over the analysis groups (L) and phases (K). This factor essentially determined how the natural structure would map into the inverted structure, and this mapping is exploited to its fullest in this block.

4.3. Feature Calculation.

GLOBAL VARIABLES REFERENCED: NAG, GROUP, PTR, SS, TYPE, REF

GLOBAL VARIABLES MODIFIED: SYCMP, POWER, Z, PF, SCZ, CABLES

LOCAL VARIABLES: K, J, L, MM, M, I, SSJMAG, SSIMAG

MODULES CALLED: SYCOMP, CABLE

DESCRIPTION:

```
DO for each analysis group (AG)
•   If this is a three-phase AG, THEN compute the symmetrical-
    component features via subroutine SYCOMP.
END
DO for each AG
•   IF this is a current AG, THEN
•   •   get the AG of its associated voltage.
•   •   DO for each phase component.
•   •   •   Compute the power.
•   •   •   IF the current is not zero, THEN
•   •   •   •   compute the impedance.
•   •   •   •   IF the voltage is not zero, THEN
•   •   •   •   •   compute the power factor.
•   •   •   END
•   •   •   IF this is a three-phase AG and the symmetrical-
            component current is not zero, THEN compute the
            symmetrical-component impedance.
•   •   END
•   END
END
Compute the cable features via subroutine CABLE.
(Notes:
    1.  The reader should be aware that all of the features
        are of complex mode.  The FORTRAN used on this
        computer automatically handles complex arithmetic
        operations.
    2.  The "ELSE" branches for current not zero were
        deliberately omitted for clarity.  In these cases,
        the features are given magnitudes of 999 for the
        impedances and zero for the power factors.  Conse-
        quently, when these features are displayed, the user
        can easily spot them and understand what has happened.
```

3. Although it might be felt that the symmetrical-component impedances should be calculated in a separate loop because the phase-component index is now a sequence index, the results are purely semantical since there are always three of each, and the program is a bit shorter in this case.)

4.5. Data Display.

GLOBAL VARIABLES REFERENCED: CASE, ETRIP, ITIMPR

GLOBAL VARIABLES MODIFIED: ITIMRF, BRK

LOCAL VARIABLES: TIME, ITIME

MODULES CALLED: TIMER

DESCRIPTION: Get the teletype break-key status (user interrupt).

```
IF an error vector threshold has been overrun,
•   THEN PERFORM PRINT,
•   ELSE CASE (based on looping menu item).
•   •   Process data continuously (4 & 5).
•   •   •   IF it is time to display data, THEN
•   •   •   •   update to check for next display time.
•   •   •   •   PERFORM PRINT.
•   •   •   END
•   •   Process only one block of data (6).
•   •   •   PERFORM PRINT.
•   •   Process data from the measured data file (7).
•   •   •   (No action).
•   END.
```

The print block is rather lengthy, so it will be subdivided as follows and discussed as separate blocks:

PRINT PROCEDURE

4.5.1. Display a general heading,
4.5.2. Display the measured data,
4.5.3. Display the feature-extraction data,
4.5.4. Display the error vectors,
4.5.5. Display the cable features.

(Note: The display of the error vectors and the cable features are described in modules EVINIT and CABLE, respectively. Therefore, sections 4.5.4 and 4.5.5 will not be presented here.)

4.5.1. Display a General Heading.

GLOBAL VARIABLES REFERENCED: SAMTIM, TITLE, CASE, OUT, CNTL

GLOBAL VARIABLES MODIFIED: BLOKID

LOCAL VARIABLES: None

DESCRIPTION: Display the time at which the measured data was sampled and the run title.

IF the processing task (looping menu item) is "process one block of data,"

THEN have the user enter a block identification.

Display the block identification.

4.5.2. Display the Measured Data.

GLOBAL VARIABLES REFERENCED: NAG, QRAW, OUT, GROUP, AGTI, PTR, NSAM, DATA

GLOBAL VARIABLES MODIFIED: None

LOCAL VARIABLES: HP, K, M, PID, I1, I2, J

DESCRIPTION:

DO for each analysis group (AG).
- IF the measured data for this AG is wanted, THEN
- • IF the heading has not yet been displayed, THEN
- • • display the "RAW DATA" heading.
- • Display the AG title and the phase identifiers.
- • DO for each sample.
- • • Display the measured data for each phase.
- • END.
- END.

END.

(Note: The mechanism for determining when to display the "raw data" heading may seem a bit awkward, but its purpose is to display this title only if some data is to be displayed.)

4.5.3. Display the Feature-extraction Data.

GLOBAL VARIABLES REFERENCED: NAG, QFFT, CASE, ETRIP, QSS, GROUP, QSYC, OUT, PTR, AGTI

GLOBAL VARIABLES MODIFIED: None

LOCAL VARIABLES: HP, K, M, I1, I2, I

DESCRIPTION:

DO for each analysis group (AG).
- IF any data is to be displayed for this AG, THEN
- • IF the header has not yet been displayed, THEN
- • • display the "Feature Extraction Block" header.
- • Set up the number of phases in this AG (M).
- • Set up channel-index pointers for the first and last phase (I1 & I2).
- • Display the AG title.

4.5.3.1. Display the spectral-component features.

4.5.3.2. Display the steady-state features.

4.5.3.3. Display the symmetrical-component features.
• END.
END.

The display of each group of features is presented in the next three sections.

4.5.3.1. Display the Spectral-component Features.

GLOBAL VARIABLES REFERENCED: QFFT, CASE, ETRIP, OUT, M, NFQ, I1, CFFT, FQPRT, K60, K

GLOBAL VARIABLES MODIFIED: None

LOCAL VARIABLES: I, J, FQP, L, PLR, TEMP, PID

MODULES CALLED: POLAR

DESCRIPTION:

IF a display of the spectral components for this AG is wanted OR the processing task (looping menu item) is "process data continuously" and an error vector threshold has been exceeded, THEN
• Display a header naming the phases
• DO for each spectral component.
• • DO for each phase:
• • • Convert the spectral component into polar format.
• • • Set a flag if the magnitude is greater than the spectral-component print threshold.
• • END
• • IF the above flag was set, THEN
• • • display the normalized spectral component harmonic number and the spectral components for each phase of this AG in polar format.
• END
END

4.5.3.2. Display the Steady-state Features.

GLOBAL VARIABLES REFERENCED: K, M, I1, I2, QSS, SS, OUT, TYPE, Z, POWER, PF, QPU

GLOBAL VARIABLES MODIFIED: None

LOCAL VARIABLES: PLR, CTMP, PID, I, J, CWORK

MODULES CALLED: POLAR

DESCRIPTION:

IF a display of the steady-state features for this AG is wanted, THEN
• IF this AG consists of only a single phase, THEN

```
•   •   convert the steady-state feature to polar format
•   •   display the steady-state feature in both
        rectangular and polar formats.
•   •   IF this AG was used to measure currents, THEN
•   •   •   convert the impedance feature to polar format.
•   •   •   display the impedance feature in both
            rectangular and polar formats.
•   •   •   IF the features are not being displayed in per-
            unit format, THEN
•   •   •   •   convert the power to kVA.
•   •   •   Convert the power to polar format.
•   •   •   Display the power in both rectangular and polar
            formats.
•   •   •   Display the power-factor features.
•   •   END
•   ELSE
•   •   Write a heading to identify each of the phases.
•   •   For each phase of this AG, convert the steady-state
        to polar format.
•   •   Display the steady-state feature in both rectangular
        and polar format for each phase of this AG.
•   •   IF this AG was used to measure currents, THEN
•   •   •   for each phase of this AG, convert the impedance
            feature to polar format.
•   •   •   Display the impedance feature in both rectangular
            and polar formats for each phase of this AG.
•   •   •   DO for each phase of this AG.
•   •   •   •   IF the features are not being displayed in
                per-unit format, THEN
•   •   •   •   •   convert the power feature to kVA.
•   •   •   •   Convert the power feature to polar format.
•   •   •   END
•   •   •   Display the power feature in both rectangular and
            polar formats for each phase of this AG.
•   •   •   Display the power-factor features for each phase
            of this AG.
•   •   END
•   END
```

4.5.3.3. Display the Symmetrical-component Features.

GLOBAL VARIABLES REFERENCED: K, M, I1, I2, QSYC, OUT, SYCMP, TYPE, SCZ

GLOBAL VARIABLES MODIFIED: None

LOCAL VARIABLES: I, J, PLR

MODULES CALLED: POLAR

DESCRIPTION:

IF a display of the symmetrical component features for this AG is wanted AND this AG is composed of three phases, THEN

- display the heading "Symmetrical Components."
- For each sequence (i.e., positive, negative, and zero) of this AG, convert it to polar format.
- Display the symmetrical-component features in both rectangular and polar format for each sequence in this AG.
- IF this AG was used to measure currents, THEN
    - for each sequence of this AG, convert the symmetrical-component impedance to polar format.
    - Display the symmetrical-component impedance in both rectangular and polar formats for each sequence in this AG.
- END

END

II.7. DETAILED DESCRIPTION OF THE EVINIT MODULE

For discussion purposes the EVINIT module can be subdivided as follows:

```
     DO Forever
1.0  Menu-item Selection.
     CASE (Depending on which item was selected.)
2.1     Display the error-vector menu.
2.2     Error-vector usage.
2.3     Set analysis group of the steady-state reference feature.
2.4     Set the "zero" detect range.
2.5     Save current error-vector thresholds on file 8.
2.6     Retrieve current error-vector thresholds from file 8.
2.7     Eliminate/include a given analysis group in the error
        vector.
2.8     Eliminate/include a given feature in the error vector.
2.9     Set error-vector thresholds.
2.10    Eliminate/include the spectral-components feature in the
        error vector.
2.11    Set the error-vector phase transform.
2.12    Exit from error-vector menu processing.
     END
   END
3.0  PROCEDURE Error Message.
```

1.0. Menu-item Selection.

GLOBAL VARIABLES REFERENCED: CNTL

GLOBAL VARIABLES MODIFIED: IRETRN

LOCAL VARIABLES: I

DESCRIPTION: A message is displayed to the user requesting him to enter an integer indicating which error-vector parameters are to be modified. This integer is chosen by referring to a display of the error-vector menu (see Section 2.1). The program then transfers control to the block of code which will allow the parameter to be changed.

If the user specifies an invalid item number, an error message is displayed via PROCEDURE Error Message.

2.1. Display the Error-vector Menu.

GLOBAL VARIABLES REFERENCED: CNTL, EVUSE, IREFAG, ZEROL, ZEROH, PXFRM, NAG, ETSS, ETZ, ETPWR, ETPF, ETR, ETX, ETSYC, ETSCZ, ETSCR, ETSCX, NFQ, EIFFT

GLOBAL VARIABLES MODIFIED: None

LOCAL VARIABLES: MENU, I, J, K

DESCRIPTION: The user enters the digit corresponding to the FORTRAN I/O unit of the file on which the error-vector menu will be displayed. The menu is then displayed in a form which briefly describes each parameter that can be changed along with its current value and an item number. In Block 1.0, the user enters this item number to indicate which parameter will be changed, and on the next line he enters the new value of the parameter.

Following the menu display, the current thresholds are displayed in a tabular format. A negative threshold indicates that no error vector should be processed for that feature component.

2.2. Error-vector Usage.

GLOBAL VARIABLES REFERENCED: CNTL

GLOBAL VARIABLES MODIFIED: EVUSE

LOCAL VARIABLES: None

DESCRIPTION: The user enters "T" or "F" depending on whether or not any error vectors are to be calculated.

2.3. Set Analysis Group of the Steady-state Reference Feature.

GLOBAL VARIABLES REFERENCED: CNTL, NAG

GLOBAL VARIABLES MODIFIED: IRETRN, IREFAG

LOCAL VARIABLES: None

DESCRIPTION: The user enters the analysis-group number of the steady-state feature which will be used to detect the beginnings and ends of cycles. This value is checked for validity, and the user is issued an error message via PROCEDURE Error Message if it is invalid.

2.4. Set the "zero" Detect Interval.

GLOBAL VARIABLES REFERENCED: CNTL

GLOBAL VARIABLES MODIFIED: ZEROL, ZEROH

LOCAL VARIABLES: None

DESCRIPTION: The user enters two floating point values which define a "zero" interval. A steady-state feature is monitored to determine whether it is inside or outside this interval, and error vector cycles are started or terminated accordingly.

2.5. Save Current Error-vector Threshold on File 8.

GLOBAL VARIABLES REFERENCED: NAG, NFQ, TITLE, ETSS, ETZ, ETPWR, ETPF, ETR, ETX, ETSYC, ETSCR, ETSCX, ETSCZ, ETFFT

GLOBAL VARIABLES MODIFIED: None

LOCAL VARIABLES: J, K

DESCRIPTION: The run title, number of analysis groups, number of spectral components, and the error-vector thresholds are written to the file assigned to FORTRAN I/O unit number 8. The file is first rewound.

Because of the large number of thresholds, this menu item makes it convenient for the user to save the current thresholds for use in a later run.

2.6. Retrieve Current Error-vector Thresholds From File 8.

GLOBAL VARIABLES REFERENCED: CNTL, NAG, NFQ

GLOBAL VARIABLES MODIFIED: ETSS, ETZ, ETPWR, ETPF, ETR, ETX, ETSYC, ETSCR, ETSCX, ETSCZ, ETFFT

LOCAL VARIABLES: N, L, J, K

DESCRIPTION: A run title, number of analysis groups, number of spectral components, and the error vector thresholds are read from the file assigned to FORTRAN I/O unit number 8. The file is first rewound.

The number of analysis groups and number of spectral components are compared with the current values. If they are not equal, an error message is generated; and control is transferred to menu item selection block. Otherwise, the thresholds just read are made the current thresholds.

2.7. Eliminate/Include a Given Analysis Group in the Error Vector.

GLOBAL VARIABLES REFERENCED: CNTL, ELIM, INCLUD, NAG, NFQ

GLOBAL VARIABLES MODIFIED: IRETRN, ETSS, ETZ, ETPWR, ETPF, ETR, ETZ, ETSYC, ETSCZ, ETSCR, ETSCX, ETFFT

LOCAL VARIABLES: ICHAR, I, J, K

DESCRIPTION: The user enters the character "E" or "I" (for eliminate or include) an an analysis-group number. If the analysis-group number or the character is invalid, an error message is issued via PROCEDURE Error Message, and the user must then reenter valid data.

Otherwise, the signs of all error-vector thresholds associated with the indicated analysis group are made positive or negative depending on whether an "I" or "E" was entered.

2.8. Eliminate/Include a Given Feature in the Error Vector.

GLOBAL VARIABLES REFERENCED: CNTL, FEAT, ELIM, INCLUD, NAG, NFQ

GLOBAL VARIABLES MODIFIED: IRETRN, ETSS, ETZ, ETPWR, ETPF, ETR, ETX, ETSYC, ETSCZ, ETSCR, ETSCX, ETFFT

LOCAL VARIABLES: ICHAR, SEL, I, L, J, K

DESCRIPTION: The user enters the character "E" or "I" (for eliminate or include), the name of a feature, and if the feature is "FFT," an integer designating the spectral component. If any of this data can be determined to be invalid, an error message is issued via PROCEDURE Error Message, and the user must then reenter valid data.

Otherwise, the signs of all error-vector thresholds associated with the indicated feature (for all analysis groups) are made positive or negative depending on whether an "I" or "E" was entered.

2.9. Set Error-vector Thresholds.

GLOBAL VARIABLES REFERENCED: CNTL, NAG, FEAT, DIGIT, SEQ

GLOBAL VARIABLES MODIFIED: IRETRN, ETFFT, ETZ, ETPWR, ETPF, ETR, ETX, ETSYC, ETSCZ, ETSCR, ETSCX, ETFFT

LOCAL VARIABLES: I, SEL, J, N, VALUE, K, L

DESCRIPTION: The user enters an analysis-group number, the name of a feature, if the feature is "FFT," an integer designating the spectral component or if the feature is associated with the symmetrical components, a character identifying the sequence, and a threshold value. If any of these data can be determined to be invalid, an error message is issued via PROCEDURE Error Message, and the user must then reenter valid data.

Otherwise the value is assigned to the designated error-vector threshold.

The reader will note that since one of the input fields can contain either numeric or alphabetic information, it is necessary to decode it in the program rather than using the format conversion codes.

2.10. Eliminate/Include the Spectral Components in the Error Vector.

GLOBAL VARIABLES REFERENCED: CNTL, ELIM, INCLUD, NAG, NFQ

GLOBAL VARIABLES MODIFIED: IRETRN, ETFFT

LOCAL VARIABLES: ICHAR, I, J, K

DESCRIPTION: The user enters the character "E" or "I" (for eliminate or include). If any other character is entered, an error message is issued via PROCEDURE Error Message, and the user must then reenter valid data. Otherwise, the signs of all error-vector thresholds associated with the "FFT" feature are made positive or negative depending on whether an "I" or "E" was entered.

2.11. Set the Error-vector Phase Transform.

GLOBAL VARIABLES REFERENCED: CNTL

GLOBAL VARIABLES CHANGED: PXFRM

LOCAL VARIABLES: None

DESCRIPTION: The user enters a "T" or "F" to indicate whether or not a phase transform is to be performed on the error vectors.

2.12. Exit from Error-vector Menu Processing.

GLOBAL VARIABLES REFERENCED: None

GLOBAL VARIABLES MODIFIED: None

LOCAL VARIABLES: None

MODULES CALLED: EVRSET

DESCRIPTION: Processing of the error vector menu items is terminated, and control is transferred into the EVRSET module and then back to the caller.

3.0. Procedure Error Message.

GLOBAL VARIABLES REFERENCED: CNTL, IRETRN

GLOBAL VARIABLES MODIFIED: None

LOCAL VARIABLES: None

DESCRIPTION: The message "input error - try again" is displayed to the user, and control is then returned to the caller.

Note that this procedure is implemented with the FORTRAN "assigned go to" facility.

II.8. DETAILED DESCRIPTION OF THE EVRSET MODULE

GLOBAL VARIABLES REFERENCED: CNTL, EVUSE

GLOBAL VARIABLES MODIFIED: N, L, ISTART, ETRIP

LOCAL VARIABLES: LWORK

DESCRIPTION: If error vectors are not being processed as indicated by variable EVUSE, control is immediately passed back to the caller. Otherwise, the user is asked if the error-vector processing is to be reset. If not, control is immediately passed back to the caller. Otherwise, several global variables are initialized so that upon next error-vector-usage processing will begin by searching for a new cycle.

II.9. DETAILED DESCRIPTION OF THE EVCALC MODULE

<u>GLOBAL VARIABLES REFERENCED</u>: EVUSE, IREFAG, ZEROL, ZEROH, NFQ, NAG, IGROUP, ITYPE, PXFRM, ETFFT, ETSS, ETSYC, ETZ, ETR, ETX, ETSCZ, ETSCR, ETSCX, ETPWR, ETPF, CFFT, SS, SYCMP, Z, SCZ, POWER, PF, FFTREF, SSREF, SYCREF, ZREF, RREF, XREF, SCZREF, SCRREF, SCXREF, POWREF, PFREF

<u>GLOBAL VARIABLES MODIFIED</u>: N, L, ISTART, NARRAY, ETRIP, ELFFT, ELSYC, ELZ, ELR, ELZ, ELSCZ, ELSCR, ELSCX, ELPWR, ELPF, EVFFT, EVSS, EVSYC, EVZ, EVR, EVX, EVSCZ, EVSCR, EVSCX, EVPWR, EVPF

<u>LOCAL VARIABLES</u>: REFVAL, VALUE, J, K, I, M

<u>MODULES CALLED</u>: CLASS, EVDIFF

<u>DESCRIPTION</u>:

```
IF error vector processing is being used, THEN
•   Get the steady-state-feature value which determines cycle
    status.
•   CASE (based on the current cycle status).
•   •   Searching for a new cycle,
•   •   •   IF the steady state is within the zero region, THEN
•   •   •   •   set the cycle status to inside a zero region.
•   •   END
•   •   Inside a zero region,
•   •   •   If the steady state breaks outside of the zero region
            on the high side only, THEN
•   •   •   •   set the cycle status to within a cycle.
•   •   END
•   •   Within a cycle,
•   •   •   count the number of data sequences within this cycle.
•   •   •   IF the steady state has returned to the zero region,
            THEN
•   •   •   •   increment the cycle counter.
•   •   •       IF there have been more than 50 cycles, THEN
•   •   •   •   •   delete the oldest data sequence count from
                    NARRAY.
•   •   •   •   Add the current data sequence count to the next
                spot in NARRAY.
•   •   •   •   Set the cycle status to inside a zero region.
•   •   •   •   Reset all the analysis-group 2 error-vector
                threshold overrun indicators.
•   •   •   •   DO for each analysis group:
•   •   •   •   •   PERFORM EVDIFF for the spectral-component
                    error vectors.
•   •   •   •   •   PERFORM EVDIFF  for the steady-state error
                    vectors.
•   •   •   •   •   IF this is a three-phase analysis group, THEN
•   •   •   •   •   •   PERFORM EVDIFF for the symmetrical-
                        component error vectors.
```

```
•  •  •  •  •  IF this is a current analysis group, THEN
•  •  •  •  •  •  PERFORM EVDIFF for the impedance error
                  vectors.
•  •  •  •  •  •  PERFORM EVDIFF for the resistance error
                  vectors.
•  •  •  •  •  •  PERFORM EVDIFF for the reactance error
                  vectors.
•  •  •  •  •  •  IF this is a three-phase analysis group,
                  THEN
•  •  •  •  •  •  •  PERFORM EVDIFF for the symmetrical-
                     component-impedance error vectors.
•  •  •  •  •  •  •  PERFORM EVDIFF for the symmetrical-
                     component-resistance error vectors.
•  •  •  •  •  •  •  PERFORM EVDIFF for the symmetrical-
                     component-reactance error vectors.
•  •  •  •  •  •  END
•  •  •  •  •  •  PERFORM EVDIFF for the power error vectors.
•  •  •  •  •  •  PERFORM EVDIFF for the power-factor error
                  vectors.
•  •  •  •  •  END
•  •  •  •  •  PERFORM CLASS
•  •  •  •  END
•  •  •  END
•  •  END
•  END
END
```

II.10. DETAILED DESCRIPTION OF THE EVREFS MODULE

GLOBAL VARIABLES REFERENCED: EVUSE, N, L, NAG, IGROUP, ITYPE, IPTR, NFQ, CFFT, SS, SYCMP, Z, SCZ, POWER, PF

GLOBAL VARIABLES MODIFIED: ETRIP, FFTREF, SSREF, SYCREF, ZREF, RREF, XREF, SCZREF, SCRREF, SCXREF, POWREF, PFREF

LOCAL VARIABLES: I, J, K, M, I1, I2

DESCRIPTION:

```
IF error vector processing is being used, THEN
•   set the overall error vector threshold indicator to false.
•   IF the steady-state feature is inside a zero region (see the
    description of the EVCALC module), THEN
•   •   DO for each analysis group.
•   •   •   Set up channel-index limits for a given analysis group.
•   •   •   DO for each phase of a given analysis group.
•   •   •   •   DO for each spectral component.
•   •   •   •   •   Set the "FFT" references to the magnitudes of
                    the "FFT" feature.
•   •   •   •   Set the steady-state reference to the magnitude of
                the steady-state feature.
•   •   •   •   IF this is a three-phase analysis group, THEN
•   •   •   •   •   set the symmetrical component reference to the
                    magnitude of the symmetrical-component feature.
•   •   •   •   IF this is a current analysis group, THEN
•   •   •   •   •   set the impedance reference to the magnitude of
                    the impedance feature.
•   •   •   •   •   Set the resistance reference to the real part
                    of the impedance feature.
•   •   •   •   •   Set the reactance reference to the imaginary
                    part of the impedance feature.
•   •   •   •   •   IF this is a three phase analysis group, THEN
•   •   •   •   •   •   set the symmetrical-component-impedance
                        reference to the magnitude of the
                        symmetrical-component-impedance feature.
•   •   •   •   •   •   Set the symmetrical-component-resistance
                        reference to the real part of the
                        symmetrical-component-impedance feature.
•   •   •   •   •   •   Set the symmetrical-component-reactance
                        reference to the imaginary part of the
                        symmetrical-component-impedance feature.
•   •   •   •   •   END
•   •   •   •   •   Set the power reference to the magnitude of the
                    power feature.
•   •   •   •   •   Set the power-factor reference to the real
                    part of the power-factor feature.
•   •   •   •   END
•   •   •   END
•   •   END
•   END
END
```

II.11. DEFINITION OF MAJOR VARIABLES

II.11.1 SEDAPS MAIN PROGRAM.

TITLE [REAL(13)]	A string of up to 52 characters containing run identification.
KOMMON [INTEGER*2(672)]	An array of 672 half-words (HW) equivalenced to the variable TITLE through B of the unlabeled common. This set of variables contains general run parameters, and this array is used to transfer this data to the raw-data disk file as a single header record.
NAG [INTEGER*2]	The number of analysis groups. An analysis group is the smallest logical grouping of one or three input channels needed to define a set of some of the simpler features.
NCH [INTEGER*2]	The number of channels. A channel consists of a sequence of measurements of a single property for some entity (e.g., current).
NSAM [INTEGER*2]	The number of elements in a single sequence of measurements. This sequence has the property that its index set maps linearly into time.
NFQ [INTEGER*2]	The number of frequencies. This variable represents the number of unique terms in the discrete Fourier transform (DFT) of the sequence of measurements from a channel.
IDELFQ [INTEGER*2]	The spacing (in Hz) between elements of the DFT of the input sequence.
K60 [INTEGER*2]	The value of the index of the element of the DFT of the input sequence which corresponds to 60 Hz. The index set is numbered 1, 2, ---, NFQ where the element whose index is 1 always corresponds to the d-c component.
AGTI [REAL(15,16)]	This is a group of strings, one string for each analysis group, for user identification of the analysis groups. Each string is up to 60 characters in length.
GROUP [INTEGER*2(16)]	An array giving the nature of each of the analysis groups as follows: 1. three-channel multiphase, 2. single-channel a-c, or 3. single-channel d-c.

TYPE [INTEGER*2(16)] — An array giving the type of measurement for each of the analysis groups as follows:
1. voltage or
2. current.

REF [INTEGER*2(16)] — An array referring to the voltage analysis group to be used in the calculation of impedance and related features. This array contains valid data only for current analysis groups.

(NOTE: The index to each element of the above three arrays refers to the analysis group number.)

PTR [INTEGER*2(3,16)] — A two-dimensional array used to map the analysis-group number and phase index into a channel index. The concept of a phase index comes from the GROUP array definition. The PTR array has three rows and 16 columns, a column for each of the analysis groups and a row for each phase. Thus for analysis group 7, phase 2, PTR (2,7) contains the channel index for this combination. (Note that for single-phase analysis groups, rows two and three are undefined.)

A and B [REAL(16)] — For each of the channels, a linear expression, A•x + B is used to map the measured value into natural units. "x" as used here is the measured channel value as read from the analog to digital converter (i.e., an integer between -512 through +511).

CASE [INTEGER*2] — The acquisition and disposition of the raw data can be handled in one of several ways termed "looping." This variable indicated the methods the user can choose as follows:
1. list the various options for looping,
2. initialize the disk to receive the raw data,
3. acquire and transfer data to disk for a certain period of time (a subset of the acquired data can be transferred),
4. process data as rapidly as possible printing results at specified intervals,
5. same as (4) and also transfer data to disk,
6. process only one sequence of data,
7. process data that has been previously stored on disk,
8. close disk file after writing has been completed, and
9. transfer of control to select new run parameters.

KOUNT [INTEGER*2]	A value derived from the sampling rate and number of channels used to directly control the sampling rate of the analog-to-digital converter (ADC).
CH [INTEGER*2(16)]	An array giving the ADC address for each of the channel indexes. It should be noted that the channel indexes are generated from the order in which the analysis-group definition was entered into the computer.
COLECT [INTEGER*2]	The number of sequences of raw data to be transferred to disk for CASE = 3.
IFAULT [INTEGER*2]	In order to detect a hardware problem in the ADC, the absolute value of the mean of a sequence of input measurements is compared to this value, and the ADC is declared functional if the mean is smaller than it. For a-c data, the mean should trends towards zero.
SAMEND [LOGICAL]	A logical variable that is set to TRUE after the last sequence of data has been read from disk for CASE = 7.
SAMTIM [INTEGER*2(6)]	The time of day at which a given sequence of data was taken. It is in the form of an integer array of six elements giving the month, day, year, hour, minute, and second.
DATA [REAL(32,16)]	A two-dimensional array containing the measured data in natural units. The rows contain elements of a sequence, and the columns contain complete sequences for each of the channels.
BLOKID [REAL(5)]	A string of 20 characters that identifies a given sequence of data. Entered by the user only when CASE = 6.
NSKIP [INTEGER*2]	Used only when CASE = 3 to determine the subset of data transferred to disk. Only the first record out of every NSKIP records is transferred.
RMTRIG [LOGICAL]	Determines whether a remote trigger will be used to set the time at which a sequence of measurements will be taken as follows: TRUE: remote trigger will be used, FALSE: a sequence will be taken when commanded by the computer.
FEATUR [COMMON LABEL]	The name of a labeled common block which contains the features computed from the measurement sequence.

CFFT [COMPLEX(17,16)]
: A complex, two-dimensional array containing the spectral features. The columns contain the spectra for each of the channels, and the rows contain each of the spectral components.

FFT [REAL(34,16]
: A two-dimensional real array that is equivalenced to CFFT. The DATA array is first transferred into this array, and then the DFT is performed in-place to produce the complex spectral components which are then accessed through CFFT.

SS [COMPLEX(16)]
: A complex array containing the steady-state features.

SYCMP [COMPLEX (16)]
: A complex array containing the symmetrical-component features.

Z [COMPLEX(16)]
: A complex array containing the impedance feature.

SCZ [COMPLEX(16)]
: A complex array containing the symmetrical-component impedance feature.

POWER [COMPLEX(16)]
: A complex array containing the power features.

PF [COMPLEX(16)]
: A complex array containing the power-factor feature in the real part and zero in the imaginary part. (Note that although this array contains only real data, it was made complex so all of the feature arrays would be of the same type.)

NOTES:
1. The arrays in the FEATUR common block are all ordered on the channel index (see PTR & CH). Access to the correct feature is typically by using the analysis-group number and phase index to retrieve the wanted channel index from the PTR array.
2. The SYCMP & SCZ arrays are defined only for three phase analysis groups.
3. The Z, SCZ, POWER, and PF arrays are defined only for current type analysis groups.

EV [COMMON LABEL]
: The name of a labeled common block which is used to communicate with the error-vector subroutines.

ETRIP [LOGICAL]
: Set in the error-vector subroutine and used to control feature printing as follows:
  - FALSE: no error vector trip has occurred, do not print features;
  - TRUE: error vector trip has occurred, print features.

TIME [INTEGER*2(16)]	An array similar to SAMTIM which is used in initial time setting and in time calculations.
CNTL [INTEGER*2]	The FORTRAN I/O unit number used to communicate with the user.
AGF [INTEGER*2]	The FORTRAN I/O unit number used to read the analysis-group-definition file.
OUT [INTEGER*2]	The FORTRAN I/O unit number used to print results.
CHNL [INTEGER*2(3,16)]	A two-dimensional array containing the channel numbers for each of the analysis groups and phases. The columns contain the values for each analysis group; for the rows, each phase. The CH array is built directly from this one.
PID [INTEGER*2(3)]	A string constant used to identify the phases ("A", "B", or "C").
VBASE} IBASE} ZBASE} PBASE} [REAL]	A set of values computed from XFMR and VLOW used to scale the voltage, current, impedance, and power, respectively, to per unit normalization.
XFMR [REAL]	Transformer rating (VA). This is a user input.
VLOW [REAL]	Low side voltage (V). This is a user input.
QRAW} QFFT} QPU } QSS } QSYC} [LOGICAL(16)]	This is a set of logical arrays, each array over the analysis group number used to control computation of and/or printing of the measured data, the spectral features, per unit normalization, steady state features, or symmetrical component features, respectively.
OREAD [LOGICAL(4)]	A logical array that indicates the user's desire after processing has been completed as follows: OREAD(4) = TRUE, terminate the program; OREAD(3) = TRUE, restart the program; OREAD(2) = TRUE, change run parameters; OREAD(1) = TRUE, select a new "looping" option.
BRK [LOGICAL]	A logical variable which is set to TRUE when the "BREAK" key is depressed on the teletype. This key is used to interrupt current processing.
HP [LOGICAL]	A logical variable used in header printing. It is set to TRUE to show that a header has been printed.

FQP
[LOGICAL]
A logical variable which is set to TRUE if none of the three (or one) phases of a spectral component exceed the threshold for printing.

SCALE
OFFSET
[REAL(3,16)]
These two two-dimensional arrays are organized in a manner similar to CHNL. SCALE is the factor to convert from the measured value in volts to natural units. OFFSET is the offset in volts. Arrays A and B are directly computed from these values.

CTMP
[COMPLEX]
A complex variable that is used in converting the power from VA to kVA when there is only one phase in an analysis group.

W
[COMPLEX(16)]
A complex array needed by the RDFT subroutine to store the sine-cosine power table.

CWORK
[COMPLEX(3)]
A complex array that is used in converting the power from VA to kVA when there are three phases in an analysis group.

PLR
[COMPLEX(3)]
A complex array that contains the features in magnitude -- phase (phasor) format. This array of three elements is computed just prior to printing the three (or one) phases of each feature.

CABLES
[COMPLEX(3,3)]
A complex two-dimensional array that contains the features as extracted by subroutine CABLE. The three columns contain the features for each of the phases: row 1, voltage drop -- phase shift; row 2, impedance difference; and row 3, symmetrical-component impedance.

TWOPI
[REAL]
A constant equal to $2 \cdot \pi$.

I1ARG
[INTEGER*2]
No longer used. It could be removed from the DATA statement.

BLANK
[REAL]
A variable used to initialize the BLOKID array to space characters for those "looping" options which do not allow the user to define it (e.g., CASE = 3, 4, and 5).

FQPRT
[REAL]
The magnitude of a spectral component must exceed this threshold to be printed.

M
[INTEGER*2]
The number of phases in an analysis group.

NFQ2
[INTEGER*2]
Two times the number of frequencies.

TEMP [REAL]	Used in converting the sampling rate (SRT) and number of samples (NSAM) into KOUNT. Also the harmonic number of a spectral component relative to the 60-Hz component.
REWIND [REAL]	An unused variable in the argument list of DISK W whose name is indicative of the action to be taken.
TIMPRT [REAL]	The time interval in minutes between printouts (used for CASE = 4 or 5).
ITIMPR [INTEGER*2]	The value of TIMPRT in 6-s increments.
ITIME [INTEGER*2]	The value of a hardware timer decrementing every 6 s.
ITIMRF [INTEGER*2]	The value of the hardware timer at which the next printout should occur.
THETA [REAL]	The phase of the 60-Hz spectral component at the beginning of a sequence of measurements in radians normalized by the DFT harmonic number of this component.
I1 [INTEGER*2]	The channel index of the first or only phase in an analysis group. Also used in selecting the spectral component for normalization of the other components.
I2 [INTEGER*2]	The channel index of the last or only phase in an analysis group.
XNORM [REAL]	The magnitude of the spectral component selected for normalizing the other components. This value can never be less than 1.0.
PUN [REAL]	Used to convert the steady-state features to per-unit normalization.
ARG [REAL]	The vector rotation in radians applied to the spectral components to correct for sampling-point offsets.
MM [INTEGER*2]	See M.
SSIMAG SSJMAG [REAL]	The magnitudes of the steady-state features for the two channels being used to compute the power factor.

II.11.2. Subroutine INPUT.

The following are variables used in the subroutine INPUT that are common with the Main Program.

TITLE	See Main Program
NAG	↓
NCH	
NSAM	
NFQ	
IDELFQ	
K60	
AGTI	
IGROUP	, Variable GROUP
ITYPE	TYPE
IREF	REF
IPTR	PTR
A	
B	
CASE	
KOUNT	
IPOLE	, Variable CH
COLECT	
IFAULT	
SAMEND	
SAMTIM	
DATA	
BLOKID	
NSKIP	
RMTRIG	↓

DSBKID [REAL(5)]	That part of the data record on disk containing BLOKID (see Main Program).
IN [INTEGER*2(512)]	An array containing the sequence of measurements made by the ADC for all channels of interest. The order of the data is channel-index 1, sample-point 1; channel-index 2, sample-point 1; --- ; channel-index NCH, sample-point 1; channel-index 1, sample-point 2; --- ; channel-index NCH, sample-point NSAM.
TIME [INTEGER*2(6)]	See Main Program.
DSKRCD [INTEGER*2(528)]	The array comprising the data in one record on disk. Consists of TIME, DSBKID, and IN.
KFLT [INTEGER*2]	Used to count the number of sequences of data read from the ADC. This value is printed whenever an ADC error is detected.
BLANK [REAL]	See Main Program.
N [INTEGER*2]	The number of sample points in a sequence of measurements taken by the ADC. Equal to NCH•NSAM.
ISTAT [INTEGER*2]	ADC status as follows: zero, ADC functional; not zero, ADC not functional.

<u>II.11.3. Subroutine SYCOMP</u>.

OUT [COMPLEX(3)]	A complex array of the symmetrical components of the three phases of a feature.
IN [COMPLEX(3)]	A complex array of the three phases of a feature.
A [COMPLEX]	A rotation of 120° represented in complex form.
AA [COMPLEX]	A rotation of -120° represented in complex form.

<u>II.11.4. Subroutine TIMER</u>.

TIME	A dummy argument integer array of six elements containing the current month, day, year, hour, minute, and second.

ITIME	A dummy argument returning the current value of a hardware counter decrementing once every six seconds.
K	A dummy argument indicating the type of processing to be performed as follows: -1, perform initialization and synchronize with the wall-clock time; zero, return the current time to the caller.
DATE	The month, day, and year part of TIME.
NOWTIM	The current value of a hardware counter documenting once every 6 s.
WALL	The wall clock time in 6-s units.
TIMREF	The previous value of the hardware counter.
TD	Used to convert the counter value to hours, minute, second format.
TDQ	= 1, whenever time passes into a new day.

II.11.5. Subroutine POLAR.

C	A complex variable in rectangular format.
POLAR	A complex variable converted to polar (magnitude-phase or phasor) format.
A	Real part of C.
B	Imaginary part of C.
TEMP	Phase part of POLAR in degrees, $0 \leq \text{TEMP} < 360$.

II.11.6. Subroutine CABLE.

The variables common with the Main Program are as follows.

TITLE	See Main Program
NAG	↓
NCH	↓
NSAM	↓
NFQ	↓
IDELFQ	↓

K60	See Main Program	
AGTI		
IGROUP		, Variable GROUP
ITYPE		TYPE
IREF		REF
IPTR		PTR
A		
B		
IOPN	Dummy argument specifying the type of processing to be performed as follows: zero, initialization; 1, compute cable features; 2, print cable features.	
SS	Dummy argument complex array transferring the steady-state features of this subroutine.	
SYCMP	Dummy argument complex array transferring the symmetrical-component features to this subroutine.	
CABLES	Dummy argument complex two-dimensional array returning the cable features to the calling routine. The three columns contain the features for each of the phases; row 1, voltage drop -- phase shift; row 2, impedance difference; and row 3, symmetrical-components impedance difference.	
DROP	A complex array containing the voltage drop for each of the three phases in polar format.	
XX	The voltage drop for a given phase in polar format.	
X	Imaginary part of XX adjusted to $-180 \le X \le 180$.	
PLR	A complex array containing the impedance difference or the symmetrical-components impedance difference in polar format for each of phases A, B, and C.	
CBL	A logical variable indicating whether cable computations are to be performed as follows: FALSE, perform no cable computations; TRUE, perform cable computations.	

JVT	The analysis-group number for the transformer voltage.
JVM	The analysis-group number for the motor voltage.
JC	The analysis-group number for the current.
M	Index for the three phases.

II.11.7. ERROR VECTOR Subroutine.

The common variables of this and the Main Program are listed below.

TITLE	See Main Program	
NAG		
NCH		
NSAM		
NFQ		
IDELFQ		
K60		
AGTI		
IGROUP		, Variable GROUP
ITYPE		TYPE
IREF		REF
IPTR		PTR
A		
B		
FEATUR		
CFFT		
SS		
SYCMP		
Z		
SCZ		

POWER	See Main Program
PF	↓
ETRIP	↓
CLASSC	A labeled common block containing error vector threshold overrun indicators for each of the features and phases of analysis group 2 as follows: zero, the threshold was not exceeded; -1, the threshold was exceeded on the negative side; 1, the threshold was exceeded on the positive side.
ELFFT	The overrun indicator for the FFT magnitude feature. Organized as a two-dimensional array with the phases indexing the columns and the spectral components indexing the rows.
ELSS	The overrun indicators for the steady-state magnitudes.
ELSYC	The overrun indicators for the symmetrical-component magnitudes.
ELZ	The overrun indicators for the impedance magnitudes.
ELR	The overrun indicators for the resistances.
ELX	The overrun indicators for the reactances.
ELSCZ	The overrun indicators for the symmetrical-component impedance magnitudes.
ELSCR	The overrun indicators for the symmetrical-component resistances.
ELSCX	The overrun indicators for the symmetrical-component reactances.
ELPWR	The overrun indicators for the power magnitudes.
ELPF	The overrun indicators for the power factors.
EVUSE	A logical variable indicating whether the error vectors are to be calculated as follows: FALSE, do not process error vectors; TRUE, process error vectors.

LWORK	A logical variable indicating whether the error vectors should be reset as follows: FALSE, do not reset; TRUE, reset.

(NOTE: The next set of arrays form a set of references to which the present value of a feature is compared to determine whether a threshold overrun has occurred. These arrays are indexed over the channel index.)

FFTREF	The reference for the FFT magnitude feature. This is a two-dimensional array organized similar to ELFFT.
SSREF	The reference for the steady-state magnitudes.
SYCREF	The reference for the symmetrical-component magnitudes.
ZREF	The reference for the impedance magnitudes.
RREF	The reference for the resistances.
XREF	The reference for the reactances.
SCZREF	The reference for the symmetrical-component impedance magnitudes.
SCRREF	The reference for the symmetrical-component resistances.
SCXREF	The reference for the symmetrical-component reactances.
POWREF	The reference for the power magnitudes.
PFREF	The reference for the power factors.
WORK	This array of three elements contains the difference between the present feature and its reference for each phase. It is used in printing this difference.
FEAT	This eleven-element array contains abbreviated names for each of the eleven features comprising the error vector. It is used by the operator to identify those features whose thresholds will be changed.

(NOTE: The next set of arrays form a set of thresholds that the difference between a feature and its reference must exceed in order to have a threshold overrun condition (error vector trip). These arrays are indexed over the analysis-group index. Arrays ETFFT, ETSYC, ETSCZ, ETSCR, and ETSCX are two dimensional with the row index referring to the spectral index for ETFFT and to the symmetrical-component index for the remaining arrays.)

ETFFT	The threshold for the FFT magnitudes. This is a two-dimensional array organized similarly to ELFFT.
ETSS	The threshold for the steady-state magnitudes.
ETSYC	The threshold for the symmetrical-component magnitudes.
ETZ	The threshold for the impedance magnitudes.
ETR	The threshold for the resistances.
ETX	The threshold for the reactances.
ETSCZ	The threshold for the symmetrical-component impedance magnitudes.
ETSCR	The threshold for the symmetrical-component resistances.
ETSCX	The threshold for the symmetrical-component reactances.
ETPWR	The threshold for the power magnitudes.
ETPF	The threshold for the power factors.
ELIM	The character "E". Used by the operator to eliminate features from inclusion in the error vector.
INCLUD	The character "I". Used by the operator to include features in the error vector.
STORE	An integer array containing the integers 0, 1, ---, NFQ-1. Used in identifying the thresholds for the FFT features during printing.
REFVAL	The channel index of the steady state reference feature.

DIGIT	An array of the integer 0, 1, ---, 9 used to identify a spectral or symmetrical-component index as entered by the operator.
SEQ	An array containing the characters P, M, Z used by the operator to identify which symmetrical component he wants to change.
CNTL	The FORTRAN I/O unit number used to communicate with the operator.
MENU	The FORTRAN I/O unit number used to display the error vector menu.
IOUT	The FORTRAN I/O unit number used to display the error vectors.
NARRAY	An array of the 50 most recent cycle counts.
IRETRN	The statement label (placed by an ASSIGN statement) to go to after giving an error message upon invalid input.
IREFAG	The analysis-group index of the steady-state reference feature.
ZEROL ZEROH	These two variables form the bounds of the zero interval. The steady-state magnitude of a reference channel falls inside and then returns to this interval to constitute an error-vector cycle.
ICHAR	Used to input the operator's include/eliminate decision. See INCLUD and ELIM.
SEL	Used to input the operator's feature name when alteration is wanted. See FEAT.
VALUE	Used to input the operator's value for an error vector threshold. It is also the magnitude of the steady-state reference feature.
ISTART	Used as the index of the next element to fill in NARRAY.
I1 I2	The starting and ending channel indexes for the three (possibly one) phases comprising an analysis group.
IFQ	An index for spectral-component elements.
TEMP	The harmonic number of a spectral component relative to the 60-Hz component.

II.11.8. Subroutine EVDIFF.

TITLE	See Main Program.	
NAG	See Main Program.	
NCH	See Main Program.	
NSAM	See Main Program.	
NFQ	See Main Program.	
IDELFQ	See Main Program.	
K60	See Main Program.	
AGTI	See Main Program.	
IGROUP	See Main Program.	Variable GROUP
ITYPE	See Main Program.	Variable TYPE
IREF	See Main Program.	Variable REF
IPTR	See Main Program.	Variable PTR
A	See Main Program.	
B	See Main Program.	
ET [REAL (ETDIM,16)]	A dummy argument transferring the error-vector threshold for a given feature to this subroutine. See ETFFT, ETSS, etc., in the Error-vector subroutine.	
FEAT [COMPLEX (FEATDM,16)]	A dummy argument transferring a given feature to this subroutine. See CFFT, SS, etc., in the Error-vector subroutine.	
REF [REAL (FEATDM,16)]	A dummy argument transferring the feature references for a given feature to this subroutine. See FFTREF, SSREF, etc., in the Error-vector subroutine.	
EV [REAL (FEATDM,16)]	A dummy argument returning the error vectors for a given feature to the Error-vector subroutine. See EVFFT, EVSS, etc., in the Error-vector subroutine.	
EL [INTEGER*2 (FEATDM,16)]	A dummy argument returning the threshold overrun indicators for a given feature to the Error-vector subroutine. See ELFFT, ELSS, etc., in the Error-vector subroutine.	

ETRIP [LOGICAL]	A dummy argument returning the overall error-vector threshold overrun indicator which is set to "TRUE" if any error vector exceeds its threshold.
FUNC [FUNCTION NAME]	A dummy argument transferring to this subroutine the name of a function for a given feature used to retrieve from the complex feature a real value needed to compute the error vector (e.g., CABS, REAL, AIMAG).
ETDIM [INTEGER*4]	A dummy argument transferring to this subroutine the dimension of the first index of the ET array (i.e., 17 for ETFFT and 1 for all others).
FEATDM [INTEGER*4]	A dummy argument transferring to this subroutine the dimension of the first index of the FEAT, REF, EV, and EL arrays (i.e., 17 for FFT, 3 for SYC, SCZ, SCR, and SCX and 1 for all others).
PXFRM [LOGICAL]	A dummy argument transferring to this subroutine the phase-transform indicator. See Error-vector subroutine.
NFEAT [INTEGER*2]	A dummy argument transferring to this subroutine the number of feature components contained in FEAT (i.e., NFQ for FFT and 1 for all others).
K [INTEGER*2]	A dummy argument transferring to this subroutine the analysis group number of the current analysis group.
M [INTEGER*2]	A dummy argument transferring to this subroutine the number of phases in the current analysis group.
IFEAT [INTEGER*2]	A feature component index. See NFEAT.
I1 [INTEGER*2]	Channel number index of the first phase in an analysis group.
I2 [INTEGER*2]	Channel number index of the second phase in an analysis group.
I3 [INTEGER*2]	Channel number index of the third phase in an analysis group.
IET [INTEGER*2]	Error-threshold index.